MUTAGENESIS OF HIV-1 GP120 V3 LOOP TO DETERMINE EFFECTS ON GP120-MEDIATED CCR5 AND CXCR4 SIGNAL TRANSDUCTION IN RESTING CD4 T CELLS

by

Huizhi Liang

A Thesis
Submitted to the
Graduate Faculty
of
George Mason University
in Partial Fulfillment of
The Requirements for the Degree
of
Master of Science
Biology

Committee:

_____ Dr. Yuntao Wu, Thesis Director

_____ Dr. Jia Guo, Committee Member

_____ Dr. Ramin M. Hakami, Committee Member

_____ Dr. James D. Willett, Director, School of Systems Biology

_____ Dr. Donna M. Fox, Associate Dean, Office of Academic Affairs and Special Programs, College of Science

_____ Dr. Peggy Agouris, Dean, College of Science

Date: _____ Spring Semester 2015
George Mason University
Fairfax, VA

MUTAGENESIS OF HIV-1 GP120 V3 LOOP TO DETERMINE EFFECTS ON GP120-MEDIATED CCR5 AND CXCR4 SIGNAL TRANSDUCTION IN RESTING CD4 T CELLS

A Thesis submitted in partial fulfillment of the requirements for the degree of Master of Science at George Mason University

by

Huizhi Liang
Bachelor of Science
George Mason University, 2010

Director: Yuntao Wu, Professor
School of Systems Biology

Spring Semester 2015
George Mason University
Fairfax, VA

DEDICATION

This is dedicated to my beloved parents, Yunyan Liang and Guocheng Wang, who educated me and supported me to reach at this level.

ACKNOWLEDGEMENTS

I thank the members of my graduate committee, Drs. Yuntao Wu, Jia Guo and Ramin Hakami, for the opportunity to pursue a master's degree under their tutelage. They have imparted on me scientific wisdom for which I am immensely grateful.

To the graduate students of Dr. Wu's lab, I convey deep appreciation for their camaraderie, discussions, visions, feedback, and support. It has been an honor to learn with them, as well as from them.

TABLE OF CONTENTS

ABSTRACT

MUTAGENESIS OF HIV-1 GP120 V3 LOOP TO DETERMINE EFFECTS ON GP120-MEDIATED CCR5 AND CXCR4 SIGNAL TRANSDUCTION IN RESTING CD4 T CELLS

Huizhi Liang, M.S.

George Mason University, 2015

Thesis Director: Dr. Yuntao Wu

The M-tropic HIV-1 viruses use CCR5 as the co-receptor for entry. The V3 loop in the M-tropic envelope protein, gp120, is largely responsible for the selection of the CCR5 co-receptor. Mutations in the V3 loop frequently lead to viral tropism switch to use CXCR4, which is associated with rapid disease progression. Recent studies from our laboratory have suggested that during viral entry, HIV-1 also triggers signal transduction through gp120 binding to CXCR4 on resting CD4 T cells. This signal transduction leads to actin dynamics, facilitating viral post entry steps. In this study, I examined the role of individual mutations in the V3 loop for viral tropism switch. We selected and mutated six amino acids in the V3 loop of the M-tropic YU2 gp120. Effects of these mutations on viral entry and viral tropism switch (R5- to X4-tropism) were analyzed. In addition, I also investigated whether these mutations alter gp120 signaling through CCR5 or CXCR4 in resting CD4 T cells. My results demonstrated that these mutations alter the ability of

HIV-1 to trigger signal through CCR5, diminishing HIV infectivity. However, these mutations were not sufficient to confer viral tropism switch and the ability to trigger signal transduction through CXCR4.

I. INTRODUCTION

A. Background of HIV-1 Infection and AIDS

Human Immunodeficiency Virus (HIV) causes Acquired Immunodeficiency Syndrome (AIDS) that affects over 33 million people worldwide. So far, there has no cure since its discovery. HIV type 1 (HIV-1) is a retrovirus which belongs to the Lentiviridae subfamily of viruses. The first patient with AIDS was recognized in 1981. Soon after in 1983, the virus was reported to be found in a patient's tissue. Gallo's group in NIH (National Institute of Health) established the causative relationship between the virus and AIDS in 1984 and in 1985 (Gallo & Montagnier, 2003; Kallings, 2008).

The onset of HIV infection is similar to mononucleosis, starting with a fever, a sore throat and a skin rash (Kallings, 2008). The stage between first exposure to the virus and clinical latency spans up to 12 weeks when HIV-specific antibodies could be detected in seroconversion (Figure 1.). During this period, the virus replicates quickly and the patient is the most infectious. Then the stabilized viral load (virus level in peripheral blood) that is specific to each patient becomes a so-called set point to determine the time from infection to development of AIDS (Kallings, 2008). Latency could last for 11 years without treatment. During this period, although the infected individuals may appear asymptomatic, the virus is actively replicating and gradually

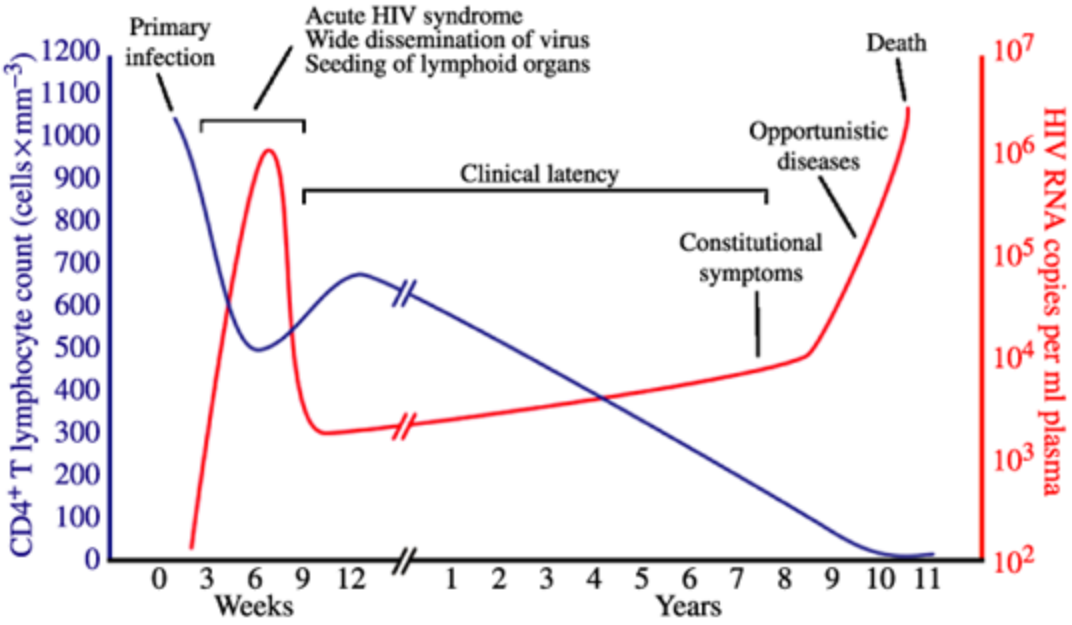

Figure 1. Typical course of HIV infection and disease. (Kallings, 2008)

destroys the immune system by a sign of CD4 T cell depletion (Kallings, 2008; Naif, 2013). When the patient has a high plasma HIV viral load and the number of CD4 T cell count is less than 200 cells x mm^{-3}, the infected individual is diagnosed with AIDS. During the phase of AIDS, the number of CD4 T cells continue to drop and the patients are more prone to opportunistic diseases like tuberculosis, pneumonia, kaposi's sarcoma, etc, as their immune systems have been compromised (Naif, 2013).

B. HIV-1 Structure, Genome and Replication Cycle

a. Structure

HIV-1 is an enveloped virus that contains two identical copies of positive sense single-stranded RNAs enclosed in a core formed by capsid (CA or p24) protein (Costin, 2007; Freed, 2001). The surface envelope protein gp120 (SU) along with the transmembrane envelope protein gp41 (TM) are anchored on the outer surface of the lipid bilayer (Figure 2.).

b. Genome

HIV-1 possesses a 9.8 kb long genome with a total of nine genes (Costin, 2007). These nine genes can be categorized into three groups: 1) structural genes –*gag*, *pol*, and *env*; 2) regulatory genes –*tat* and *rev*; 3) accessory genes –*vpu*, *vpr*, *vif*, and *nef* (Costin, 2007). The *gag* gene encodes a polyprotein precursor $Pr55^{Gag}$ which can be cleaved by the viral protease (PR) to the mature Gag protein matrix (MA or p17), capsid,

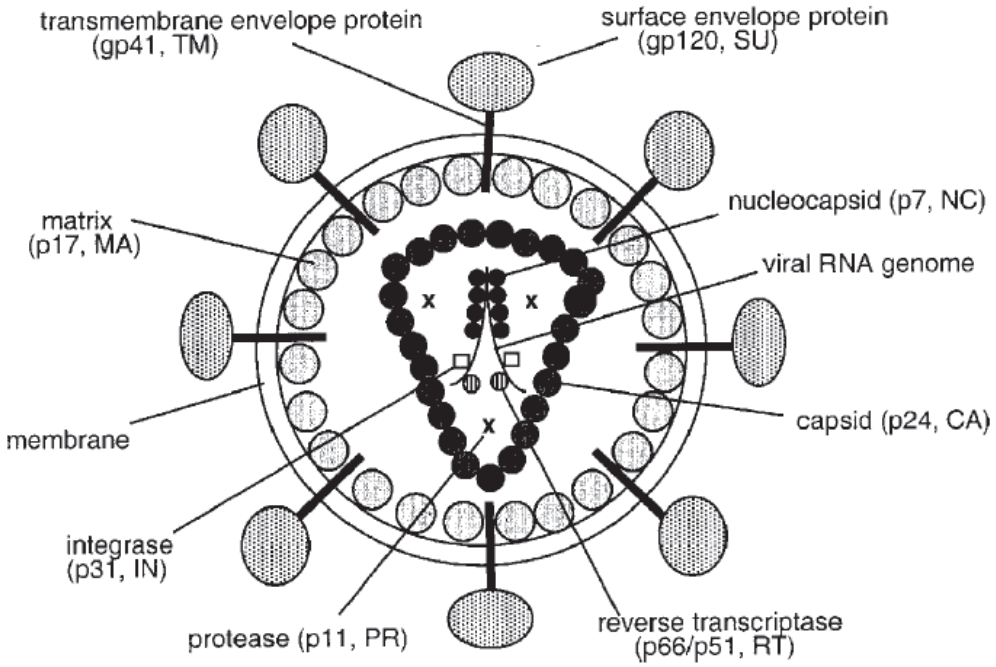

Figure 2. Diagram of a typical HIV particle structure (Freed, 2003).

nucleocapsid (NC or p7), p6, and two spacer peptides p1 and p2 (Figure 3.) (Freed, 2003). These structural proteins induce the transformation of a virion with MA remaining associated with the inner surface of the viral membrane and CA forming a shell around the two single-stranded RNAs that have been shrouded by NC (Freed, 1998). The *pol* gene encodes three functional enzymes that are essential in the virus life cycle and pre-existing in the mature virions. They are protease (PR), reverse transcriptase (RT), and integrase (IN) (Freed, 2003). The *env* gene only encodes the viral protein Env which is required for binding and entry into the host cell (Arrildt *et al*, 2012). The Env precursor, named as gp160, is cleaved by a cellular protease into surface glycoprotein gp120 (SU) and transmembrane glycoprotein gp41 (TM) during trafficking from the nucleus to the cell surface where budding of the viral particle takes place (Freed, 2003).

The regulatory proteins Tat and Rev are both RNA binding proteins. The major function of *tat* (transactivator of transcription) is to enhance HIV-1 gene expression such as chromatin remodeling, phosphorylation of RNA polymerase II, transactivation of viral genes, and binding to a specific structure of HIV-1 mRNAs (Romani et al, 2010; Freed, 2001). Rev (regulator of expression of viral protein) protein is responsible for viral RNA export (Freed, 2003). Since there's a need for unspliced RNAs to be served as mRNA for Gag and GagPol polyprotein precursors and as genomic RNAs for progeny virions, and a need for partially spliced mRNA encoding Env, Vif, Vpu, and Vpr proteins in the

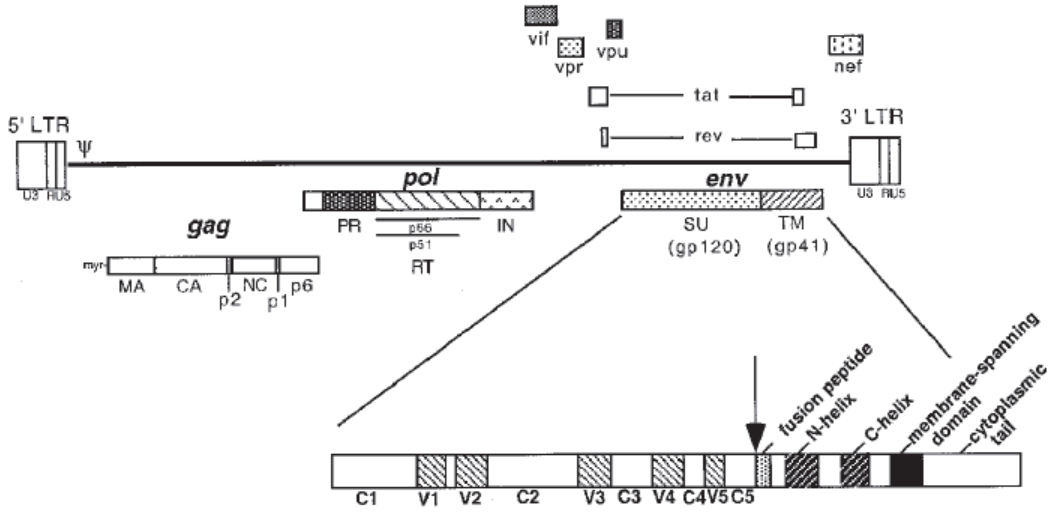

Figure 3. Organization of HIV genome (Freed, 2003).

cytoplasm, Rev is required for the transportation of these large-sized RNAs (Freed, 2003). Rev accomplished it by binding to the Rev responsive element (known as RRE) which is present in all unspliced and partially spliced HIV-1 RNAs (Freed, 2003). The Rev-RRE complex is then able to interact with cellular nuclear export machinery to transport the unspliced or partially spliced form of RNA from nucleus to the cytosol (Freed, 2003).

The four accessory or auxiliary proteins Vpu, Vpr, Vif, and Nef are not essential for viral replication. However, they do contribute to the efficiency of virus spread and disease induction in vivo (Freed, 2003). Vpu (viral protein u) is capable of down-regulating of CD4 expression and enhancing viral particle release (Costin, 2007). Vpr (viral protein r) has three functions: 1) weakly stimulates gene expression from HIV LTR; 2) arrests the cell cycle in the G2 phase; 3) facilitates the translocation of HIV-1 preintegration complex (PIC) to the nucleus (Costin, 2007; Freed, 2001). Vif (viral infectivity factor) is reported to be essential for viral replication in certain cell lines and in some "non-permissive" cell types such as PBMCs, macrophages, and primary lymphocytes (Costin, 2007; Freed, 2003). Nef stands for negative factor. It functions in downregulation of surface CD4 and major histocompatibility class I (MHC I) molecules in host cells (Freed, 2001). In addition of stimulating HIV virion infectivity, Nef is also reported to interact with K^+ channels (Costin, 2007).

c. Replication Cycle

HIV entry initiates with the binding of gp120 and its primary host cell receptor CD4 which can be found on the surface of CD4+ T cells, monocytes, dendritic cells, and brain microglia (Younai, 2013). After binding to CD4 receptor, CCR5 or CXCR4 coreceptors are required by the virus for further anchorage and fusion process (Younai, 2013). Following fusion with the host cell, the viral particle is uncoated and the two copies of single-stranded viral RNA are reverse transcribed into double stranded DNA for integration by the pre-existing viral reverse transcriptase (Freed, 2003) (Figure 4.). Once the linear viral DNA has formed, it will be translocated into cell nucleus and integrated into host genome. After integration, a variety of genetic materials, proteins, and enzymes necessary to the formation of a new viral particle could be produced by host cell replication machinery (Younai, 2013). Virion assembles in the cytoplasm and then buds off from the plasma membrane. Shortly after budding, the viral protease cleaves the Gag and GagPol polyproteins to generate mature infectious virus (Freed, 2001; Marsden & Zack, 2013).

C. Envelope Glycoprotein gp120

The entry of HIV-1 into a target cell requires surface Env glycoprotein gp120 and CD4 receptor as well as coreceptors CCR5/CXCR4 on macrophages and T-lymphocytes, respectively. The initiation step involves binding of CD4 to gp120 glycoprotein which induces conformational changes in gp120. The conformational change in gp120 leads to the exposure and/or formation of antigenic epitopes recognized

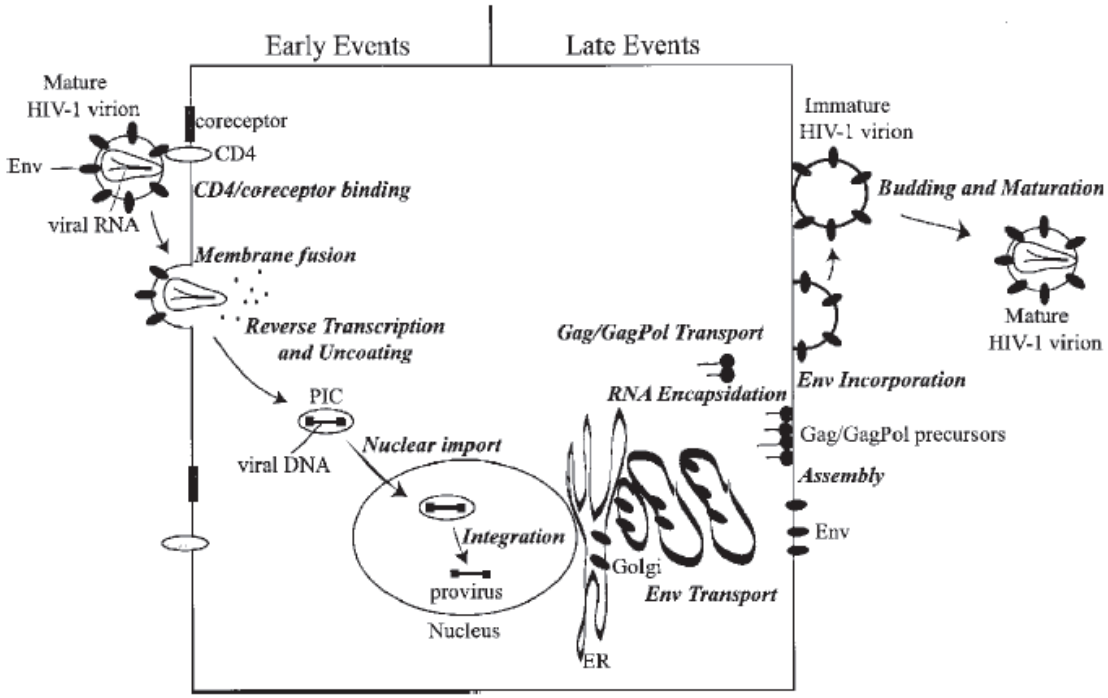

Figure 4. HIV replication cycle (Freed, 2003).

by the coreceptors. After binding to the coreceptors the transmembrane glycoprotein gp41 undergoes structural rearrangements that mediate the fusion process to facilitate viral entry into the host cell (Hsu and Bonvin, 2004).

The functional env complex is a trimer that contains three monomeric gp120 surface glycoproteins attached to each other via noncovalent bond (Hartley *et al*, 2005). The monomeric gp120 is organized into five conserved regions (C1-C5) and five highly variable domains (V1-V5) (Freed, 2001). The conserved regions which are interspersed with V1-V5 contain many important gp120 elements for receptor binding and fold into a core. The first four variable regions (V1-V4) are incorporated into large, surface-exposed loops by intramolecular disulfide bonds in gp120 (Xiang et al, 2002).

The first crystallized structure of a monomeric gp120 core was revealed by Kwong et al in 1998. According to this study, the five conserved regions (C1—C5) and five variable loops (V1—V5) of gp120 are organized into the inner domain and the outer domain with a connecting region known as the bridging sheet (Figure 5.) (Kwong *et al*, 1998). Sequence comparison of a number of HIV-1 isolates revealed that the gp120 is highly variable between isolates (Freed and Martin, 1995).

Many experiments have been performed by investigators in order to figure out the features of each region. One study showed that a proteolytic fragment of gp120 with most of its C3, C4, and C5 conserved regions retains the ability to bind CD4 (Chirmule and Pahwa, 1996). The

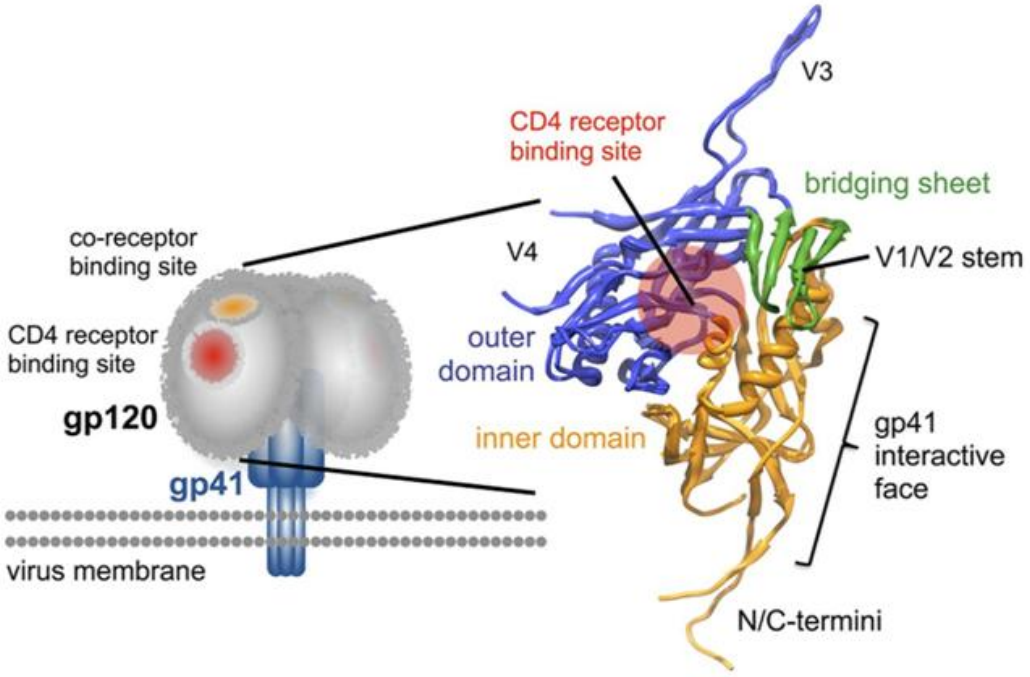

Figure 5. HIV-1 envelope glycoprotein gp120 structure (Miklos Guttman *et al*, 2012).

fact that C1 and C5 regions are accessible to antibody on monomeric gp120 but not on gp120-gp41 complex revealed that these two regions could be the main contact interface with gp41 (Pantophlet and Buron, 2006). It was proposed that major segments of C2, C3, and C4 regions form a buried, relatively hydrophobic core in gp120 (Pantophlet and Buron, 2006).

In contrast to the conserved regions, the variable regions in gp120 are well exposed on the surface (Pantophlet and Buron, 2006). The function of V4 and V5, located on the proximal end of the outer domain, are not clear so far, but V4 is suggested to be involved in gp160 folding (Thali *et al*. 1993; Pantophlet and Buron, 2006). V1/V2 loops which are located at the distal end of the inner domain function in blocking the conserved regions from antibody neutralization and provide some additional protection for the variable loops beside the core (Wyatt *et al*. 1993; Cao et al. 1997). Removal of the V1/V2 variable loops enables the envelope protein to bind CXCR4 without the involvement of CD4 binding (Basmaciogullari *et al*, 2002).

D. The V3 Loop and Tropism

Two major targets of HIV-1 are macrophages and CD4 T lymphocytes. Both express the CD4 receptor, and have two different seven transmembrane chemokine co-receptors; macrophages have CCR5 and T cells contain CXCR4 receptors. The engagements of the virus with these receptors and consequent signal transduction are critical for viral infection, permitting viral entry and facilitating post-entry events. Viruses using the CCR5, CXCR4, or both are termed R5, X4, and R5X4, respectively

(Hoffman et al, 2002). People get infected by being exposed to HIV infected body fluids. The patients' immune system will be destroyed over time as T cells will be depleted by viral infection. Clinical data showed that in the early stage of HIV-1 infection, the predominant virus type is R5. And at later stage of disease progression, the viruses in 50% of the patients will mutate and become X4. Patients with X4 virus infection are usually associated with an accelerated loss of CD4 T cells and an increased likelihood of progressing to AIDS (Connor et al, 1994; Koot et al, 1993; Richman et al, 1994). However, 50% of the patients who are infected with HIV-1 clade B develop to AIDS without detectable X4 HIV-1 quasispecies (Scoggins, 2000). Though most studies have shown that R5 replicate slower in tissue cultures and stimulated PBMCs than R5X4 or X4 isolates, many AIDS patients die with exclusively R5 (Scoggins, 2000). Data have shown that some R5 isolates replicate more quickly at the late stage of disease, especially after an AIDS diagnose is made (Scoggins, 2000).

One of the differences between R5 and X4 viruses is the usage of co-receptor. After binding to CD4, the surface protein gp160 of HIV will undergo a conformational change, revealing the co-receptor binding site, most notably the third hypervariable loop region V3 (Sander et al, 2007).

The V3 loop is found on the distal end of the outer domain (Kwong *et al*, 1998). This disulfide-bonded loop has 35 amino acids and is the major determinant of co-receptor usage (Figure 6.) (Sander *et al*, 2007). The structure of the loop is roughly divided into three entities: the crown of the loop, the N-terminal stem and the C-terminal

stem that flank the crown (Cormier and Dragic, 2002). The crest, or the tip of the loop, has a conserved amino acid motif, Gly-Pro-Gly, that is found in all HIV-1 strains and is important in binding to CCR5 (Cormier and Dragic, 2002). The Cormier group showed that the C-terminal segment is conserved as well by sequence comparison of V3 loop from different HIV-1 isolates, whereas the variability occurs in the region flanking the crest (Cormier and Dragic, 2002).

V3 is not involved in CD4 binding, but it is important to define the tropism of a CD4-bound env complex. Substitutions of the V3 region of an X4 virus with an R5 strain converted the virus to become macrophage-tropic (Hartley *et al*, 2005). It is believed that the switch of tropism from R5 to X4 is associated with an increase in the net positive charge of V3 (Hartley *et al*, 2005). They have proposed a simple model of coreceptor switching that the substitutions of V3 sequence directly destroy a coreceptor binding site and create a new one within V3 itself. However, a previous study has shown that the removal of the glycan on 301N site on V3 could also change an R5 virus into an X4, indicating the model mentioned before is oversimplistic (Hartley *et al*, 2005). But it is possible that the removal of glycan increases the net positive charge of V3 by revealing the previously masked positively charged amino acid residues or loss of a negatively charged carbohydrate moiety (Hartley *et al*, 2005). The 11/25 rule is more widely accepted which suggest that the charge change of the residues at positions 11 and 25 on V3 is used to predict viral tropism: a positively charged amino acid at the position 11, 24, or 25 defines X4; otherwise R5 (Cardozo *et al*, 2007). According to previous structural and mutagenic analyses, bridging sheet is also required in concert with the V3 loop for

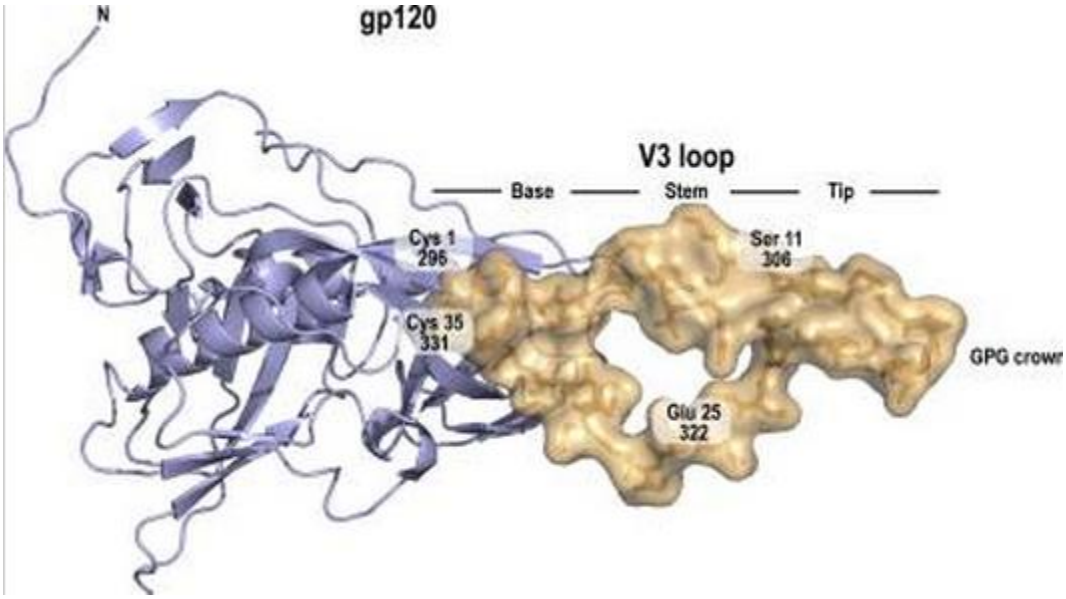

Figure 6. Crystal structure with the V3 loop (Sander *et al*, 2007).

coreceptor binding in the CD4-bound gp120 complex (Hsu and Bonvin, 2004).

E. Gp120 and Signal Transduction

The cytoskeleton is known to support cell shape, facilitating in cell motility and trafficking within the cytosol. The actin cytoskeleton is a dynamic structure and has been reported to be important in cell motility and migration (Spear *et al*, 2012).

Because the binding of gp120 and coreceptor causes signal transduction in the host cell, we use cofilin as an indicator to detect signaling. Cofilin is a severing protein that functions in regulating actin polymerization rate. It exists in two forms: an active dephosphorylated form and an inactive phosphorylated form. In unstimulated, resting T cells, it is mainly in its inactive form and is activated by dephosphorylation of serine 3 by phosphatases (Moriyama et al., 1996; Agnew et al., 1995). Cofilin activity is negatively regulated by LIM kinases 1 and 2 (Arber et al., 1998; Yang et al., 1998). Only the dephosphorylated form of cofilin interacts with the actin cytoskeleton and is capable of translocating into the nucleus. Cofilin is involved in two main activities of human T lymphocytes: chemotaxis and T cell activation (Samstag et al., 2003). Furthermore, cofilin has been proposed to be an important early signaling molecule utilized by HIV-1 viruses when establishing the latent infection in resting human CD4 T cells (Yoder et al., 2008). It has been demonstrated that the binding of viral gp120 envelope glycoprotein with the CXCR4 co-receptor activates cofilin and helps the virus to overcome the cortical actin restriction in resting T cells (Figure 7.) (Yoder *et al*., 2008). Dephosphorylation of cofilin accompanies human T cell activation by co-stimulatory signals (Samstag *et al*,

1994; Nebl *et al*, 1996). Studies have shown that HIV needs a dynamic cytoskeleton to accomplish viral entry, postentry DNA synthesis, and nuclear migration in resting T cells (Spear *et al*, 2012). Our lab has demonstrated that when HIV gp120 binds to its primary receptor CD4 and coreceptor CXCR4, it triggers the Rac-PAK-LIMK-cofilin pathway in CD4 T cell, resulting in an early actin polymerization (Yoder *et al*., 2008). The activation of cortical actin leads to a transient blockage of CXCR4 internalization. Following fusion, the viral preintegration complex (PIC) is believed to anchor onto the cortical actin for reverse transcription. The intracellular migration of PIC is promoted by cofilin-mediated treadmilling in the cell (Spear *et al*, 2012).

F. Study Aims and Experimental Design

The suggested mutation sites are provided by Dr. Vaisman and Dr. Masso. They retrieved the YU2 (R5) V3 loop sequence from patients with AIDS diagnosis whose data are in LANL HIV Sequence Database, and compared it with YU2 sequence. The most frequent mutation sites were chosen for mutagenesis. We started with single-site mutation first.

At the beginning, we cloned the YU2 (provided by Dongyang Yu) Env fragment into a smaller plasmid called pUC19 as the original plasmid is too large for PCR. Restriction enzymes EcoR1 and Sal I were used for digestion of YU2 and pUC19 plasmids. After ligation, transformation and screening, positive clones were selected and sent out for sequencing. Once the sequence was confirmed, this pUC19-YU2 served as template for PCR during Mutagenesis.

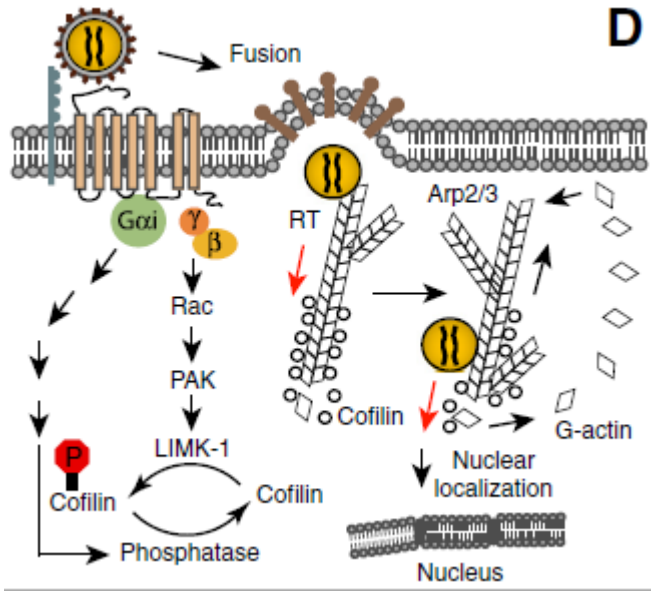

Figure 7. Model of actin dynamics in HIV-1 infection of T cells (Spear *et al*, 2012).

In order to generate mutants, we followed the mutagenesis kit instructions to design primers that contain mutation sites in the middle. After PCR, the PCR products with mutation underwent digestion and transformation. The purpose of digesting the PCR products with Dpn I was to remove the parental pUC19-YU2 template. The mixture was then delivered into the high efficiency XL10-Gold Ultracompetent cells. These cells can repair the nicks in the mutated plasmids. After transformation, clones were sent out for sequencing. The confirmed positive mutants were then cloned into pNL-Δψ-Env(gp160) for viral particle assembly later.

pNL-Δψ-YU2-Env along with the helper plasmid NL4-3 (encodes all HIV structural genes except the Env glycoprotein) were assembled into viral particles by co-transfecting into 293T cells. Viruses were harvested at 48 hours post transfection and filter through a 0.45μM filter.

To measure the infectivity and signaling pathway effects, a reporter monoclonal cell line was made. Two helper plasmids along with pNL-GFP-puro-RRE-SA were used to assemble the viral particles. pCMVΔ8.2 plasmid encodes all HIV structural genes except the Env glycoprotein, and its mRNA is also missing the packaging signal Ψ. pHCMV-G provides the envelope and allows pantropic endocytic fusion. The plasmid pNL-GFP-puro-RRE-SA contains green fluorescent protein. The lentiviral particles were introduced into an R5 cell line named A3R5.7 cells. Then the bulk population of the transfected cells was diluted and grown in a 96-well plate for monoclonal cell line selection under the selection pressure of puromycin.

In order to test the infectivity of the YU2 Env mutant viruses, we measured the GFP positive percentage after cells were challenged with viruses. Two indicator cell lines were used in this assay: CD4+CXCR4+ indicator cell line (Clone X), CD4+CCR5+ indicator cell line (A3R5.7-GFP).

We speculated that the mutations in YU2 (R5) V3 loop may trigger the signal transduction through CXCR4 in CD4 T cells without giving rise to the X4 tropism. Primary cells were used and the activation of major regulator cofilin which is involved in actin rearrangment was evaluated by intracellular staining.

II. MATERIALS AND METHODS

A. YU2 env Template Production

Double digestion of laboratory strain pNL-Δψ-YU2-Env plasmid genome and pUC19 (obtained from GeneArt® Site-Directed Mutagenesis Kit, Invitrogen, Carlsbad, California) was carried out with EcoRI and Sal I (New England Biolabs, Ipswich, MA) according to manufacturer guidelines. A total of 2 μg of each plasmid was digested. Following digestion, pUC19 was dephosphorylated with 1 unit of calf intestinal alkaline phosphatase (CIP) (New England Biolabs, Ipswich, MA) and NEBuffer 3. The dephosphorylation reaction took place at 37 ℃ for 20 minutes. The CIAP was then heat-inactivated by incubating the reaction mixture at 80 ℃ for 20 minutes. Dephoshporylated pUC19 was then cooled to room temperature for 20 minutes.

The entire digestion reaction for both plasmids was run on a 1% agarose gel. The 2.7 kb and 2.6 kb fragments that resulted from the digestion of pNL-Δψ-YU2-Env and de-phosphorylated pUC19, respectively, were excised from the gel and purified with the QIAquick Gel Extraction Kit® (Qiagen, Valencia, CA) as instructed by the manufacturer protocol. The purified DNA was eluted with distilled water and a small amount of the purified pNL-Δψ-YU2-Env and pUC19 fragments were run on a 1% agarose gel to view and confirm the presence and quality of a 2.7 kb band for pNL-Δψ-YU2-Env and a 2.6 kb band for pUC19.

The purified 2.7 kb fragment generated from double digestion of pNL-Δψ-YU2-Env was ligated to the dephosphorylated 2.6 kb fragment generated from pUC19. For the ligation, the pNL-Δψ-YU2-Env fragment was combined with the dephosphorylated pUC19 fragment at a 3:1 amount ratio, along with T4 DNA Ligase Buffer, and 1 unit of T4 DNA Ligase (New England Biolabs, Ipswich, MA) in a total volume of 20 µl. The new plasmid was renamed as pUC19-YU2.

pUC19-YU2 was transformed into OneShot DH5α competent cells (Invitrogen, Carlsbad, CA). A vial of OneShot cells was thawed on ice, and then 50 µl of cells was transferred to a pre-chilled 14 ml round-bottom polypropylene Falcon tube (BD Biosciences, Rockville, MD) and combined with 5 µl of the pUC19-YU2 ligase. Cells were heat-shocked at 42 ℃ for 30 seconds in a water bath. Cells were incubated with 1 ml of room-temperature SOC media in a shaker (225 rpm) for one hour at 37 ℃. The cells were spread on 1% LB-agar plates with ampicillin (100 µg/µl) in various volumes. Plates were incubated overnight at 37 ℃.

The following day, several colonies were individually cultured in 5 ml of liquid LB media with 5 µl of ampicillin (100 µg/µl) in preparation for a small-scale plasmid purification with the QIAprep Spin Miniprep Kit (Qiagen, Valencia, CA). The cultures were incubated in a shaker (225 rpm) overnight at 37 ℃. Plasmid purification was carried according to the provided protocol. The plasmids were digested with Bgl I, EcoRI and Sal I (New England Biolabs, Ipswich, MA), NEBuffer 3, 10X BSA for 2 hours and run on a 1% agarose gel to view the release of the 2.7 kb fragment. For storage of the successful clones, 850 µl of the remaining bacterial culture for each successful

colony was mixed with 150 µl of sterile glycerin (Fisher Scientific, Hampton, NH) and stored at -80 ℃.

YU2 *env* was prepared for sequence analysis by Genewiz, Inc. (Germantown, MD). 2,000 ng of DNA template was sent out and the primer was made by the company. Sequencing primers are listed in Table 1. The sequence of YU2 *env* was analyzed by Pustell matrix alignment on MacVector®.

B. pUC19-YU2 Mutants Production

pUC19-YU2 was amplified by PCR using the PTC-200 Peltier Thermal Cycler (MJ Research, Hercules, CA). The primers specific for the 5' and 3' ends of pUC19-YU2 mutants were designed. Primer design took into account the specifications of the QuickChange® Site-directed Mutagenesis Kit protocol (Stratagene, La Jolla, California). Primers for mutagenesis were between 25-45 bases in length with the desired mutation occurring in the middle of the primer. Upon receipt, primers were diluted with sterile RNAase-free water to obtain a final concentration of 10 µM and stored at -20 ℃ until the time of use. Primers used for the amplification of pUC19-YU2 mutants are listed in Table 3. The reaction consisted of 1 µl of pUC19-YU2 (25ng/ µl) template, 5 µl of 10x Reaction buffer, 1 µl of 2mM dNTP mix, 1 µl of forward primer (10 µM), 1 µl of reverse primer (10 µM), 2.5 U of *PfuTurbo* DNA polymerase (2.5 U/ µl), and PCR water in a total reaction volume of 50 µl.

A PCR temperature gradient was prepared to determine the most efficient annealing temperature for the primers. The PCR cycles were as follows: step 1) 95 ℃ for 30 seconds; step 2) 95 ℃ for 30 seconds; step 3) annealing temperature (55-73 ℃)

for 1 minute; step 4) 68 ℃ for 6 minutes; 16 cycles of steps 2 to 4. The following temperatures were tested for step 3: 55, 56.4, 60, 65.7, 70.2, and 72.6 ℃. A quantitative 1% agarose gel was run to determine which annealing temperature most efficiently amplified *env*. The gel was stained with ethidium bromide and imaged with the Alpha Innotech Imager (Alpha Innotech, San Leandro, CA).

Dpn I restriction enzyme (New England Biolabs, Ipswich, Massachusetts) was directly added to each amplification reaction to digest the methylated, nonmutated parental DNA template after PCR cycles were completed. The digestion took place at 37 ℃ for 2 hours. The reaction was then chilled on ice prior to being transformed into chemically competent cells.

For the transformation, 4 μl of the β-mercaptoethanol (β-ME) mix provided with the kit was added into a prechilled 14 ml round-bottom polypropylene Falcon tube (BD Biosciences, Rockville, MD) along with 100 μl of XL10-Gold ® ultracompetent cells (Stratagene, La Jolla, California), following manufacturer guidelines. The cells were incubated on ice for 10 minutes and gently swirled every 2 minutes. 10 μl of the Dpn I-treated DNA was added to each aliquot of cells afterwards. Cells were then subjected to a 42 ℃ heat bath for 30 seconds and then transferred to ice for 2 minute. After heat-pulsing, 900 μl of SOC media (2% tryptone, 0.5% yeast extract, 10 mM NaCl, 2.5 mM KCl, 10mM $MgCl_2$, 10 mM $MgSO_4$, 20 mM glucose) (Invitrogen, Carlsbad, California) was added into the reaction mixture and the cells were incubated in the Lab Line shaking incubator (Analytical Instruments, LLC, Golden Valley, MN) (225 rpm) at 37 ℃ for 1 hour. Cells were then spread with sterile glass beads on 1.5% agar plates of Luria-

Bertani medium (1% tryptone, 0.5% yeast extract, 0.5% NaCl, pH 7.2-7.4; LB) containing ampicillin (final concentration of 100 µl/ml) in volumes ranging from 10 – 300 µl, and incubated overnight at 37 °C.

A total of ten mutants were screened for the presence of YU2 *env*. Each mutant was individually cultured in 5 ml of liquid LB media with 5 µl ampicillin (100 µg/µl) and incubated overnight in a shaker (250 rpm) at 37 ℃. The cultures were centrifuged at 13,000 rpm for 1 minute and underwent plasmid purification using the QIAprep Spin Miniprep Kit® (Qiagen, Valencia, California). The purification process was carried out according to the manufacturer protocol. DNA was eluted with distilled water, and the DNA was diluted ten times with sterile RNAase-free water (total volume 50 µl) in preparation for an optical density reading with the Eppendorf BioPhotometer (Eppendorf, Westbury, New York). All ten mutants DNA were sent to Genewiz, Inc. for sequencing.

Six confirmed samples were then triple digested to verify that YU2 *env* was properly cloned. Approximately 500 ng of DNA was combined with 1µl each of Bgl I, EcoR I and Sal I, 2 µl of NEBuffer 3, 1 µl of 10x BSA (New England Biolabs, Ipswich, Massachusetts) and enough sterile water to bring volume to 20 µl. Digestion took place at 37 ℃ for 2 hours. The digestion products were run on a 1% agarose gel to confirm the presence of digested DNA. Successful cloning produced four DNA fragments of 2.7kb, 1.3kb, 1.1kb, and 200 bp in length. Plasmid containing the cloned YU2 *env* gene was sent out for sequencing (Genewiz Inc., Germantown, MD) to confirm whether there had desired mutations. 2,000 ng of each mutant DNA template was sent out and the primer was made by the company. Sequencing primers are listed in Table 2. The sequences of

YU2 *env* mutations were analyzed against the wild-type nucleotide sequence of HIV-1 YU2 env by Pustell matrix alignment on MacVector®. Each of the successful mutant clones was renamed pUC19-YU2 with its mutation site after "YU2" and a number after mutation site to denote the colony number from which the plasmid originated; i.e. pUC19-YU2-(N-H)-1, pUC19-YU2-(S-G)-2, etc. For storage of the successful clones, 850 µl of the remaining bacterial culture for each successful colony was mixed with 150 µl of sterile glycerin (Fisher Scientific, Hampton, NH) and stored at -80 ℃.

C. Generating pNL-Δφ-YU2-Env Mutants

Double digestion of pNL-Δφ-YU2-Env was carried out with with EcoRI and Sal I (New England Biolabs, Ipswich, MA) according to manufacturer guidelines. Triple digestion of pUC19-YU2(N-H), pUC19-YU2(S-G), pUC19-YU2(N-P), pUC19-YU2(N-T), pUC19-YU2(L-F), and pUC19-YU2(E-Q) were carried out with with Bgl I, EcoRI and Sal I (New England Biolabs, Ipswich, MA) according to manufacturer guidelines. A total of 2 µg of each plasmid was digested. Following digestion, pNL-Δφ-YU2-Env was dephosphorylated with 1 unit of calf intestinal alkaline phosphatase (CIAP) (New England Biolabs, Ipswich, MA) and NEBuffer 3. The dephosphorylation reaction took place at 37 ℃ for 20 minutes. The CIAP was then heat-inactivated by incubating the reaction mixture at 80 ℃ for 20 minutes. Dephoshporylated pNL-Δφ-YU2-Env was then cooled to room temperature for 20 minutes.

The entire digestion reaction for both plasmids was run on a 1% agarose gel. The 2.7 kb and 7.0 kb fragments that resulted from the digestion of pUC19-YU2(N-H), pUC19-YU2(S-G), pUC19-YU2(N-P), pUC19-YU2(N-T), pUC19-YU2(L-F), pUC19-YU2(E-Q) and de-phosphorylated pNL-Δφ-YU2-Env, respectively, were excised from the gel and

purified with the QIAquick Gel Extraction Kit® (Qiagen, Valencia, CA) as instructed by the manufacturer protocol. The purified DNA was eluted with distilled water and a small amount of the purified pUC19-YU2(N-H), pUC19-YU2(S-G), pUC19-YU2(N-P), pUC19-YU2(N-T), pUC19-YU2(L-F), pUC19-YU2(E-Q) and de-phosphorylated pNL-Δφ-YU2-Env fragments were run on a 1% agarose gel to view and confirm the presence and quality of a 2.7 kb band for mutants and a 7.0 kb band for pNL-Δφ-YU2-Env.

The purified 2.7 kb fragment generated from triple digestion of pUC19-YU2 mutants was ligated to the dephosphorylated 7.0 kb fragment generated from pNL-Δφ-YU2-Env. For the ligation, the pUC19-YU2 mutant fragment was combined with the dephosphorylated pNL-Δφ-YU2-Env fragment at a 3:1 amount ratio, along with T4 DNA Ligase Buffer, and 1 unit of T4 DNA Ligase (New England Biolabs, Ipswich, MA) in a total volume of 20 μl. The new clone was renamed pNL-Δφ-YU2-Env(x) whereas "x" referred to the mutation site, e.g. pNL-Δφ-YU2-Env(N-H).

pNL-Δφ-YU2-Env(N-H), pNL-Δφ-YU2-Env(S-G), pNL-Δφ-YU2-Env(N-P), pNL-Δφ-YU2-Env(N-T), pNL-Δφ-YU2-Env(L-F), and pNL-Δφ-YU2-Env(E-Q) was each transformed into OneShot DH5α competent cells (Invitrogen, Carlsbad, CA). A vile of OneShot cells was thawed on ice, and then 50 μl of cells was transferred to a pre-chilled 14 ml round-bottom polypropylene Falcon tube (BD Biosciences, Rockville, MD) and combined with 5 μl of the pNL-Δφ-YU2-Env mutants ligase. Cells were heat-shocked at 42 ℃ for 30 seconds in a water bath. Cells were incubated with 1 ml of room-temperature SOC media in a shaker (225 rpm) for one hour at 37 ℃. The cells

were spread on 1% LB-agar plates with ampicillin (100 μg/μl) in various volumes. Plates were incubated overnight at 37 ℃.

The following day, several colonies were individually cultured in 5 ml of liquid LB media with 5 μl of ampicillin (100 μg/μl) in preparation for a small-scale plasmid purification with the QIAprep Spin Miniprep Kit (Qiagen, Valencia, CA). The cultures were incubated in a shaker (225 rpm) overnight at 37 ℃. Plasmid purification was carried according to the provided protocol. The plasmids were digested with Bgl I, EcoRI and Sal I (New England Biolabs, Ipswich, MA), NEBuffer 3, 10X BSA for 2 hours and run on a 1% agarose gel to view the release of the 2.7 kb fragment. For storage of the successful clones, 850 μl of the remaining bacterial culture for each successful colony was mixed with 150 μl of sterile glycerin (Fisher Scientific, Hampton, NH) and stored at -80 ℃.

D. HIV-1 Wild type Particles and Mutant Viral Particles Production

HIV-1 viruses were generated using the 293T cell line derived from human embryonic kidney epithelial cells. HIV-1 YU2 control viruses were produced by transfecting the 293T cell line with pNL-Δφ-YU2-Env and NL4-3 (KFS)Δgp160. HIV-1 envelope control viruses were produced by transfecting the 293T cell line with NL4-3 (KFS)Δgp160 alone. HIV-1 YU2 mutant viruses were produced by transfecting the 293T cell line with pNL-Δφ-YU2-Env(mutant) and NL4-3 (KFS)Δgp160. For each virus, 3 x 10^6 cells were seeded in 10 cm cell culture Petri dishes (BD Biosciences, Rockville, MD) and cultured overnight at 37 ℃ in 10 ml of Gibco® Dulbecco's Modified Eagle Medium (DMEM) with 10% fetal calf serum (Invitrogen, Carlsbad, CA) and grown to 80%

confluence. The following day, 10 μg of NL4-3 (KFS)Δgp160 and 10 μg of pNL-Δφ-YU2-Env or pNL-Δφ-YU2-Env(mutant), or 20 μg of NL4-3 (KFS)Δgp160 were combined with 1.5 ml of serum-free DMEM in a 5-ml round-bottom polystyrene Falcon tube. In a separate Falcon tube, 60 μl of Lipofectamine (Invitrogen, Carlsbad, CA) was added to 1.5 ml of serum-free DMEM, and both the Lipofectamine mixture and the DNA mixture were incubated at room temperature for 5 minutes. The DNA-containing medium was added to the Lipofectamine -containing medium to bring the total volume of the transfectant mixture to 3 ml. The mixture was incubated at room temperature for 20 minutes. The medium from the Petri dishes was discarded and 5 ml of pre-warmed fresh serum-free DMEM was added to each dish. The Lipofectamine-DNA mixture was gently administered to the Petri dish, which was then gently swirled to mix and then incubated for 6 hours at 37 ℃. 6 hours later, the serum-free DMEM in the Petri dishes was discarded and 10 ml of pre-warmed DMEM with 10% FBS was gently added to each dish.

Viral particles were harvested 48 hours after transfection. The medium from the Petri dish was collected and centrifuged for 5 minutes in 14 ml round-bottom Falcon tube at approximately 1200 rpm. The supernatant was filtered through a 10 cc syringe (Becton, Dickinson and Company, Franklin Lakes, NJ) fitted with a 0.45 μm filter cartridge (Millipore, Billerica, MA), and 500 μl aliquots of the viral filtrate were stored at -80 ℃.

E. Surface Staining of A3R5.7 Cell Line

A3R5.7 cells (Obtained from NIH AIDS Reagent Program) are derived from the human T-lymphoblastoid cell line A3.01. These cells naturally express CD4, CXCR4 and

α4β7 and were engineered to constitutively express CCR5 under G418 (geneticin sulfate) selection. Surface staining of CD4, CXCR4, and CCR5 was done to verify the existence of these receptors. Six 5 ml round bottom tubes were labeled as #1-#6 and each contained 5 x 10^5 of A3R5.7 cells in 200 µl 10% RPMI. 3.5 ml of PBS plus 0.1% BSA was added to each tube and the cells were pelleted at 4 ℃ and 400 rpm for five minutes. Supernatant was decanted. Cells were resuspended in less than 100 µl residual medium. 1 µl (5.5 mg/ml) of Mouse IgG (Jackson ImmunoResearcH) was added to tubes #1, 2, 4, and 5 and 1 µl (5.5 mg/ml) of Rat IgG (Jackson ImmunoResearcH) was added to tubes #3 and 6 to block non-specific association with Fc receptors. To each tube, appropriate amount of the respective, indicated antibodies were added and incubated on ice, and in the dark, for 30 minutes. 5 µl FITC-Labeled IgG1k Mouse Isotype (BD Pharmingen) for CD4 was added to tube #1. 20 µl PE/Cy5-Labeled Mouse IgG2ak Isotype for CXCR4 (BD Pharmingen) was added to tube #2. 20 µl PE-Rat IgG2ak Isotype for CCR5 (BD Pharmingen) was added to tube #3. 20 µl FITC-anti-human CD4 (BD Pharmingen) was added to tube #4. 20 µl PE/Cy5-anti-human CXCR4 (Biolegend) was added to tube #5. 20 µl PE-anti-human CCR5 (BD Pharmingen) was added to tube #6. After the 30-minute incubation, cells were washed with 2 ml cold PBS + 0.1% BSA and pelleted at 4° C and 1200 rpm for five minutes. The supernatant was discarded. 200 µl PBS plus 0.1% BSA and 200 µl of 2% paraformaldehyde were added to each tube to resuspend the cells for flow cytometric analysis on a FACSCalibur (BD Biosciences). Isotype staining was ensured under 10^1 in each respective fluorescence channel and the relative expression of CD4, CXCR4, and CCR5 was then determined.

F. Construction of Monoclonal Cell Line with CCR5 Co-receptor and GFP

pNL-GFP-RRE-SA(Puro) (bacterial stock obtained from Taylor's Clone I, plasmid was extracted using QIAprep Spin Miniprep Kit) lentiviral particles were generated using the 293T cell line derived from human embryonic kidney epithelial cells. pNL-GFP-RRE-SA(Puro) lentiviral particles were produced by transfecting the 293T cell line with pNL-GFP-RRE-SA(Puro), pCMVΔ8.2 and pHCMVG. 3 x 10^6 of 293T cells were seeded in 10 cm cell culture Petri dishes (BD Biosciences, Rockville, MD) and cultured overnight at 37 °C in 10 ml of Gibco® Dulbecco's Modified Eagle Medium (DMEM) with 10% fetal calf serum (Invitrogen, Carlsbad, CA) and grown to 80% confluence. The following day, 12 μg of pNL-GFP-RRE-SA(Puro), 9 μg of pCMVΔ8.2 and 3 μg of pHCMVG were combined with 1.5 ml of serum-free DMEM in a 5-ml round-bottom polystyrene Falcon tube. In a separate Falcon tube, 60 μl of Lipofectamine (Invitrogen, Carlsbad, CA) was added to 1.5 ml of serum-free DMEM, and both the Lipofectamine mixture and the DNA mixture were incubated at room temperature for 5 minutes. The DNA-containing medium was added to the Lipofectamine -containing medium to bring the total volume of the transfectant mixture to 3 ml. The mixture was incubated at room temperature for 20 minutes. The medium from the Petri dishes was discarded and 5 ml of pre-warmed fresh serum-free DMEM was added to each dish. The Lipofectamine-DNA mixture was gently administered to the Petri dish, which was then gently swirled to mix and then incubated for 6 hours at 37 ℃. 6 hours later, the serum-free DMEM in the Petri dishes was discarded and 10 ml of pre-warmed DMEM with 10% FBS was gently added to each dish.

Viral particles were harvested 48 hours after transfection. The medium from the Petri dish was collected and centrifuged for 5 minutes in 14 ml round-bottom Falcon tube at approximately 1200 rpm. The supernatant was filtered through a 10 cc syringe (Becton, Dickinson and Company, Franklin Lakes, NJ) fitted with a 0.45 μm filter cartridge (Millipore, Billerica, MA). The filtered supernatant was then transferred to Vivaspin ultrafiltration spin column (Sartorius Stedim Biotech GmbH, Goettingen, Germany) which has a membrane cut-off of 100,000 molecular size and concentrated to 500 μl at 7500 rpm for 20 minutes. The viral filtrate was stored at -80 ℃.

2 x 10^5 of A3R5.7 cells were transfected with concentrated pNL-GFP-RRE-SA(Puro) lentiviral particles and were incubated at 37 ℃ for 48h in 1 mL of RPMI with 10% fetal calf serum (Invitrogen, Carlsbad, CA) and G418.

After 48 hours, 10 μl puromycin (Gibco, Cat. No. A11138-03, stock conc. = 10mg/ml, work conc. = 1ug/ml) was added to the 1 mL transfected cells and incubated at 37 ℃ for 2 days. Then the transfected cells were transferred to T25 flask under G418 and puromycin selection. During cell growth, cells were centrifuged at 1200 rpm for 5 minutes and supernant was filtered through a 10 cc syringe (Becton, Dickinson and Company, Franklin Lakes, NJ) fitted with a 0.45 μm filter cartridge (Millipore, Billerica, MA) and collected as conditional medium. After 25 ml of conditional medium was collected, the cells were diluted with 10% FBS RPMI to a final cell count of 50 cells in 25 ml fresh 10% FBS RPMI. When combined with 25 ml conditional medium, there were 50 cells in 50 ml 10% FBS RPMI with puromycin and G418. The 50 ml medium

containing 50 cells was added to a 96-well plate, each well was added 200 μl of cell culture (final concentration 0.5 cell/well).

The 96-well plate was incubated at 37 ℃ for 3-4 weeks and was screened under microscope. Wells containing cells were selected and cells in each well were transferred to 12-well plates with 2 ml 10% RPMI under G418 and puromycin selection. The selected single cell clones was renamed as pNL-GFP-RRE-SA($Puro^+$) with a number to denote the cell clone number from which the clone originated; i.e. pNL-GFP-RRE-SA($Puro^+$)-1, pNL-GFP-RRE-SA($Puro^+$)-2.

Each cell clone maintained in 10% RPMI with G418 and puromycin were aliquoted to 5 ml falcon tube, 2 x 10^5 cells/tube. 200 μl YU2 wild type viruses were added to each tube and incubated at 37 ℃ for 2 hours. After 2 hours, 3 mL of serum-free RPMI was added to each tube and centrifuged at 1200 rpm for 5 minutes. The supernatant was discarded. 1 ml of 10% RPMI with G418 and puromycin was added back to each tube. The cells were incubated at 37 ℃ for 48 hours and the percentage of GFP-expressing cells was determined for each infection by flow cytometry. The monoclonal cell line pNL-GFP-RRE-SA($Puro^+$)-8 which had the highest GFP-expressing percentage was selected and stored in 70% FBS DMSO at -80 ℃.

G. M-tropic HIV-1 Infection of Clone X Cells and pNL-GFP-RRE-SA($Puro^+$)-8 Cells

The Clone X cell line is derived from the CEM-SS suspension cell line that has been modified to express green fluorescent protein (GFP) and luciferase when the Clone

X cells are infected with HIV-1. The Clone X cells are used exclusively in the laboratory in which this study was conducted and are also commercially unavailable at this time.

Clone X cells maintained in RPMI with 10% FBS were diluted to a concentration of 2 x 10^6 cells/ml, and 200 µl of cells was aliquoted to nine 5 ml tubes labeling from #1-9. Tube #1 was left uninfected as negative control. Tube #2 was infected with single-cycle YU2 wild type viruses. Tube #3 was infected with NL4-3 (KFS)Δgp160. Six mutant viruses were added to six tubes #4-9, respectively. All viruses were calculated and used in equal p24 amount. The amount of virus used for each infection were calculated by multiplying the volume of virus used to infect Clone X cells by the p24 concentration (pg/ml) value obtained for each mutant from a p24 ELISA. Cells were spinoculated at 1200 rpm for 2 hours at room temperature. The cells were incubated for 48 hours at 37 ℃ and the percentage of GFP expression of each infection was determined by flow cytometry.

300 µl of infected Clone X cells were transferred into a 5 ml round-bottom polystyrene FACS tube (BD Biosciences, Rockville, MD) and analyzed with the Becton-Dickinson FACSCalibur flow cytometer (Becton Dickinson, Rockville, MD). Propidium iodide (Fluka) was added (2 µg/mL) before flow cytometry to exclude dead cells. After each round of flow cytometry, 300 µl fresh 10% RPMI was added back to tubes #1-9. Data were collected and analyzed every other day with the CellQuest Software.

The infection of pNL-GFP-RRE-SA($Puro^+$)-8 Cells with mutant viruses was the same as Clone X infection, except the medium used was 10% RPMI with G418 and puromycin.

H. HIV-1 p24 ELISA

HIV-1 replication was measured by p24 release. In preparation for a p24 ELISA, 10 µl of lysis buffer was added to 90 µl of each mutant virus. The virus was then serial diluted in RPMI containing 10% FBS to obtain 10x, 100x, 1000x, and 10,000x dilutions. A p24 standard was also serial diluted. 100 µl diluted p24 standard and viral preparations were individually loaded into the wells of a 96-well ELISA plate coated with anti-p24 antibody. Procedures were executed according to the manufacturer protocol of the p24 ELISA kit (Beckman Coulter).

The wells containing the diluted samples were covered with an adhesive cover and the plate was incubated for 1 hour at 37 ℃. The wells were washed three times with 1x washing buffer using the EL_X 50 Auto Strip Washer (BIOTEK Instruments, Inc., Winooski, VT). The washing buffer was discarded and 100 µl of biotinylated HIV-immunoglobulin was applied to the wells. The plate was sealed and incubated for 1 hour at 37 ℃. After the incubation with the biotin reagent, the wells were washed three times with washing buffer. 100 µl of 1:150 diluted of Streptavidin-HRP antibodies was added into each test well. The plate was sealed and incubated for 45 minutes at 37 ℃. The plate was washed three times. The washing buffer was discarded from the plate. And the plate was inverted and patted dry to remove the residual buffer. 100 µl of freshly-made peroxidase substrate was added to each ELISA well. The peroxidase substrate was made of 300 µl 4mg/ml Tetramethyl-benzidine (TMB) DMSO solution, 5 µl 30% H_2O_2, and 10 mL 0.1M Sodium Acetate solution. The plate was immediately placed into the $EL_X 800_{IU}$

Ultra Microplate Reader (BIOTEK Instruments, Inc., Winooski, VT) for a kinetic assay (625 nm).

A standard curve was generated based on the concentration values of the p24 standard. The results were used to calculate viral mutants' p24 amount.

I. Purification of Primary Human $CD4^+$ T Cells

$CD4^+$ T-cells were purified from blood obtained from healthy individuals using the Dynal® Biotech T-cell Negative Isolation Kit (Invitrogen, Carlsbad, CA). The blood was diluted at a 1:1 ratio with room temperature Gibco Dulbecco's phosphate buffered saline (PBS) (Invitrogen, Carlsbad, CA) containing 1% BSA (Fisher Scientific, Hampton, NH), and 35 ml of the diluted blood was carefully layered on top of 15 ml of room temperature CellGro FICOLL® lymphocyte separation media (Mediatech, Inc., Herndon, VA) in a 50 ml Falcon Tube (BD Biosciences, Rockville, MD). The blood-FICOLL layer was centrifuged for 20 minutes (830 rpm, without brake) at room temperature in the Sorvall RT600 Refrigerated Centrifuge (DuPont). Platelets were removed by pipetting out 20 ml of the top-most layer of the gradient, and the blood was centrifuge for another 20 minutes (1290 rpm, without brake) at room temperature. The top-most layer occurring above the interface of PBMCs was removed. The PBMC interface was collected and transferred into a clean 50 ml Falcon Tube and washed by centrifugation three times with cold PBS-0.1% BSA at a total volume of 50 ml for 5 minutes (1400 rpm, with brake) at 4 C. Prior to the third wash, 10 µl of the suspended cells were removed and added to 10 µl of Trypan Blue for a PBMC count.

The provided antibody mix was added to the PBMCs (20 µl antibody/100µl cell suspension) suspended in cold PBS-BSA at a concentration of 10^7 cells/100 µl. Fetal Bovine Serum (FBS) was also added to the cells at a concentration of (20 µl antibody/100µl cell suspension). The antibody-cell-FBS mixture was incubated on a rocker for 20 minutes at 4 C. Depletion Dynabeads for the Negative Isolation Kit (100 µl/10^7 cells) were washed twice with cold PBS-0.1% BSA in a 14 ml round-bottom polypropylene Falcon tube by applying the tube to a magnetized tube holder and allowing the beads to adhere to the side of the tube before discarding the supernatant. Beads were resuspended at a concentration of 100 µl/10^7 cells in cold PBS-0.1% BSA and kept on ice. Following incubation of PBMCs with the antibody mix and FBS, the antibodies were washed away with PBS by centrifugation for 5 minutes (1200 rpm, with brake) at 4 ℃. Cells were resuspended in PBS at a concentration of 10^7 cells/900 µl and the washed beads were incubated with the cells at room temperature for 15 minutes on a rocker.

T-lymphocytes were isolated by applying the tube of cell-bead mixture to the magnetized tube holder and allowing the beads to adhere to the side of the tube for two minutes at room temperature. The supernatant was transferred to a clean Falcon tube and applied to the magnet for two minutes two more times, for a total of three applications to the magnet. A cell count of the newly isolated $CD4^+$ and $CD8^+$ T-cells was performed by removing and applying 10 µl of the cell suspension to 10 µl of Trypan blue, prior to pelleting the cells at room temperature for 5 minutes (1200 rpm, with brake).

$CD4^+$ T-cells were further purified from solution by resuspending the cells in cold PBS-0.1% BSA at a concentration of 5 x 10^6 cells/100 µl and combining the cells with

anti-human CD8 (BD Pharmagen, San jose, CA) and anti-human CD11b (BD Pharmagen, San jose, CA) antibody (1/3 μl per 10^6 cells for both antibodies), and anti-human CD19 (BD Pharmagen, San jose, CA) antibody (1/5 μl per 10^6 cells).

In order to get a population of memory cells, CD45RA antibody (BD Pharmagen, San jose, CA) was added at a concentration of 0.1 μl per 10^6 cells. To get a total CD4 T cell population without CCR5, CD195 antibody (BD Pharmagen, San jose, CA) was added instead of CD45RA at the same concentration mentioned above.

The antibody-cell mixture was incubated at 4 ℃ for 20 minutes on a rocker. Pan mouse IgG-conjugated to magnetic beads (100 μl/10^7 cells) were washed twice as described previously and kept on ice. Unbound antibody was washed from the cells and the cell pellet was resuspended in PBS-0.1% BSA at a concentration of 10^7 cells/900 μl prior to incubation with the beads for 15 minutes. The magnet was used to separate $CD8^+$ T-cells from the supernatant, which was collected and applied to the magnet two more times as described for the PBMCs. After the third application to the magnet, cells were counted and pelleted for 5 minutes (1200 rpm, with brake) at 4 ℃. Cells were resuspended in RPMI (with 10% FBS) at a concentration of 1 x 10^6 cells/ml in a Corning tissue culture flask (Sigma-Aldrich, St. Louis, MO) and maintained in a cell culture incubator at 37 ℃ overnight prior to use for p-cofilin intracellular staining with challenge of YU2 mutants.

J. Cofilin Phosphorylation in Viral Mutants Stimulated CD4 T Cells

In preparation of intracellular staining of phosphor-cofilin in YU2 mutants infected CD4+ T cells, 500 ul of half million purified CD4+ T cells were aliquoted into

ten 5 ml Falcon Tubes (BD Biosciences, Rockville, MD). 200 ul of viruses with equal p24 amount was added to each corresponding tube and incubated for appropriate time. After incubation, 28.4 ul of 37% formaldehyde was added to each tube to obtain a final concentration of 1.5% formaldehyde (1:24). Cells were then pelleted at 1200rpm for 5 min and permeabilized by resuspending with vigorous vortexing in 500ul ice-cold MeOH per tube and incubated at 4 ℃ for at least 10 min. Cells were washed twice with 2ml/tube staining buffer (4% BSA in PBS). Supernatant was discarded and about 100 ul staining buffer was left in each tube. 1ul (1:100) p-cofilin antibody(Cell signaling Technology, Inc. Danvers, MA) was added to each tube except for the negative control. After 1 hour incubation at room temperature, cells were washed twice with 2ml/tube staining buffer (4% BSA in PBS). Supernatant was discarded and about 100 ul staining buffer was left in each tube. 0.5 ul (1:200) secondary antibody (Alexa Fluor 488 chicken anti-Rabbit Molecular Probes) (Invitrogen, Carlsbad, CA) was added to each tube. Cells were incubated at room temperature in dark for 30 minutes. After washing with staining buffer twice, cells were resuspend in 200ul 1% paraformaldehyde and analyze by flow cytometry using the FACSCalibur (Becton Dickinson, Rockville, MD). Data were collected and analyzed with the CellQuest software program.

III. RESULTS

A. YU2 env Sequencing

In preparation of performing site-directed mutagenesis, pYU2 was sent to Genewiz, Inc. for sequencing. Table 1 lists all the primers used for sequencing the env part of pYU2. Figure 8 shows the DNA sequence of YU2 env from EcoRI cutting site to SalI cutting site. The DNA sequence in blue is the open reading frame of YU2 env, and the sequence in red is the V3 loop in YU2 env. Black underlines indicate the mutation sites. Figure 9 shows the total 35 amino acid sequence of V3 loop.

B. Cloning of pNL-Δψ-YU2-Env

a. Generating pNL-Δψ-Env(gp160) vector

YU2 env was cloned into plasmid pNL-Δψ-Env(gp160). However, pNL-Δψ-Env(gp160) plasmid was about 10 kb and its size was too large to be a vector. As a result, pNL-Δψ-Env(gp160) was digested with restriction enzyme MfeI to reduce its size (Figure 11). After digestion, pNL-Δψ-Env(gp160) underwent self-ligation. Figure 15A and 15B show the MfeI digested pNL-Δψ-Env(gp160) before and after gel extraction. The 8.5 kb fragment of pNL-Δψ-Env(gp160) was recovered and the DNA was transformed into Stbl 3 cells. Clones were selected and screened by EcoRI and XhoI double digestion. The positive clones gave two bands: 7.0 kb and 1.5 kb (Figure 15C). The vector with the reduced size was named as pNL-Δψ-Env(gp160)(ΔMfeI).

b. Clone of YU2 env into pNL-Δψ-Env(gp160)(ΔMfeI)

The plasmids pNL-Δψ-Env(gp160)(ΔMfeI) and pYU2 (Figure 10) were both digested with EcoRI and XhoI (Figure 16A and 16C). The 7.0 kb DNA fragment of vector pNL-Δψ-Env(gp160)(ΔMfeI) (Figure 16B) and 3.1 kb DNA fragment of insert pYU2 env (Figure 16D) were recovered. The 7.0 kb vector was dephosphorylated with calf intestinal alkaline phosphatase (CIP) for 30 minutes before ligation. After transformed into Stbl 3 cells, clones were selected and digested with EcoRI and XhoI. Correct clones gave two bands: 7.0 kb and 3.1 kb (Figure 16E). The new clone was named as pNL-Δψ-YU2-Env.

c. Clone of YU2 env into pUC19

As pNL-Δψ-YU2-Env was approximately 10 kb in size, it was too large for PCR (polymerase chain reaction). Therefore, YU2 env was cloned into a smaller vector called pUC19. Restriction enzymes EcoRI and SalI were used to cut both pNL-Δψ-YU2-Env and pUC19 for recovery of a 2.7 kb fragment from pNL-Δψ-YU2-Env (Figure 17B) and a 2.6 kb fragment from pUC19 (Figure 17A). Vector pUC19 was dephosphorylated and ligated with YU2 env insert. The ligated plasmid was transformed into OneShot DH5α competent cells. Clones were screened with EcoRI and SalI digestion. Positive clones gave one band as the sizes of vector and insert were similar: 2.6-2.7 kb (Figure 17C).

C. Mutagenesis of V3 loop in YU2 env

Dr. Vaisman and Dr. Masso retrieved the YU2 (R5) V3 loop sequence from patients with AIDS diagnosis whose data were in LANL HIV Sequence Database. Those

patients were R5 infected and had rapid disease progression. They compared the patients' sequences with YU2 wild type sequence and provided us with ten most frequently mutated sites in patients' sequences according to their calculated mathematical model. Forward and reverse primers (Table 3) were designed such that a particular residue of choice was mutated to desired amino acid during a PCR-based mutagenesis. Plasmid pUC19-YU2 was used as DNA template. Successful PCR produces a 5.3 kb band on 1% agarose gel after electrophoresis. However, due to the small amount of PCR product, sometimes there is no band showing on the gel. According to the manufacturer's manual, the phenomenon was normal and the transformation could proceed even though there was no band. Section A in all Figures 18-27 shows the PCR product in 1% agarose gel, respectively. Section B in all Figures 18-27 shows the results of triple digestion of each mutant with EcoRI, SalI, and BglI. Section F in Figures 18-23 and section C in Figure 24-27 show the results of sequence alignment data of comparing pUC19-YU2 mutant with YU2 env open reading frame. pUC19-YU2 mutants were sent to Genewiz, Inc for sequencing using the primer listed in Table 2. The nick in the linear graph of sequence alignment indicated that there was mismatch in mutant when compared to YU2 open reading frame. Sequence analysis of V3 loop gene verified that mutagenesis was successful for each intended mutant with the exception of 20-L-W, 22-T-A, 25-E-D, and 29-D-N.

Six confirmed pUC19-YU2 mutants were then cloned back to pNL-Δψ-YU2-Env. Those pUC19-YU2 mutants were triple digested with EcoRI, SalI, and BglI. Vector pNL-Δψ-YU2-Env was double digested with EcoRI and SalI. 2.7 kb DNA fragment of

pUC19-YU2 mutant was recovered. 7.0 kb DNA fragment of pNL-Δψ-YU2-Env was recovered as well. Sections C and D in Figures 18-23 show the digestion and recovery results. After transformation, pNL-Δψ-YU2-Env mutant clones were digested with EcoRI and SalI for screening positive clones (Section E in Figure 18-23).

D. Production of Control and Mutant Viruses

HIV-1 YU2 viruses were produced by transfecting the 293T cell line with pNL-Δφ-YU2-Env and NL4-3 (KFS)Δgp160. HIV-1 envelope control viruses were produced by transfecting the 293T cell line with NL4-3 (KFS)Δgp160 alone. HIV-1 YU2 mutant viruses were produced by transfecting the 293T cell line with pNL-Δφ-YU2-Env mutants and NL4-3 (KFS)Δgp160. Once harvested at 48 hours, the titer of the purported wild-type and mutant viruses were assessed by a p24 ELISA assay. Based on the p24 ELISA assay results for the wild-type virus, the viral titer of each mutant was normalized to reflect the same viral concentration as the wild-type virus by adjusting the volume of mutant virus to be used in each infection (data not shown).

E. Production of A3R5.7 Monoclonal Cell Line

a. Surface Staining of A3R5.7 Cell Line

A3R5.7 cells (Obtained from NIH AIDS Reagent Program) are derived from the human T-lymphoblastoid cell line A3.01. These cells naturally express CD4, CXCR4 and α4β7. They were engineered to constitutively express CCR5 under G418 (geneticin sulfate) selection. Surface staining of CD4, CXCR4, and CCR5 was done to verify the existence of these receptors. Equal amount of cells were aliquoted into six tubes containing one type of antibody or isotype. Cells were stained, washed, and fixed before

flow cytometry analysis. The green peak in each graph shows the isotype of CD4, CXCR4, and CCR5 receptors, respectively. The right-shifted peaks verify the existence of CD4, CXCR4 and CCR5 receptors (Figure 28).

b. Selection of A3R5.7 Monoclonal Indicator Cell Line

Before testing the infectivity of the mutants in cells, an R5 indicator cells was required. As A3R5.7 cells contain CD4, CXCR4, and CCR5 receptors, GFP (green fluorescence protein) reporter system could be introduced into the cell line. pNL-GFP-RRE-SA(Puro) (bacterial stock obtained from Taylor Goad's Clone I, plasmid was extracted using QIAprep Spin Miniprep Kit) lentiviral particles were generated using 293T cells. A3R5.7 cells were transfected with pNL-GFP-RRE-SA(Puro) lentiviral particles and selected under G418 and puromycin pressure. The GFP percentage of each selected single cell clone was assessed by YU2 infection and analyzed by flow cytometry (Figure 29). According to the flow cytometry result, A3R5.7 clone #8 had the highest infectivity.

F. Infectivity of Mutant Viruses in Indicator Cell Lines

a. Infection of A3R5.7 Cells with YU2 Mutants

In order to test the infectivity of mutants in CCR5-expressed cell line, A3R5.7 Clone #8 cells were challenged with equal amount of pNL-Δφ-YU2-Env wildtype virus, NL4-3 (KFS)Δgp160 envelope control viruses, and pNL-Δφ-YU2-Env mutant viruses. The cells were infected for two hours at 1200 x g, washed, and incubated for a week. During the incubation, GFP expression was assessed at 2 dpi (days post infection), 4 dpi, and 6 dpi. Flow cytometry analysis of the A3R5.7 cells showed that all the YU2 mutants

lost infectivity except 13-N-P mutant for which GFP expression was 0.34% (Figure 30). This result implied that those mutation sites were crucial for the CCR5 coreceptor binding upon viral entry. However, as A3R5.7 cells express both CXCR4 and CCR5 coreceptors, it was difficult to determine which coreceptor was responsible for the infectivity of 13-N-P mutant.

b. Infection of Clone X Cells with YU2 Mutants

In order to test the infectivity of mutants in CXCR4-expressing cell line, Clone X cells were used as the indicator cell line. Clone X cells were derived from the CEM-SS suspension cell line that has been modified to express green fluorescent protein (GFP) and luciferase when the cells are infected with HIV-1. The cells were challenged with equal amount of pNL-Δφ-YU2-Env wildtype virus, NL4-3 (KFS)Δgp160 envelope control viruses, and pNL-Δφ-YU2-Env mutant viruses. Clone X cells were centrifuged for two hours at 1200 x g, washed, and incubated for a week. During the incubation, GFP expression was assessed at 2 dpi (days post infection), 4 dpi, and 6 dpi. Flow cytometry analysis of the Clone X cells showed that all the YU2 mutants lost infectivity in CXCR4-expressing cells (Figure 31). The 0.00% infectivity of 13-N-P mutant suggested that the 0.34% GFP expression in A3R5.7 cells was due to CCR5 coreceptor.

G. Signal Transduction of Memory Cells Following Stimulation with Mutants

a. Time Course of Intracellular P-cofilin Staining during Wild-type Infection

An infection time course was conducted on memory cells purified from blood, using the pNL-Δφ-YU2-Env wildtype virus and NL4-3 (KFS)Δgp160 envelope control virus to establish the time point at which actin depolymerization showed the greatest

difference between the two. For each staining, half million memory cells were infected with equal amount of pNL-Δφ-YU2-Env wildtype virus and NL4-3 (KFS)Δgp160 envelope control virus for 5 minutes, 10 minutes, 15 minutes, 30 minutes, and 60 minutes. The time point at which p-cofilin activity differed most between pNL-Δφ-YU2-Env wildtype and NL4-3 (KFS)Δgp160 was selected for subsequent experiments on mutants (Figure 32, 34 & 36). All results showed that p-cofilin activity is activated through the engagement of gp120 and CCR5 coreceptor. The change in p-cofilin levels indicated that the actin dynamics was activated upon viral entry. This phenomenon is consistent with our lab's actin dynamic model based on the observations of X4 viruses and CXCR4 cells engagement, meaning that R5 viruses utilize CCR5 to overcome the actin barrier.

b. P-cofilin Intracellular Staining in Mutant Virus-stimulated Memory T Cells

Once the time point of p-cofilin intracellular staining was established, the memory cells from the same donor were infected with equal amount of pNL-Δφ-YU2-Env wildtype virus, NL4-3 (KFS)Δgp160 envelope control virus, and all six mutants for 10 or 15 minutes, depending on the previous YU2 time course experiment. The negative control contained neither viruses nor p-cofilin antibody. Another tube without virus had p-cofilin antibody. P-cofilin antibody was added to each tube except for the negative control and incubated for 1 hour. Secondary antibody was added to each tube and incubated for 30 minutes before examined by flow cytometry. The p-cofilin activity changed by mutant viruses was determined based on comparison to the data generated from the uninfected cells and wild-type virus-infected cells. According to the flow

cytometry analysis, p-cofilin levels fluctuated in donor# 04172014 (Figure 33). However, p-cofilin decreased in most of the mutants except for 13-N-P when compared to the p-cofilin percentage in pNL-Δφ-YU2-Env wildtype in donor# 04222014 (Figure 35). The degree of p-cofilin decrease varied among mutants 13-N-H, 11-S-G, 13-N-T, 20-L-F, and 25-E-Q. Change of p-cofilin activity was the characteristic used to determine if the mutated amino acid residue is a contributor to the V3 loop domains that contribute to actin dynamics activation. There was no pattern shown in two donors to predict the p-cofilin change. All data indicated that the mutants could still trigger actin dynamics even though they had lost infectivity on CCR5+ cells. Figure 36 shows that at 15 min there was a significant change in p-cofilin. But when mutants were used to stimulate the cells for 15 min, the p-cofilin of YU2 wild type challenged cells exhibited no change as compared to the negative control (Figure 37). As the experimental settings were the same in those two experiments, it was hard to explain why the cells were not activated at 15 min. Thus, the data of this donor# 08052014 was not used for data interpretation.

H. Signal Transduction in Mutant-stimulated CXCR4+CCR5- T cells

a. Surface Staining of CXCR4+CCR5- T cells

CXCR4+CCR5- T cells were purified from blood. Antibody CD195 (anti-CCR5) was added during the blood purification process to eliminate cells that express CCR5 coreceptors. In order to verify the effectiveness of CD195 antibody, CXCR4 and CCR5 surface staining was done on the purified total CD4 T cell population. Equal amount of cells were aliquoted into four tubes containing one type of antibody or isotype. Cells were stained, washed, and fixed before flow cytometry analysis. The green peak in each

histogram shows the isotype of CXCR4 and CCR5 receptors, respectively. The right-shifted peaks verify the existence of CXCR4 receptors (Figure 38). The red peak in CCR5 staining histogram was almost identical to its green isotype peak (Figure 38), meaning that there was no CCR5 coreceptor in CXCR4+CCR5- T cells population.

b. Time Course of Intracellular P-cofilin Staining during Wild-type Infection

An infection time course was conducted on memory cells purified from blood, using the pNL-Δφ-YU2-Env wildtype virus and NL4-3 (KFS)Δgp160 envelope control virus to establish the time point at which actin depolymerization was at greatest difference between the two. For each staining, half million of total CD4 T cells (CCR5-) were infected with equal amount of pNL-Δφ-YU2-Env wildtype virus and NL4-3 (KFS)Δgp160 envelope control virus for 5 minutes, 10 minutes, 15 minutes, 30 minutes, and 60 minutes. A tube containing only cells was set as a negative control. The time point at which p-cofilin activity differed most between pNL-Δφ-YU2-Env wildtype and NL4-3 (KFS)Δgp160 was selected for subsequent experiments for mutants (Figure 39, 41 & 43).

c. Time Course of P-cofilin Intracellular Staining during Infection with Mutants

Once the time point of p-cofilin intracellular staining was established, the total CD4 T cells (CCR5-) from the same donor were infected with equal amount of pNL-Δφ-YU2-Env wildtype virus, NL4-3 (KFS)Δgp160 envelope control virus, and all six mutants for 15 minutes. The negative control contained either no virus or p-cofilin antibody. Another tube without virus had p-cofilin antibody. P-cofilin antibody was added to each tube except for the negative control and incubated for 1 hour. Secondary

antibody was added to each tube and incubated for 30 minutes before examined by flow cytometry. The p-cofilin activity changed by mutant viruses was determined based on comparison to the data generated from the uninfected cells and wild-type virus-infected cells. According to the flow cytometry analysis, p-cofilin did not change significantly in all the mutants challenged cells (Figure 40, 42 & 44). It suggested that these mutations were unable to trigger actin dynamics in CXCR4+CCR5- cells.

IV. DISCUSSION

Based on the model of actin dynamics with HIV-1 infection from our lab built, actin depolymerization in resting $CD4^+$ T-cells is believed to aid the viral post-entry process and permits the virus to use the cell as a reservoir during latency as is observed *in vitro*. The purpose of this study was to mutate the V3 loop in gp120 glycoprotein of a CCR5 HIV-1 strain YU2 in an attempt to identify the mutations responsible for inducing actin depolymerization in resting $CD4^+$ T-cells without tropism change. Identification of mutations that stimulate actin depolymerization in resting $CD4^+$ T-cells is important to cast light on the clinical phenomena observed in patients that die from AIDS with exclusive R5 isolates.

At first, Geneart site-directed mutagenesis kit from Invitrogen was used to generate mutants. However, many attempts were done and all of them failed. Therefore, we switched to QuikChange site-directed mutagenesis kit by Strategene. There are several differences between the two systems. Invitrogen kit uses AccuPrime™ *Pfx* DNA polymerase that results in two linear PCR products; whereas Stragegene kit uses PfuTurbo DNA polymerase to produce nicked circular strands. Invitrogen kit uses DH5α-T1 competent E. coli cells as host for recombinant DNA. The host cell could circulate the linear mutated DNA, and *Mcr*BC endonuclease would digest the methylated parental DNA. Strategene kit has a different system. It requires DpnI to digest the nonmutated,

methylated parental DNA *in vitro*. XL10-Gold ® ultracompetent cells that are capable of repairing the nicks in the mutated plasmid are used as host cells. By using Strategene kit, six mutants were successfully generated. However, the generation of four mutants at the locations 20-L-W, 22-T-A, 25-E-D, and 29-D-N failed. The possible reason of the failure might be the high GC content within the primers. More attempts should be done to produce the mutants. Or, DNA synthesis of the plasmid containing desired mutations could be done commercially.

In the process of making monoclonal CCR5+ indicator cell line, I also encountered some problems. U937 cells which are known to have CCR5 coreceptors on the surface were used for making the indicator cell line at the beginning. But after the surface staining of the cells, it was surprising to find out that the level of CCR5 was very low. And YU2 wild type virus could not infect the cells. Later, IFN-γ was added to cell culture to stimulate the emergence of CCR5 according to Zella *et al* (Zella *et al*, 1998). HIV-1 YU2 viruses were used to infect the IFN-γ treated U937 cells. The results showed that there was no infection of these cells (data not shown), probably due to the inhibitory effect of IFN-γ on infections. Subsequently, A3R5.7 cells that have both CXCR4 and CCR5 coreceptors on surface were used to make the indicator cell line. When screening for cell clones, only clones with rapid proliferation and high infectivity were selected. Following this criteria, clone #8 was selected to be the indicator cell line for subsequent experiments.

Because R5 viruses are generally known to replicate slower than X4 viruses, it takes more than three days to reach the peak infectivity, whereas X4 viruses reach peak infectivity at 3 dpi based on previous observations. The data shown in Figure 29 was obtained on day seven post infection. The infectivity in Figures 30 and 31 was measured on day four post infection. And we used spinoculation to enhance the viral infectivity.

The data of infectivity of mutants on CCR5+ cell line showed that all the mutants lost infectivity except the mutant 13-N-P which retained limited infectivity. And the mutants could not infect CXCR4+ cell line either, indicating that single mutation was not able to switch viral tropism. However, these single mutations are crucial in viral entry as all the mutants could not infect CCR5+ cells anymore. The mechanism of how they affect binding is unclear. Additional studies need to be done to understand the role of the mutations in V3 loop. The mutations may cause conformational change of gp120 so that it is no longer functional in binding to receptors. Another explanation could be that the mutations changed the net charge in V3 loop region so that it could not bind to CCR5 coreceptors as CCR5 is naturally neutral or less negative than CXCR4. The commonly used 11/25 rule predicts an X4 strain in the presence of positively charged amino acids at positions 11 or 25 of the V3 loop. . Mutant 11-S-G carried a change from a polar, hydrophilic serine to a non-polar, hydrophobic glycine. Mutant 25-E-Q carried a change from a negatively charged glutamic acid/glutamate to a polar, hydrophilic glutamine. Glycine and glutamine are not positively charged amino acids, so they did not contribute to X4 viral switch. Asparagine at position 13 is a polar, hydrophilic amino acid. It was mutated either to histidine and threonine that have the same properties, or to proline,

which is non-polar and hydrophobic. Leucine at position 20 was mutated to phenylalanine. Both amino acids are non-polar and hydrophobic. All those mutations abolished the infectivity in mutants.

All the experiments of intracellular staining of p-cofilin in primary cells were repeated three times. P-cofilin level increased in all memory cells from three different donors with YU2 wild type infection. The degree of the change and the time point at which peak activity was reached varied due to donor variations. In the first donor (Donor# 04182014), cells with no virus and p-cofilin antibody were tested. But we excluded that sample in later experiments because we only needed to find out the time point at which the YU2 stimulated cells had highest p-cofilin level change. Ideally, the p-cofilin change for each mutant on primary cells should have been measured at each time point that we did for YU2 wild type. But due to the shortage of cells purified from blood, we could test the p-cofilin level on mutants-stimulated cells only at one time point. In donor# 08062014, we chose 15 minutes as the time point for subsequent experiment as the p-cofilin level was about 30% in YU2-stimulated memory cells (Figure 36). However, when using the same amount of YU2 viruses to infect the same amount of memory cells from the same donor for 15 minutes, the result showed that there was no p-cofilin change (Figure 37). The reason might be that 15 minutes was not the “right” time point for p-cofilin to be activated in this experiment. Therefore, the results from this donor were not used for analysis as the positive control data was not consistent with the previous data showed in Figure 36. Although previous infectivity data showed that mutants had lost infectivity in CCR5+ cell line, intracellular staining data suggested that

these mutants could still affect the p-cofilin level somehow. The change of p-cofilin level in memory cells with mutant stimulation might be related to partial contact of gp120 with the CCR5 coreceptor.

The results of YU2 wild type viruses stimulating the primary cells with no CCR5 coreceptor present on surface met our prediction. There was no p-cofilin change due to the lack of CCR5. The mutants did not activate p-cofilin in those cells as well. All results were consistent in three donors. Our hypothesis was that the mutations in YU2 V3 loop could trigger signal transduction without giving rise to X4 tropism. The results indicated that these single mutations in V3 region could not trigger signal transduction in CXCR4+ cells.

The data generated from this study provided limited information about the mechanism of mutations in V3 loop mediating actin dynamics in resting CD4+ T cells. In future studies, more mutations should be done, such as double mutations, triple mutations, etc. The function and role of each amino acid in V3 loop and structural changes of gp120 due to mutations need to be investigated. More regulators of actin dynamics could be measured, such as Arp2/3, WASP, and LIMK. Additionally, because V3 loop is not the sole determinant of coreceptor usage, V1/V2, and β19 regions should also be studied as these regions are related to tropism switch. There are new questions raised from this research. As memory CD4 T cells contribute 30% of the population of total CD4 T cells, how do the R5 viruses manage to deplete CXCR4+ CD4 T cells in patients? Employment of apoptosis assay is necessary for the mutant-stimulated cells to

see whether the mutation can activate apoptotic pathway in cells by contacting CXCR4 coreceptors on cell surface without viral entry.

V. TABLES AND FIGURES

Table 1. Primers used for sequencing YU2 envelope in pYU2 plasmid.

Primer	Sequence
pYU2-env-primRA	5’-GGGGCATACATTGCTTTTC -3’
pYU2-env-primFB	5’-GTACAAGACCCAACAACAATAC -3’
pYU2-env-primRC	5’-CCACTAGTAGTAGCTG-3’
pYU2-env-primFD	5’-GCTGACGGTACAGGCCAGAC -3’
pYU2-env-primRE	5’-CAGCTACTACTAGTGG -3’
pYU2-env-primFF	5’-AGAGACAGAGACAGATC -3’

Table 2. Primers used for sequencing pUC19-YU2 mutant plasmid.

Primer	Sequence
Mut Seq	5’- CATACATTATTGTGCCCCG -3’

Table 3. Primers used for generating pUC19-YU2 mutants. The underlines indicate the desired mutations. F: Forward; R: Reverse.

Primer	Sequence
11 S-G F	5'- CCAACAACAATACAAGAAAA**GGA**ATAAATATAGGACCAGGGAG -3'
11 S-G R	5'- CTCCCTGGTCCTATATTTAT**TCC**TTTTCTTGTATTGTTGTTGG -3'
13 N-H F	5'- ACAATACAAGAAAAAGTATA**CAC**ATAGGACCAGGGAGAGCATTGT-3'
13 N-H R	5'-ACAATGCTCTCCCTGGTCCT**ATG**TGTATACTTTTTCTTGTATTGT -3'
13 N-P F	5'- ACAATACAAGAAAAAGTATA**CCA**ATAGGACCAGGGAGAGCATT -3'
13 N-P R	5'- AATGCTCTCCCTGGTCCTAT**TGG**TATACTTTTTCTTGTATTGT -3'
13 N-T F	5'- ACAATACAAGAAAAAGTATA**ACT**ATAGGACCAGGGAGAGCATT -3'
13 N-T R	5'- AATGCTCTCCCTGGTCCTAT**AGT**TATACTTTTTCTTGTATTGT -3'
20 L-F F	5'- ATATAGGACCAGGGAGAGCA**TTT**TATACAACAGGAGAAATAAT -3'
20 L-F R	5'- ATTATTTCTCCTGTTGTATA**AAA**TGCTCTCCCTGGTCCTATAT -3'
20 L-W F	5'- ATATAGGACCAGGGAGAGCA**TGG**TATACAACAGGAGAAATAAT -3'
20 L-W R	5'- ATTATTTCTCCTGTTGTATA**CCA**TGCTCTCCCTGGTCCTATAT -3'
22 T-A F	5'- GACCAGGGAGAGCATTGTAT**GCA**ACAGGAGAAATAATAGGAGA -3'
22 T-A R	5'- TCTCCTATTATTTCTCCTGT**TGC**ATACAATGCTCTCCCTGGTC -3'
25 E-D F	5'- GAGCATTGTATACAACAGGA**GAT**ATAATAGGAGATATAAGACA -3'
25 E-D R	5'- TGTCTTATATCTCCTATTAT**ATC**TCCTGTTGTATACAATGCTC -3'
25 E-Q F	5'- GAGCATTGTATACAACAGGA**CAA**ATAATAGGAGATATAAGACA -3'
25 E-Q R	5'- TGTCTTATATCTCCTATTAT**TTG**TCCTGTTGTATACAATGCTC -3'
29 D-N F	5'- CAACAGGAGAAATAATAGGA**AAT**ATAAGACAAGCACATTGTAA -3'

29 D-N R	5’- TTACAATGTGCTTGTCTTAT**ATT**TCCTATTATTTCTCCTGTTG -3’

AATTCTGCAACAACTGCTGTTTATTCATTTCAGAATTGGGTGTCAACATAGCA
GAATAGGCATTATTCAACAGAGGAGAGCAAGAAGAAATGGAGCCAGTAGAT
CCTAACCTAGAGCCCTGGAAGCATCCAGGAAGTCAGCCTAGGACTGCTTGTA
ACAATTGCTATTGTAAAAAGTGTTGCTTTCATTGCCAAGTTTGTTTTACAAAA
AAAGGCTTAGGCATCTCCTATGGCAGGAAGAAGCGGAGACAGCGACGAAGA
CCTCCTCAGGACAGTCAGACTCATCAAAGTTCTCTATCAAAGCAGTAAGTAG
TACATGTACTGCAATCTTTACAAGTATTAGCAATAGTAGCATTAGTAGTAGCA
ACAATAATAGCAATAGTTGTGTGGACCATAGTATTCATAGAATATAGGAAAA
TATTAAGACAAAGGAAAATAGACAGGTTAATTAATAGAATAACAGAAAGAG
CAGAAGACAGTGGCAATGAGAGCGACGGAGATCAGGAAGAATTATCAGCAC
TTGTGGAAAGGGGGCACCTTGCTCCTTGGGATGTTGATGATCTGTAGTGCTGC
AGAACAATTGTGGGTCACAGTCTATTATGGGGTACCTGTGTGGAAAGAAGCA
ACCACCACTCTATTTTGTGCATCAGATGCTAAAGCATATGATACAGAGGTAC
ATAATGTTTGGGCCACACATGCCTGTGTACCCACAGACCCCAACCCACAAGA
AGTAAAATTGGAAAATGTGACAGAAAATTTTAACATGTGGAAAAATAACATG
GTAGAACAAATGCATGAGGATATAATCAGTTTATGGGATCAAAGCCTAAAGC
CATGTGTAAAATTAACTCCACTCTGTGTTACTTTAAATTGCACTGATTTAAGG
AATGCTACTAATACCACTAGTAGTAGCTGGGAAACGATGGAGAAAGGAGAA
ATAAAAAACTGCTCTTTCAATATCACCACAAGCATAAGAGATAAGGTACAGA
AAGAATATGCACTTTTTTATAACCTTGATGTAGTACCAATAGATAATGCTAGC
TATAGGTTGATAAGTTGTAACACCTCAGTCATTACACAGGCCTGTCCAAAGGT
ATCCTTTGAGCCAATTCCCATACATTATTGTGCCCCGGCTGGTTTTGCGATTCT
AAAATGTAATGATAAAAAGTTCAATGGAACAGGACCATGTACAAATGTCAGC
ACAGTACAATGTACACATGGAATTAGGCCAGTAGTATCAACTCAACTGCTGT
TAAATGGCAGTCTAGCAGAAGAAGAGATAGTAATTAGATCTGAAAATTTCAC
AAACAATGCTAAAACTATAATAGTACAGCTGAACGAATCTGTAGTAATTAAT
TGTACAAGACCCAACAACAATACAAGAAAAAGTATAAATATAGGACCAGGG
AGAGCATTGTATACAACAGGAGAAATAATAGGAGATATAAGACAAGCACAT
TGTAACCTTAGTAAAACACAATGGGAAAACACTTTAGAACAGATAGCTATAA
AATTAAAAGAACAATTTGGGAATAATAAAACAATAATCTTTAATCCATCCTC
AGGAGGGGACCCAGAAATTGTAACACACAGTTTTAATTGTGGAGGGGAATTT
TTCTACTGTAATTCAACACAACTGTTTACTTGGAATGATACTAGAAAGTTAAA
TAACACTGGAAGAAATATCACACTCCCATGTAGAATAAAACAAATTATAAAT
ATGTGGCAGGAAGTAGGAAAAGCAATGTATGCCCCTCCCATCAGAGGACAA
ATTAGATGTTCATCAAATATTACAGGGCTGCTATTAACAAGAGATGGTGGTA
AGGACACGAACGGGACTGAGATCTTCAGACCTGGAGGAGGAGATATGAGGG
ACAATTGGAGAAGTGAATTATATAAATATAAAGTAGTAAAAATTGAACCATT
AGGAGTAGCACCCACCAAGGCAAAGAGAAGAGTGGTGCAGAGAGAAAAAA
GAGCAGTGGGACTAGGAGCTTTGTTCCTTGGGTTCTTGGGAGCAGCAGGAAG
CACTATGGGCGCAGCGTCAATAACGCTGACGGTACAGGCCAGACAATTATTG
TCTGGTATAGTGCAACAGCAGAACAATCTGCTGAGGGCTATTGAGGCGCAAC
AGCACCTGTTGCAACTCACAGTCTGGGGCATCAAGCAGCTCCAGGCAAGAGT
CCTGGCTGTGGAAAGATACCTAAGGGATCAACAGCTCCTAGGGATTTGGGGT
TGCTCTGGAAAACTCATTTGCACCACTACTGTGCCTTGGAATACTAGTTGGAG

TAATAAATCTCTGAATGAAATTTGGGATAACATGACTTGGATGAAGTGGGAA
AGAGAAATTGACAATTACACACACATAATATACTCCTTAATTGAACAATCGC
AGAACCAACAAGAAAAGAATGAACAAGAATTATTGGCATTAGATAAATGGG
CAAGTTTGTGGAATTGGTTTGACATAACAAAATGGCTGTGGTATATAAAAAT
ATTCATAATGATAGTAGGAGGCTTGATAGGTTTAAGAATAGTTTTTGTTGTAC
TTTCTATAGTGAATAGAGTTAGGCAGGGATACTCACCATTATCGTTTCAGACC
CACCTCCCAGCTCAGAGGGGACCCGACAGGCCCGACGGAATCGAAGAAGAA
GGTGGAGAGAGAGACAGAGACAGATCCGGTCCATTAGTGGATGGCTTCTTAG
CAATTATCTGGGTCGAC

Figure 8. Sequence of YU2 env from EcoRI to SalI cutting site (2.7 kb). Red dotted line:

EcoRI site (first), and SalI site (last). Blue: YU2 open reading frame. Red: V3 loop.

Black underline: mutation sites.

CTRPNNNTRKSINIGPGRALYTTGEIIGDIRQAHC

Figure 9. Amino acid sequence of V3 loop in YU2 env (35 aa). Red: mutation sites.

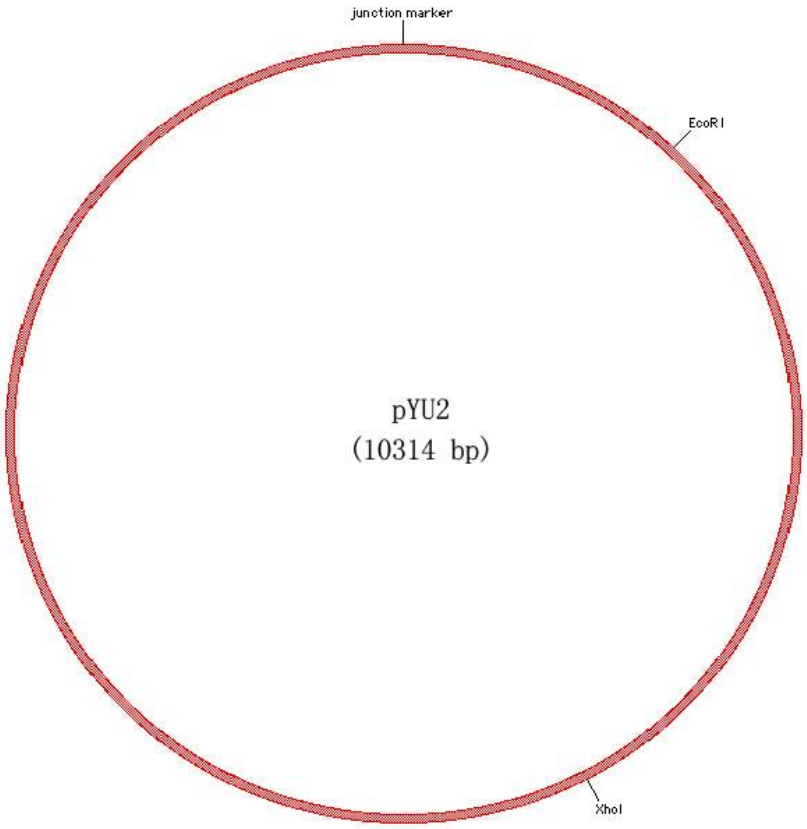

Figure 10. Map of pYU2 plasmid showing the EcoRI and XhoI sites.

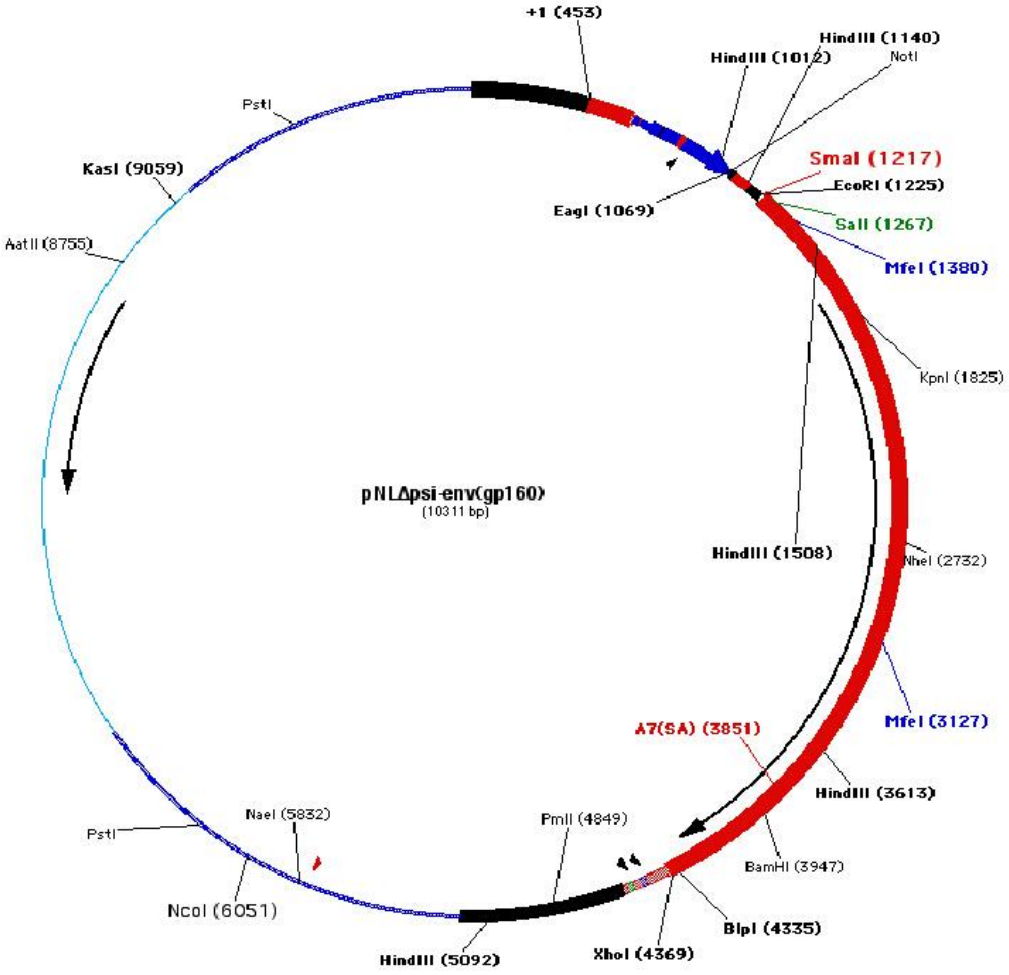

Figure 11. Map of pNL-Δψ-Env(gp160) plasmid showing the MfeI cutting sites.

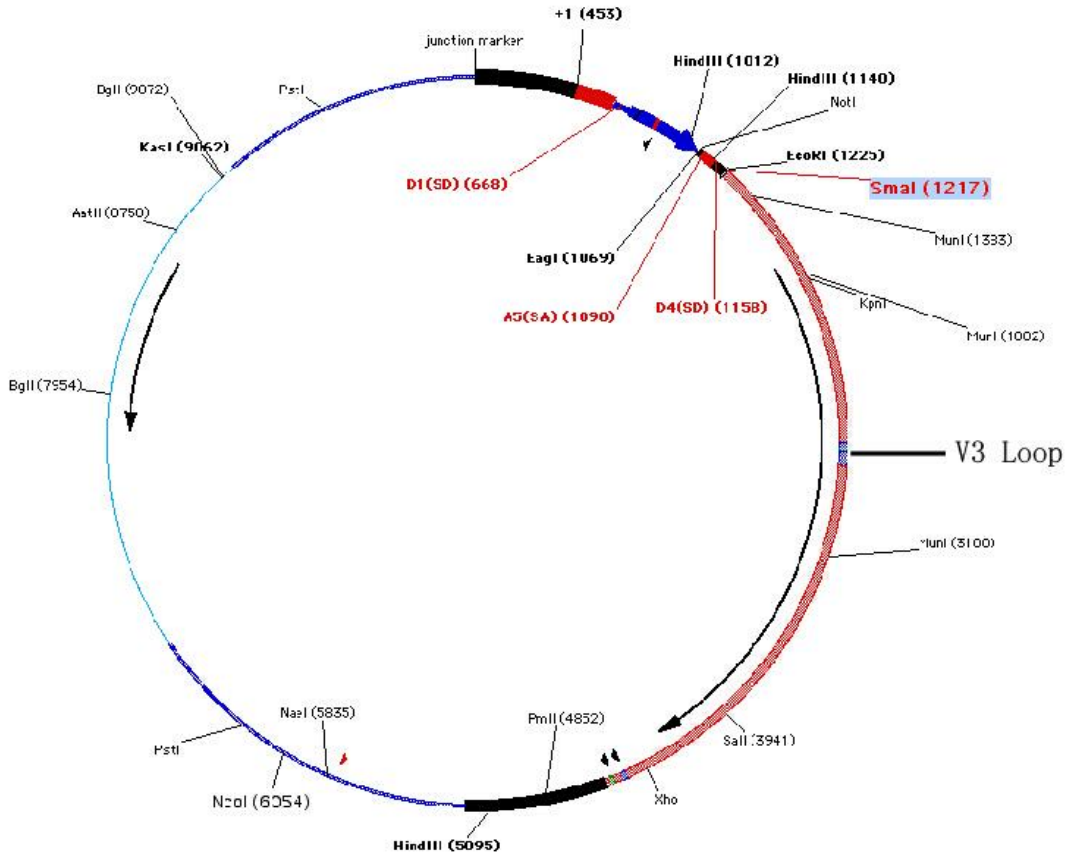

Figure 12. Map of pNL-Δψ-YU2-Env plasmid showing EcoRI, SalI, and XhoI cutting sites.

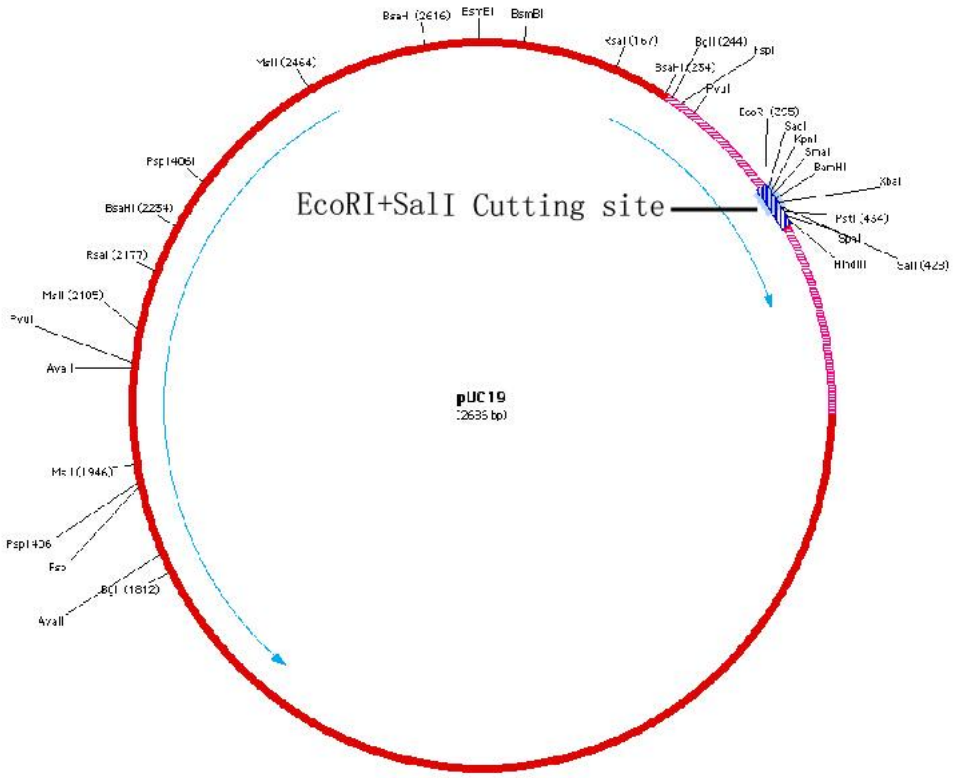

Figure 13. Map of pUC19 plasmid (2.6kb).

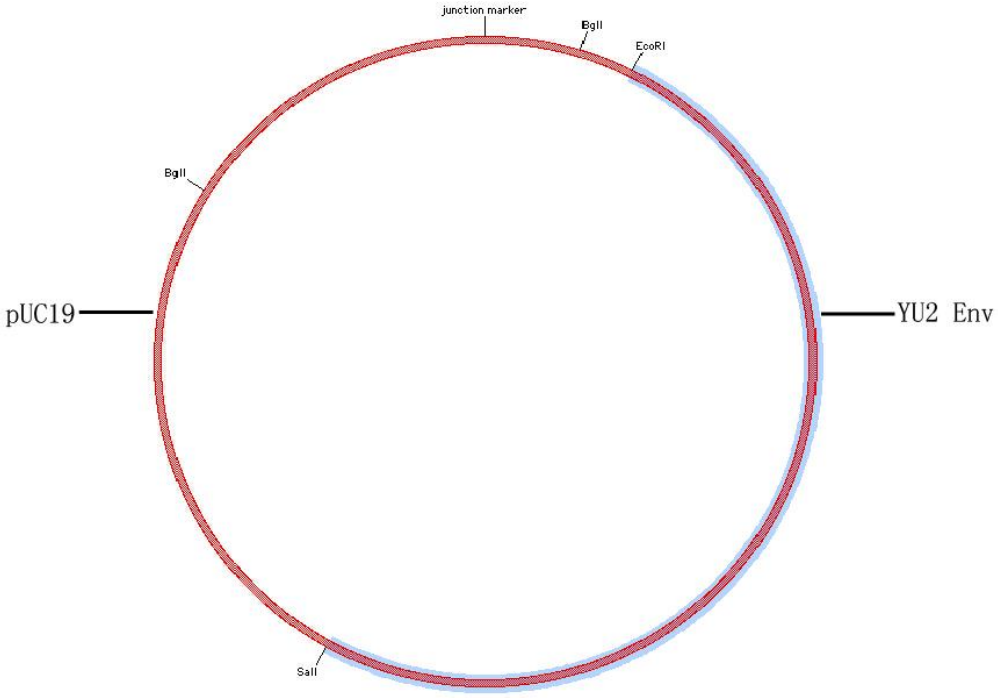

Figure 14. Map of pUC19-YU2 plasmid (5.3kb) showing EcoRI and SalI cutting sites.

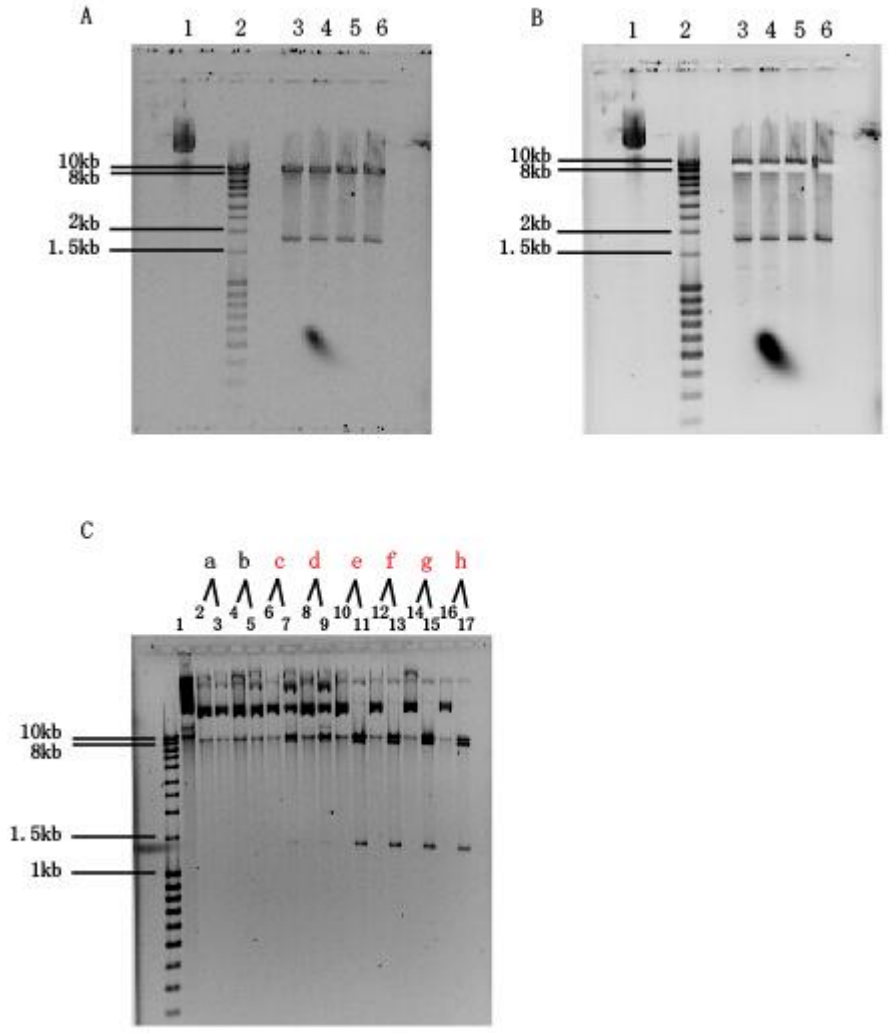

Figure 15. **A**. Digestion of pNL-Δψ-Env(gp160) with MfeI. **B**. Recovery of 8.5 kb fragment of pNL-Δψ-Env(gp160). **C**. Double digestion of pNL-Δψ-Env(gp160)(ΔMfeI) clones with EcoRI and XhoI. Letters a-b represent Clones #1-8. Number 1 is DNA ladder. Numbers under letters: even numbers represent uncut pNL-Δψ-Env(gp160)(ΔMfeI) plasmid clone #1-8. Odd numbers represent digested pNL-Δψ-Env(gp160)(ΔMfeI) plasmid clone #1-8. Red letter c-h represent positive clones #3-8.

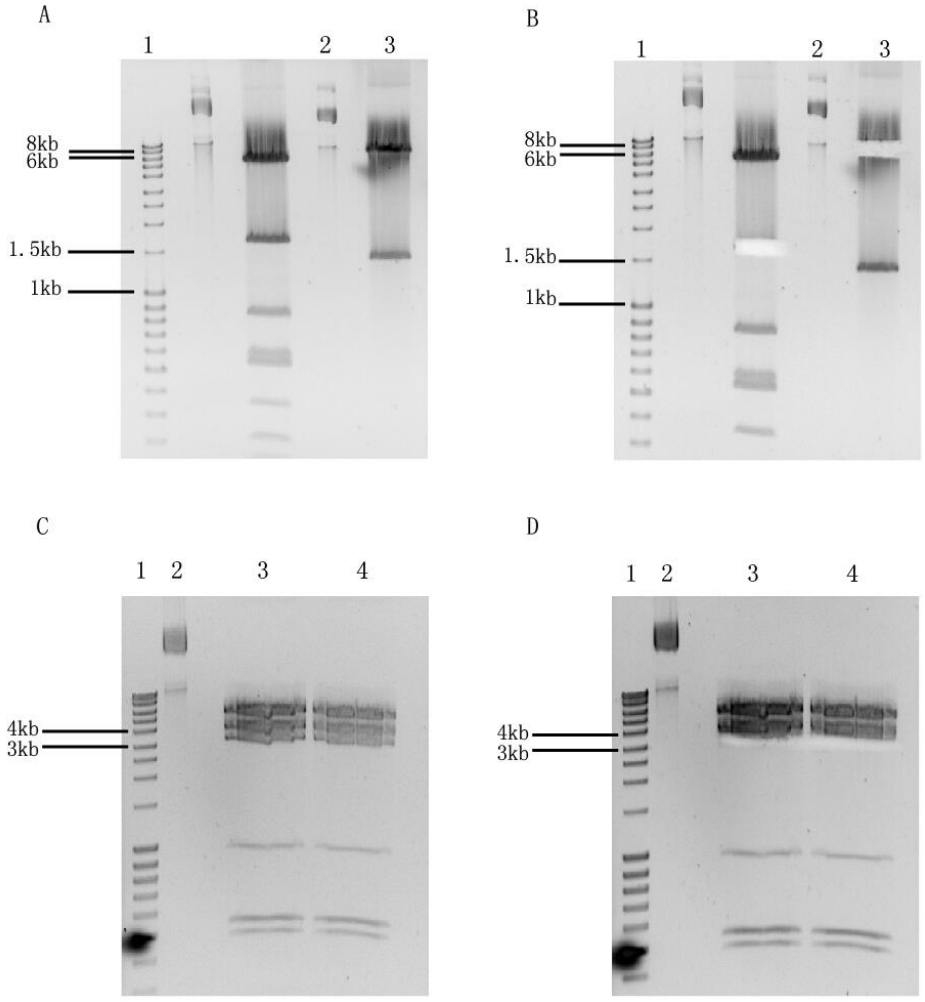
A
1
2
3
8kb
6kb
1.5kb
1kb
B
1
2
3
8kb
6kb
1.5kb
1kb
C
1
2
3
4
4kb
3kb
D
1
2
3
4
4kb
3kb

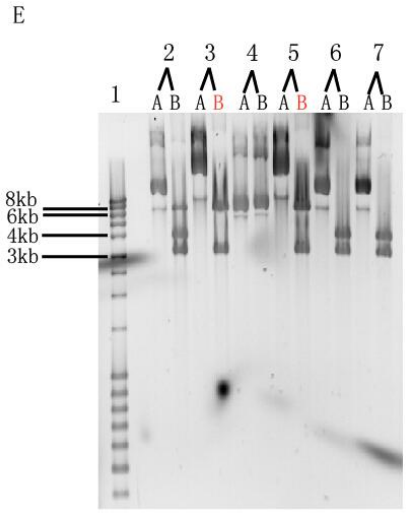

Figure 16. **A**. Digestion of pNL-Δψ-Env(gp160)(ΔMfeI) with EcoRI and XhoI. 1: DNA ladder; 2: uncut pNL-Δψ-Env(gp160)(ΔMfeI); 3: pNL-Δψ-Env(gp160)(ΔMfeI) with EcoRI and XhoI. **B**. Recovery of 7.0 kb fragment of pNL-Δψ-Env(gp160)(ΔMfeI). 1: DNA ladder; 2: uncut pNL-Δψ-Env(gp160)(ΔMfeI); 3: pNL-Δψ-Env(gp160)(ΔMfeI) with EcoRI and XhoI. **C**. Digestion of pYU2 clones with EcoRI and XhoI. 1: DNA ladder; 2: uncut pYU2; 3 & 4: pYU2 with EcoRI and XhoI. **D**. Recovery of 3.1 kb fragment of pYU2. 1: DNA ladder; 2: uncut pYU2; 3 & 4: pYU2 with EcoRI and XhoI. **E**. Screening of pNL-Δψ-YU2-Env, digested with EcoRI and XhoI. Letters A represents uncut Clones #1-6. Letters B represents Clones #1-6 digested with EcoRI and XhoI. Number 1 is DNA ladder. Number 2-7 represent Clones #1-6. Red letters represent positive clones.

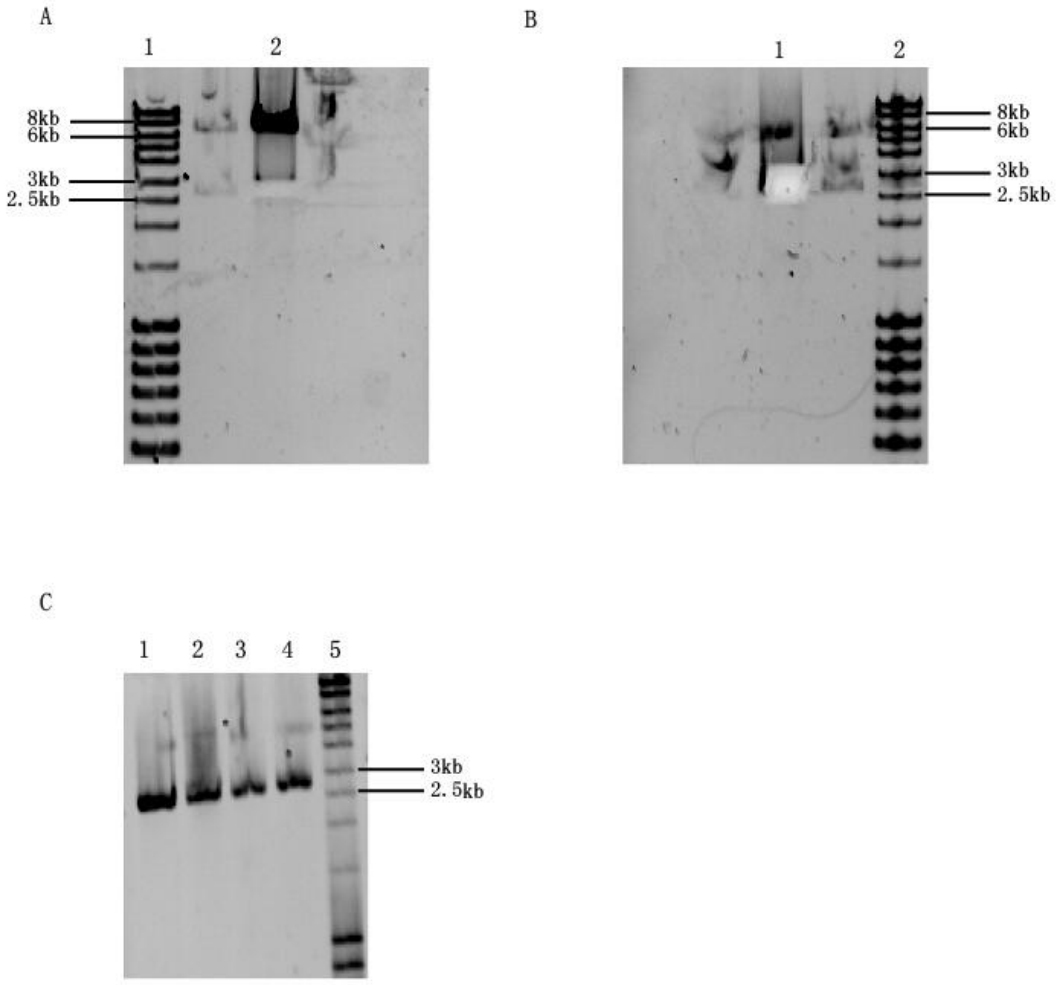

Figure 17. **A**. Digestion of pNL-Δψ-YU2-Env with EcoRI and SalI and recovery of 2.7 kb fragment. 1: DNA ladder; 2: pYU2 cut with EcoRI and SalI. **B**. Digestion of pUC19 with EcoRI and SalI and recovery of 2.6 kb fragment. 1: pUC19 cut with EcoRI and SalI; 2: DNA ladder. **C**. Double digestion of pUC19-YU2 clones with EcoRI and SalI. 5: DNA ladder; 1-4: pUC19-YU2 clones cut with EcoRI and SalI.

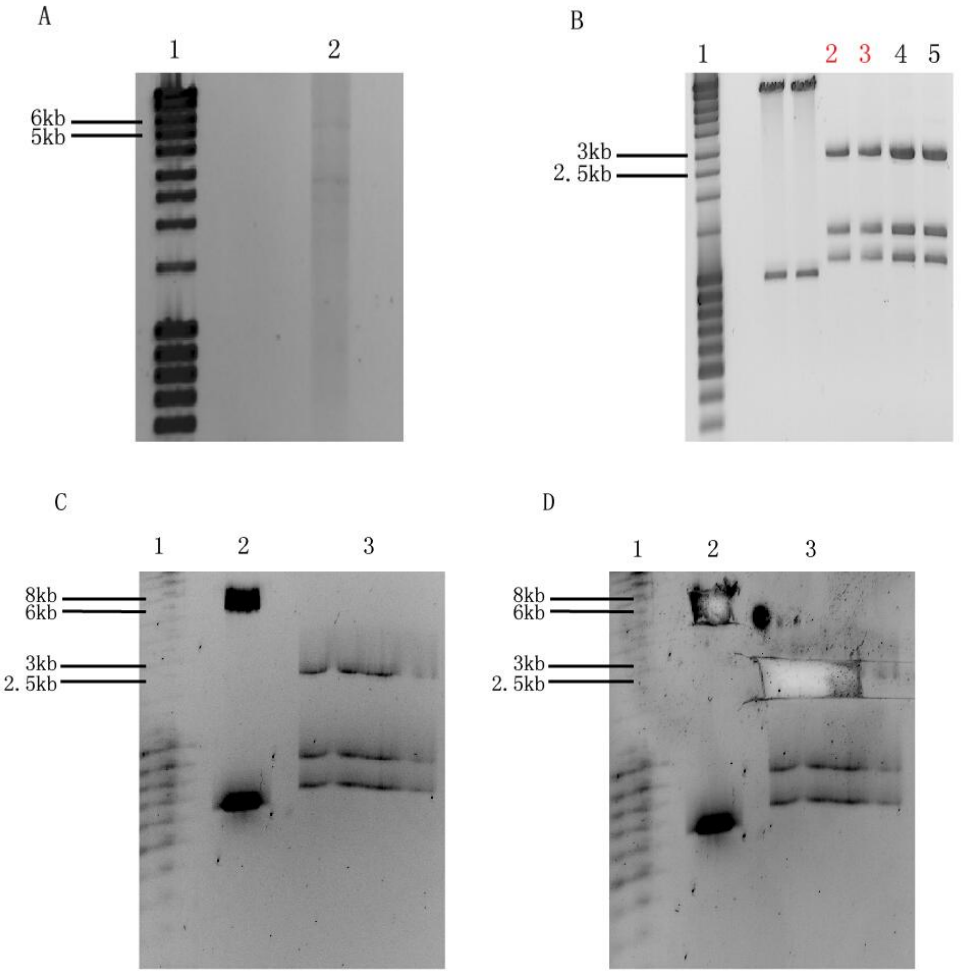
A
1
2
6kb
5kb
B
1
2
3
4
5
3kb
2. 5kb
C
1
2
3
8kb
6kb
3kb
2. 5kb
D
1
2
3
8kb
6kb
3kb
2. 5kb
E
1
2
3
4
5
6
7
8kb
6kb
3kb
2. 5kb
F
Window Size = 10
Min. % Score = 80
Hash Value = 6
Strand = Both
Jump = 1
Scoring Matrix: DNA database matrix
mut YU2 11N to HF (ove#18F454
100
150
200
250
300
350
400
450
600
700
800
900
1000
1100
1200
YU2 Env ORF

Figure 18. **A**. PCR of pUC19-YU2(N-H). 1: DNA ladder; 2: PCR product of pUC19-YU2(N-H) (5.3kb). **B**. Screening of pUC19-YU2(N-H) mutant clones, digested with EcoRI, SalI, and BglI. 1: DNA ladder; 2 & 3: pUC19-YU2(N-H) cut with EcoRI, SalI, and BglI. **C**. Digestion of pNL-Δψ-YU2-Env plasmid and confirmed positive pUC19-YU2(N-H) clone. 1: DNA ladder; 2: pNL-Δψ-YU2-Env cut with EcoRI and SalI; 3: pUC19-YU2(N-H) cut with EcoRI, SalI, and BglI. **D**. Recovery of 7.0 kb fragment of pNL-Δψ-YU2-Env. Recovery of 2.7 kb fragment of pUC19-YU2(N-H). 1: DNA ladder; 2: pNL-Δψ-YU2-Env cut with EcoRI and SalI; 3: pUC19-YU2(N-H) cut with EcoRI, SalI, and BglI. **E**. Screening of pNL-Δψ-YU2-Env(N-H), digested with EcoRI and SalI. 1: DNA ladder; 2-7: pNL-Δψ-YU2-Env(N-H). Red numbers represent positive clones. **F**. Sequence alignment data of pUC19-YU2(N-H) with pNL-Δψ-YU2-Env open reading frame.

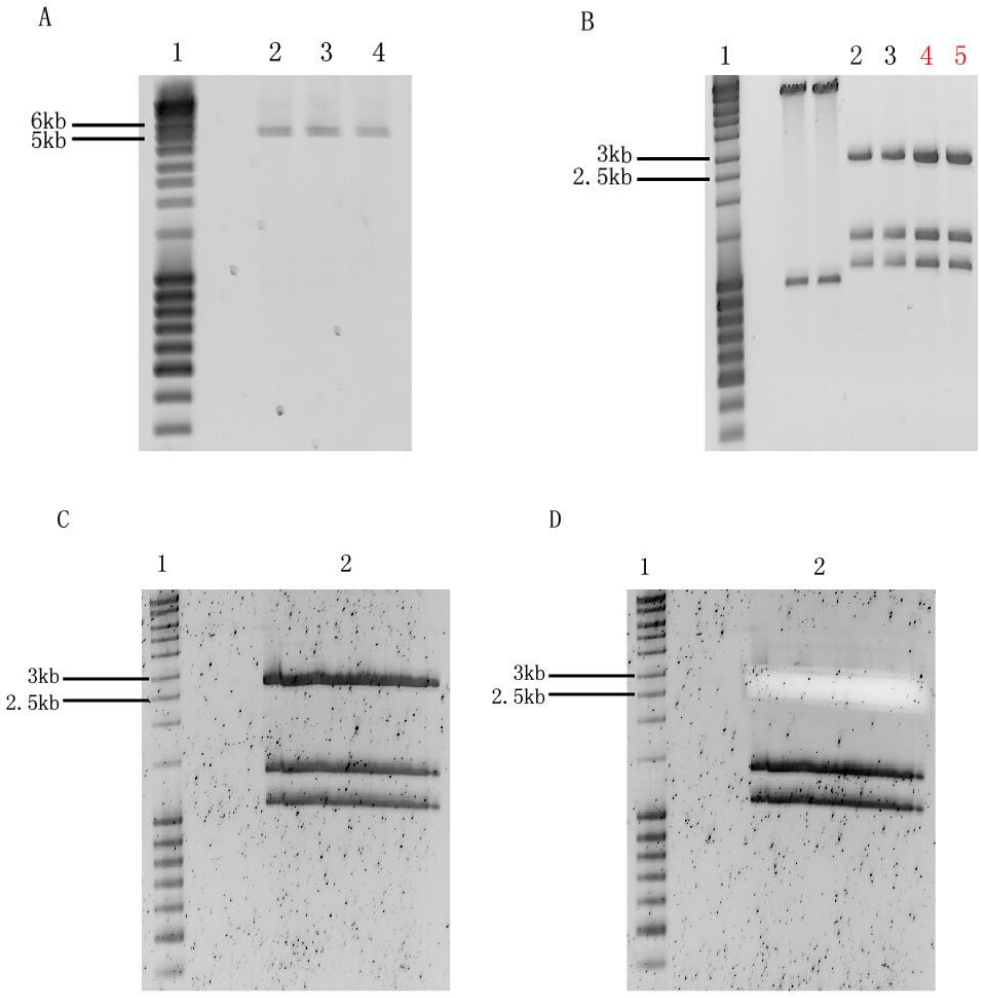
A
1
2
3
4
6kb
5kb
B
1
2
3
4
5
3kb
2. 5kb
C
1
2
3kb
2. 5kb
D
1
2
3kb
2. 5kb

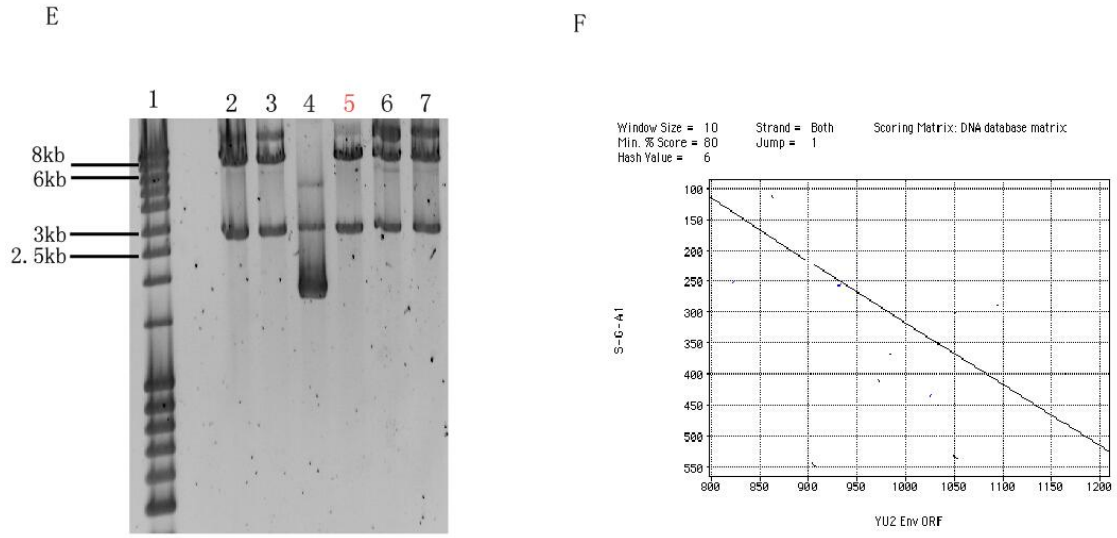

Figure 19. **A**. PCR of pUC19-YU2(S-G). 1: DNA ladder; 2-4: PCR product of pUC19-YU2(S-G) (5.3kb). **B**. Screening of pUC19-YU2(S-G) mutant clones, digested with EcoRI, SalI, and BglI. 1: DNA ladder; 4 & 5: pUC19-YU2(S-G) cut with EcoRI, SalI, and BglI. **C**. Digestion of confirmed positive pUC19-YU2(S-G) clone. 1: DNA ladder; 2: pUC19-YU2(S-G) cut with EcoRI, SalI, and BglI. **D**. Recovery of 2.7 kb fragment of pUC19-YU2(S-G). 1: DNA ladder; 2: pUC19-YU2(S-G) cut with EcoRI, SalI, and BglI. **E**. Screening of pNL-Δψ-YU2-Env(S-G), digested with EcoRI and SalI. 1: DNA ladder; 2-7: pNL-Δψ-YU2-Env(S-G). Red numbers represent positive clones. **F**. Sequence alignment data of pUC19-YU2(S-G) with pNL-Δψ-YU2-Env open reading frame.

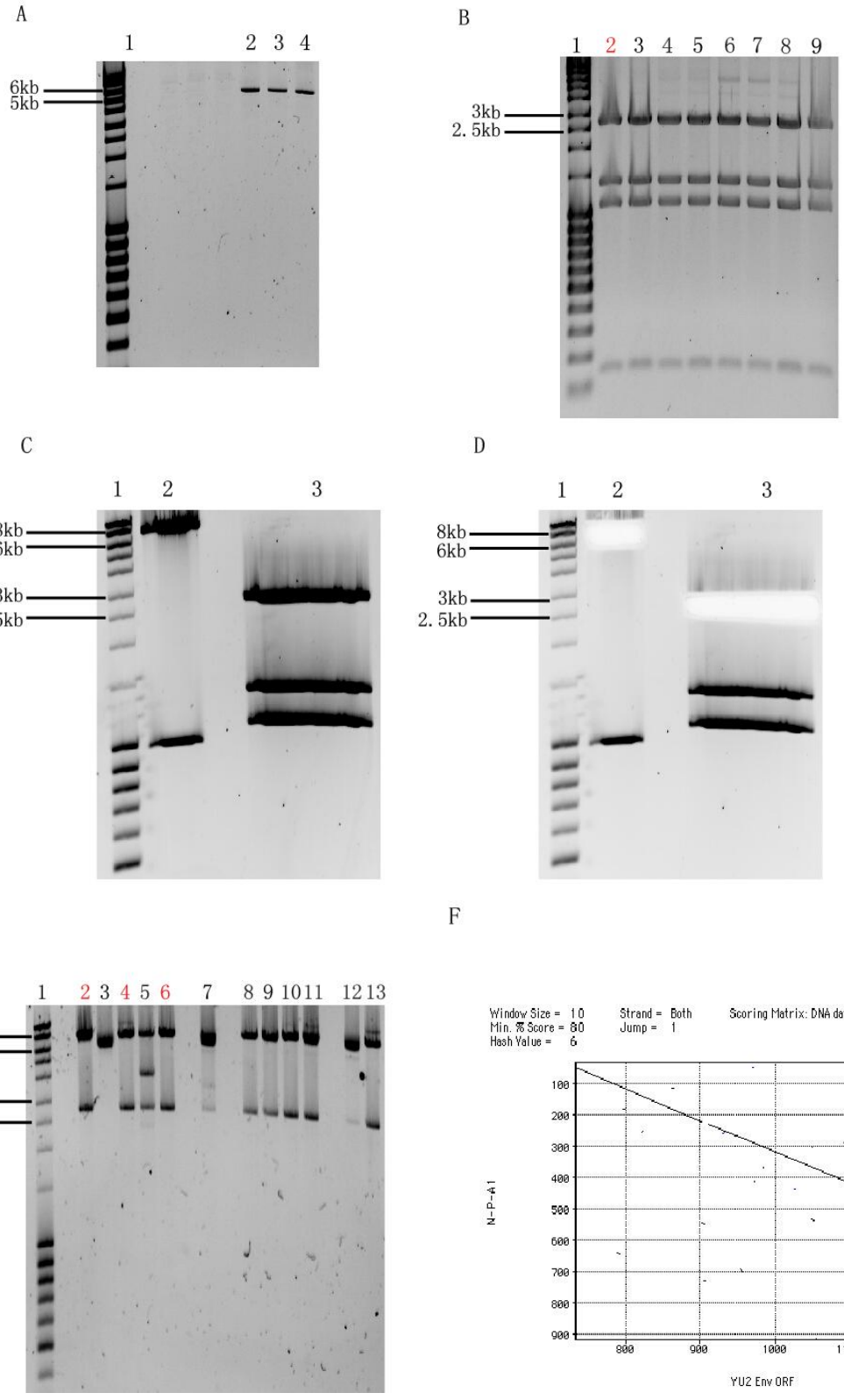
A
1 2 3 4
6kb
5kb
B
1 2 3 4 5 6 7 8 9
3kb
2.5kb
C
1 2 3
8kb
6kb
3kb
2.5kb
D
1 2 3
8kb
6kb
3kb
2.5kb
E
1 2 3 4 5 6 7 8 9 10 11 12 13
8kb
6kb
3kb
2.5kb
F
Window Size = 10
Min. % Score = 80
Hash Value = 6
Strand = Both
Jump = 1
Scoring Matrix: DNA database matrix
N-P-A1
100
200
300
400
500
600
700
800
900
800
900
1000
1100
1200
YU2 Env ORF

Figure 20. **A**. PCR of pUC19-YU2(N-P). 1: DNA ladder; 2-4: PCR product of pUC19-YU2(N-P) (5.3kb). **B**. Screening of pUC19-YU2(N-P) mutant clones, digested with EcoRI, SalI, and BglI. 1: DNA ladder; 2: pUC19-YU2(N-P) cut with EcoRI, SalI, and BglI. **C**. Digestion of pNL-Δψ-YU2-Env plasmid and confirmed positive pUC19-YU2(N-P) clone. 1: DNA ladder; 2: pNL-Δψ-YU2-Env cut with EcoRI and SalI; 3: pUC19-YU2(N-P) cut with EcoRI, SalI, and BglI. **D**. Recovery of 7.0 kb fragment of pNL-Δψ-YU2-Env. Recovery of 2.7 kb fragment of pUC19-YU2(N-P). 1: DNA ladder; 2: pNL-Δψ-YU2-Env cut with EcoRI and SalI; 3: pUC19-YU2(N-P) cut with EcoRI, SalI, and BglI. **E**. Screening of pNL-Δψ-YU2-Env(N-P), digested with EcoRI and SalI. 1: DNA ladder; 2-6: pNL-Δψ-YU2-Env(N-P). Red numbers represent positive clones. **F**. Sequence alignment data of pUC19-YU2(N-P) with pNL-Δψ-YU2-Env open reading frame.

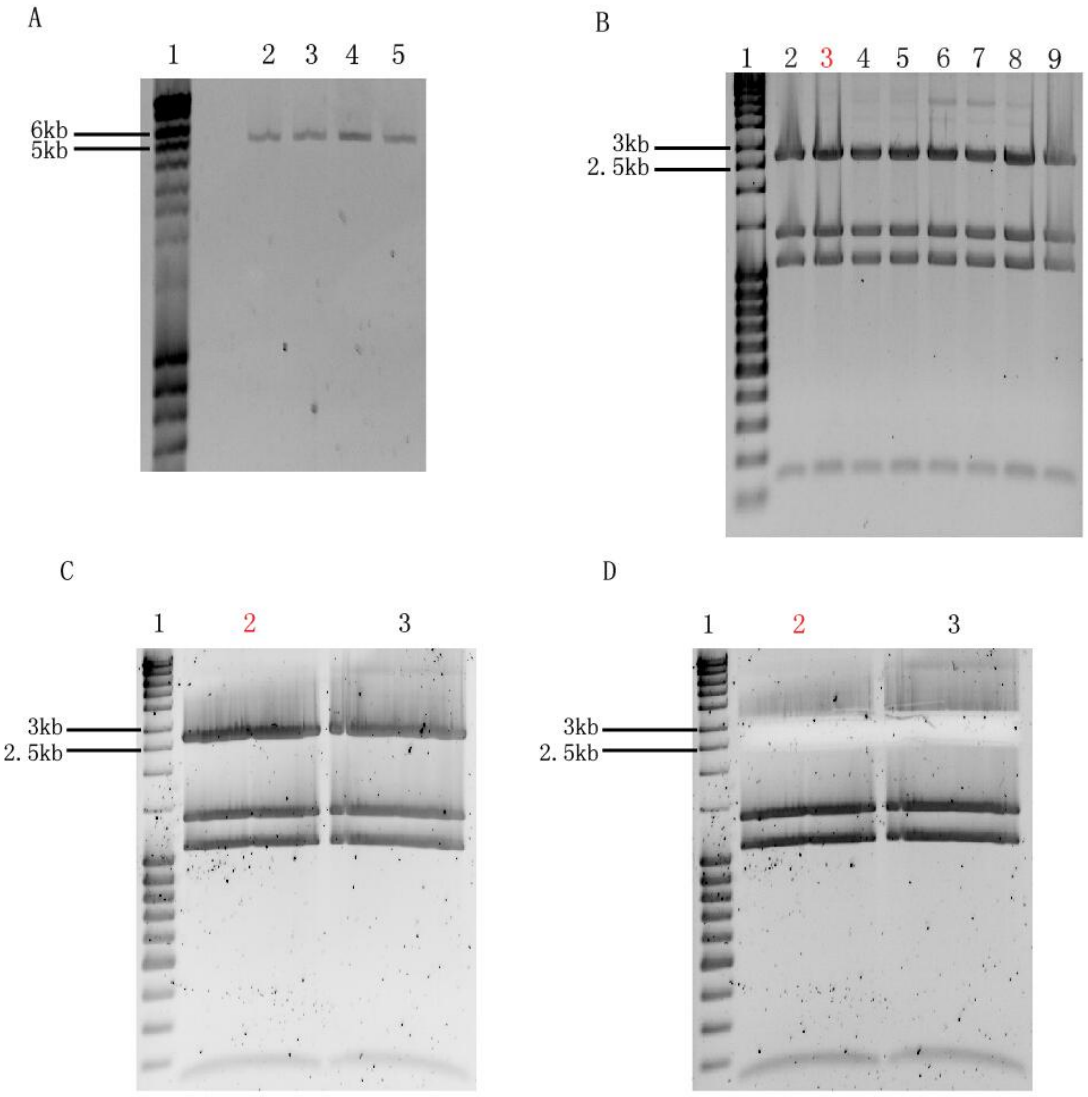
A
1 2 3 4 5
6kb
5kb
B
1 2 3 4 5 6 7 8 9
3kb
2. 5kb
C
1 2 3
3kb
2. 5kb
D
1 2 3
3kb
2. 5kb

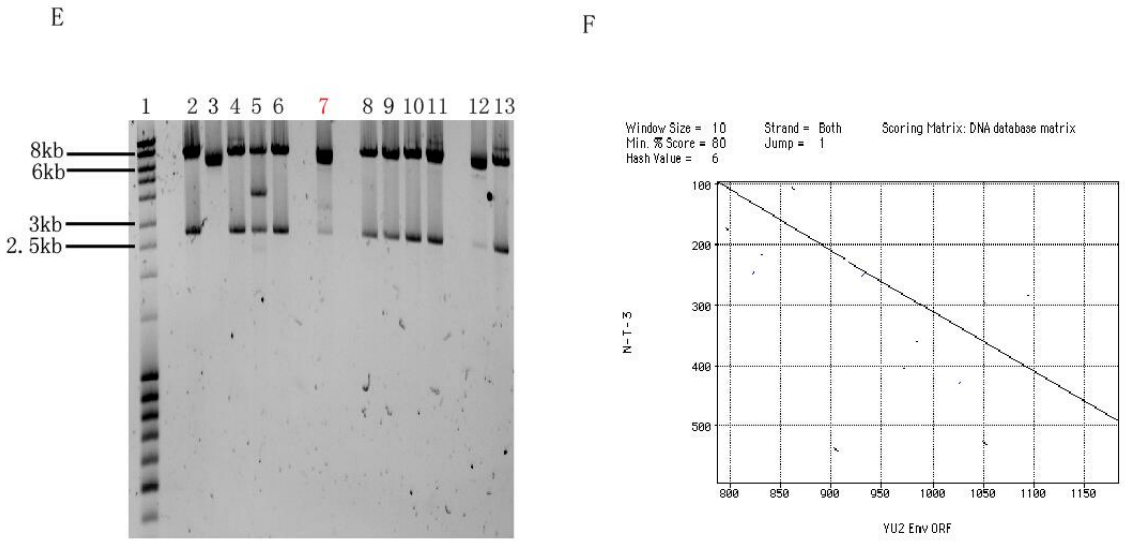

Figure 21. **A**. PCR of pUC19-YU2(N-T). 1: DNA ladder; 2-5: PCR product of pUC19-YU2(N-T) (5.3kb). **B**. Screening of pUC19-YU2(N-T) mutant clones, digested with EcoRI, SalI, and BglI. 1: DNA ladder; 3: pUC19-YU2(N-T) cut with EcoRI, SalI, and BglI. **C**. Digestion of confirmed positive pUC19-YU2(N-T) clone. 1: DNA ladder; 2: pUC19-YU2(N-T) cut with EcoRI, SalI, and BglI. **D**. Recovery of 2.7 kb fragment of pUC19-YU2(N-T). 1: DNA ladder; 2: pUC19-YU2(N-T) cut with EcoRI, SalI, and BglI. **E**. Screening of pNL-Δψ-YU2-Env(N-P), digested with EcoRI and SalI. 1: DNA ladder; 7: pNL-Δψ-YU2-Env(N-T). Red numbers represent positive clones. **F**. Sequence alignment data of pUC19-YU2(N-T) with pNL-Δψ-YU2-Env open reading frame.

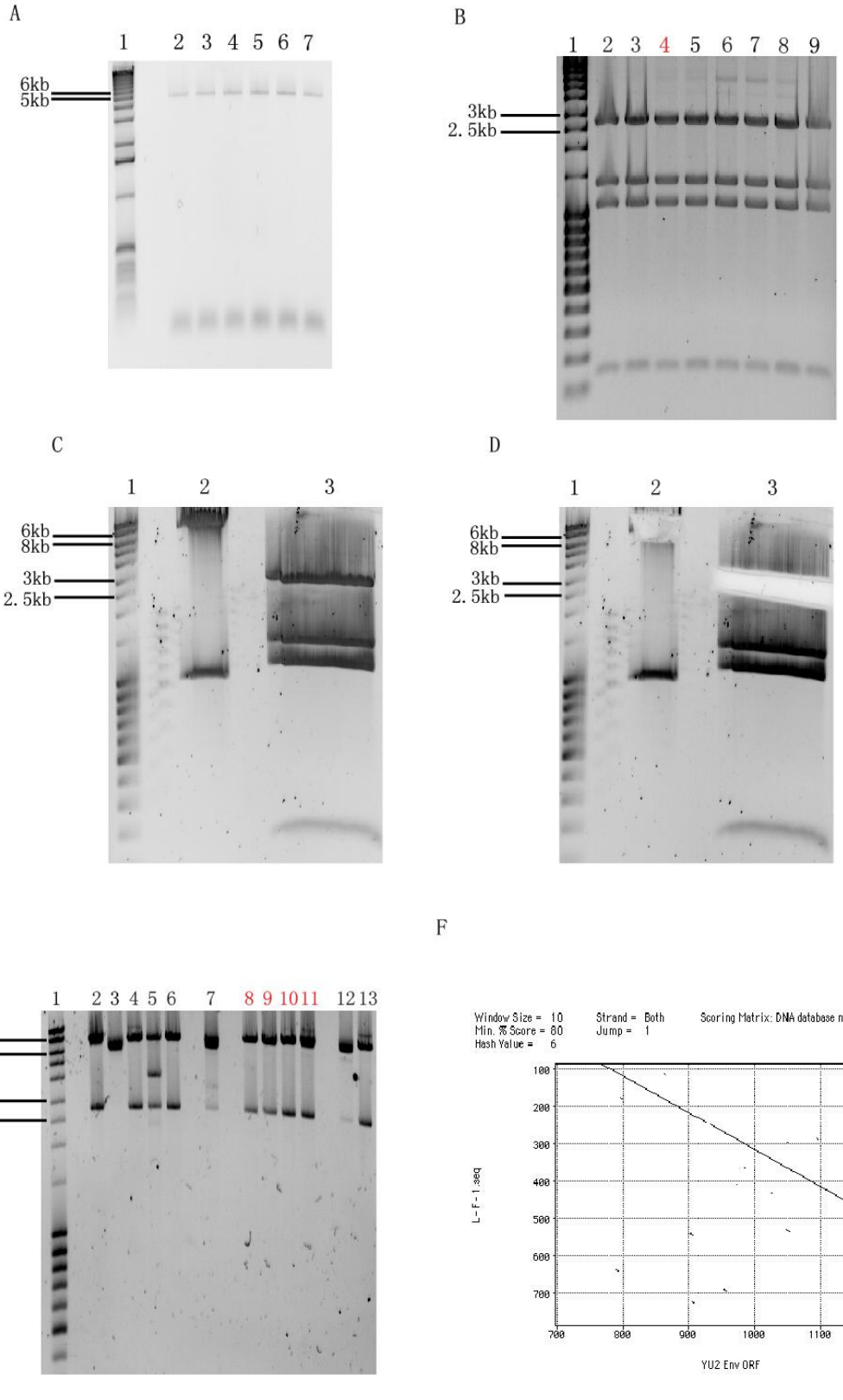
A
1 2 3 4 5 6 7
6kb
5kb
B
1 2 3 4 5 6 7 8 9
3kb
2. 5kb
C
1 2 3
6kb
8kb
3kb
2. 5kb
D
1 2 3
6kb
8kb
3kb
2. 5kb
E
1 2 3 4 5 6 7 8 9 10 11 12 13
8kb
6kb
3kb
2. 5kb
F
Window Size = 10
Min. % Score = 80
Hash Value = 6
Strand = Both
Jump = 1
Scoring Matrix: DNA database matrix
L-F-1.seq
100
200
300
400
500
600
700
700
800
900
1000
1100
1200
YU2 Env ORF

Figure 22. **A**. PCR of pUC19-YU2(L-F). 1: DNA ladder; 2-7: PCR product of pUC19-YU2(L-F) (5.3kb). **B**. Screening of pUC19-YU2(L-F) mutant clones, digested with EcoRI, SalI, and BglI. 1: DNA ladder; 4: pUC19-YU2(L-F) cut with EcoRI, SalI, and BglI. **C**. Digestion of pNL-Δψ-YU2-Env plasmid and confirmed positive pUC19-YU2(L-F) clone. 1: DNA ladder; 2: pNL-Δψ-YU2-Env cut with EcoRI and SalI; 3: pUC19-YU2(L-F) cut with EcoRI, SalI, and BglI. **D**. Recovery of 7.0 kb fragment of pNL-Δψ-YU2-Env. Recovery of 2.7 kb fragment of pUC19-YU2(L-F). 1: DNA ladder; 2: pNL-Δψ-YU2-Env cut with EcoRI and SalI; 3: pUC19-YU2(L-F) cut with EcoRI, SalI, and BglI. **E**. Screening of pNL-Δψ-YU2-Env(L-F), digested with EcoRI and SalI. 1: DNA ladder; 8-11: pNL-Δψ-YU2-Env(L-F). Red numbers represent positive clones. **F**. Sequence alignment data of pUC19-YU2(L-F) with pNL-Δψ-YU2-Env open reading frame.

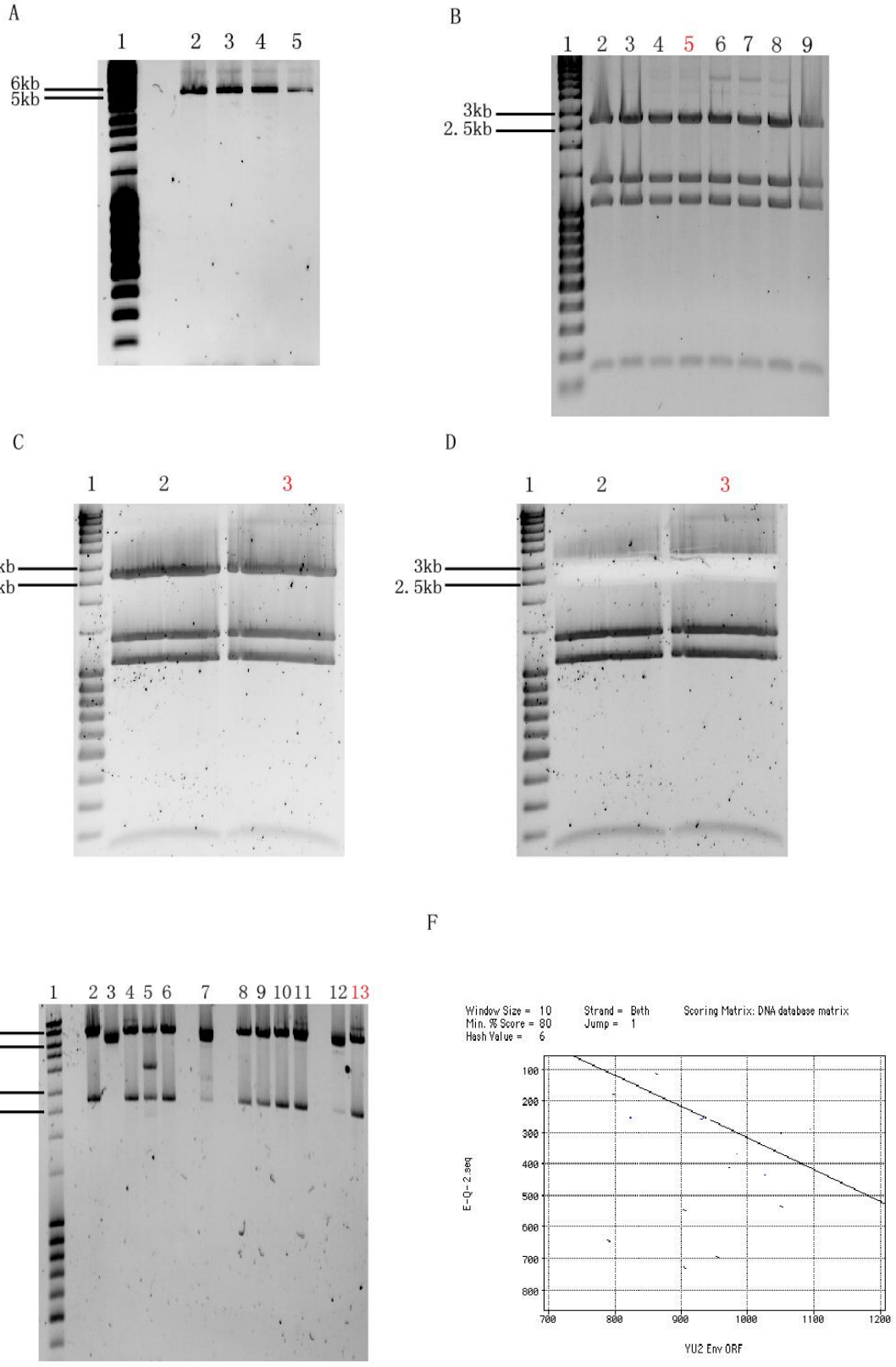
A
1 2 3 4 5
6kb
5kb
B
1 2 3 4 5 6 7 8 9
3kb
2. 5kb
C
1 2 3
3kb
2. 5kb
D
1 2 3
3kb
2. 5kb
E
1 2 3 4 5 6 7 8 9 10 11 12 13
8kb
6kb
3kb
2. 5kb
F
Window Size = 10
Min. % Score = 80
Hash Value = 6
Strand = Both
Jump = 1
Scoring Matrix: DNA database matrix
E-Q-2.seq
100
200
300
400
500
600
700
800
700
800
900
1000
1100
1200
YU2 Env ORF

Figure 23. **A**. PCR of pUC19-YU2(E-Q). 1: DNA ladder; 2-5: PCR product of pUC19-YU2(N-T) (5.3kb). **B**. Screening of pUC19-YU2(E-Q) mutant clones, digested with EcoRI, SalI, and BglI. 1: DNA ladder; 5: pUC19-YU2(E-Q) cut with EcoRI, SalI, and BglI. **C**. Digestion of confirmed positive pUC19-YU2(E-Q) clone. 1: DNA ladder; 3: pUC19-YU2(E-Q) cut with EcoRI, SalI, and BglI. **D**. Recovery of 2.7 kb fragment of pUC19-YU2(E-Q). 1: DNA ladder; 3: pUC19-YU2(E-Q) cut with EcoRI, SalI, and BglI. **E**. Screening of pNL-Δψ-YU2-Env(E-Q), digested with EcoRI and SalI. 1: DNA ladder; 12 & 13: pNL-Δψ-YU2-Env(E-Q). Red numbers represent positive clones. **F**. Sequence alignment data of pUC19-YU2(E-Q) with pNL-Δψ-YU2-Env open reading frame.

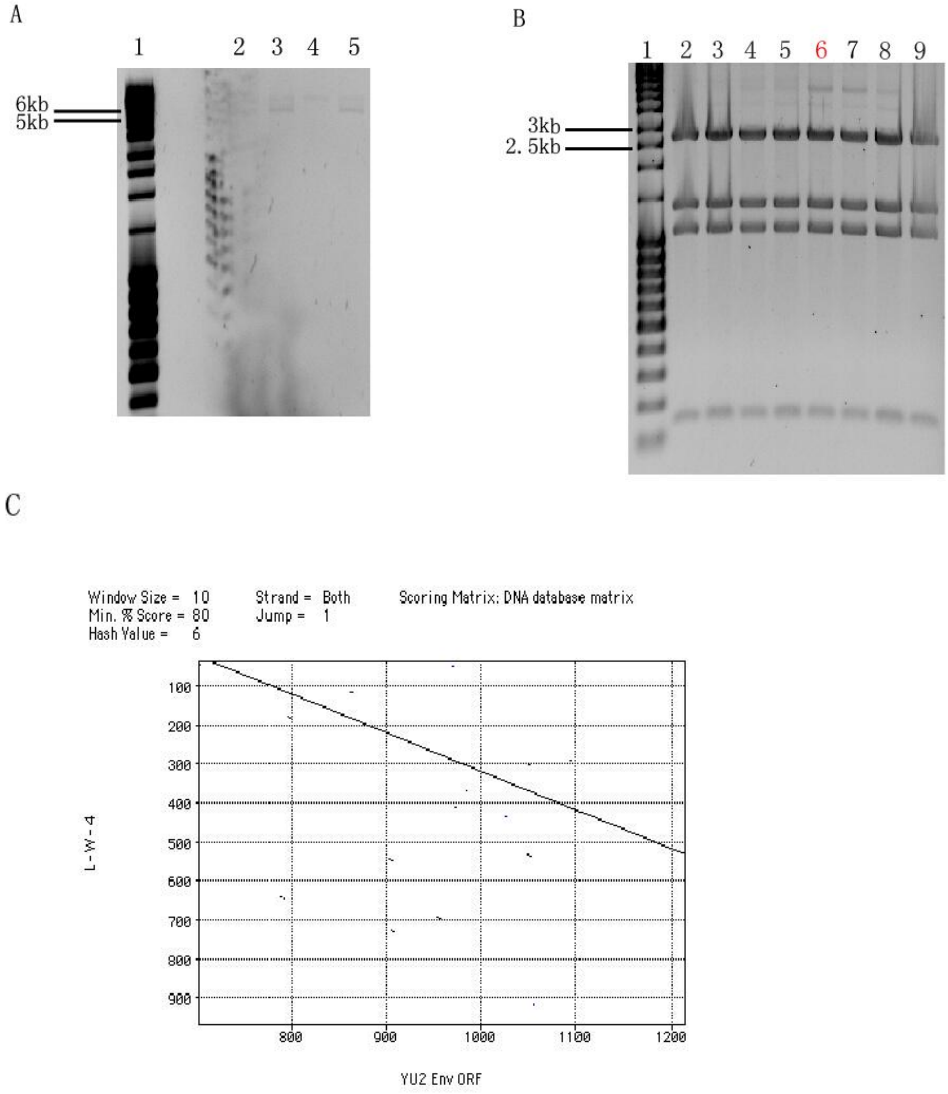

Figure 24. **A**. PCR of pUC19-YU2(L-W). 1: DNA ladder; 2-5: PCR product of pUC19-YU2(L-W) (5.3kb). **B**. Screening of pUC19-YU2(L-W) mutant clones, digested with EcoRI, SalI, and BglI. 1: DNA ladder; 6: pUC19-YU2(L-W) cut with EcoRI, SalI, and BglI. **C**. Sequence alignment data of pUC19-YU2(L-W) with pNL-Δψ-YU2-Env open reading frame.

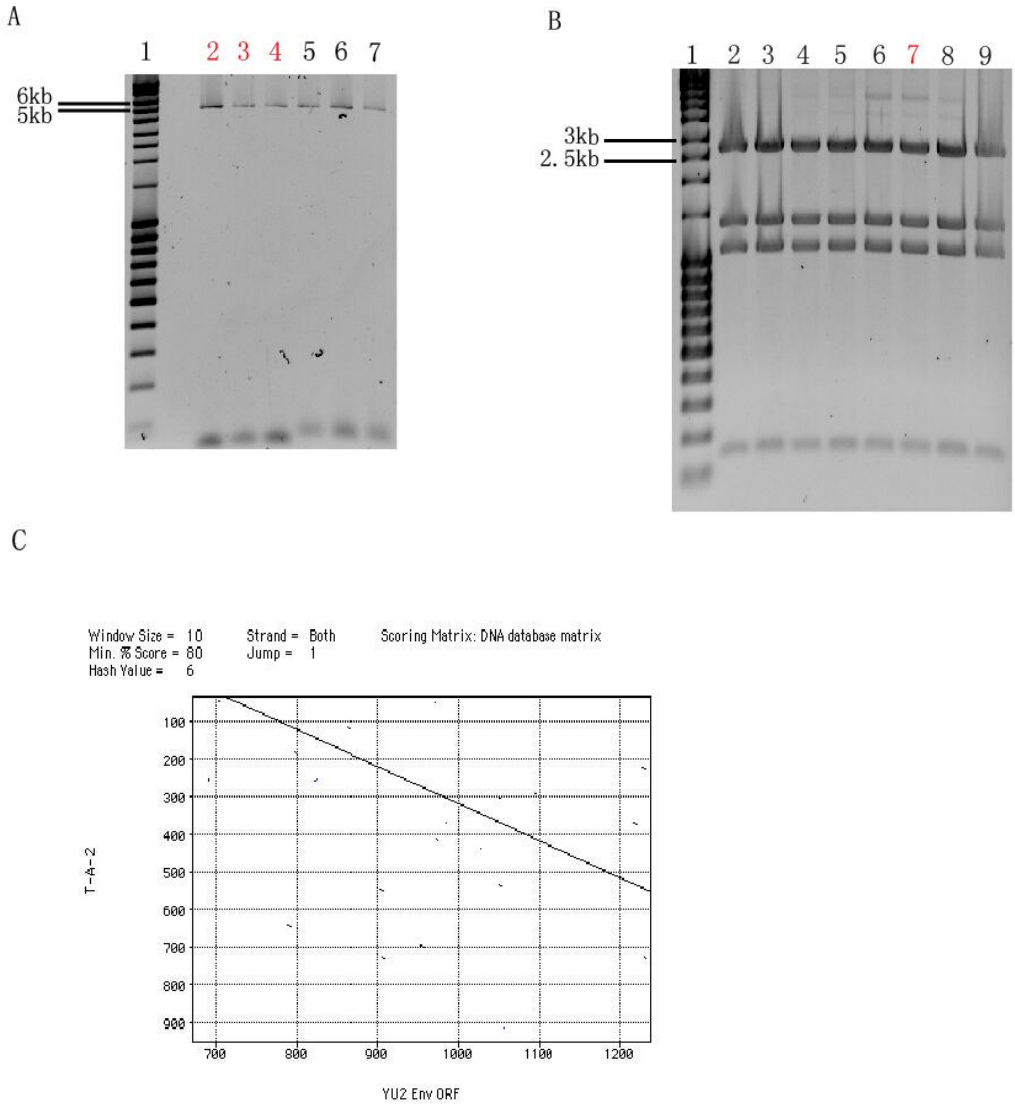

Figure 25. **A**. PCR of pUC19-YU2(T-A). 1: DNA ladder; 2-4: PCR product of pUC19-YU2(T-A) (5.3kb). **B**. Screening of pUC19-YU2(T-A) mutant clones, digested with EcoRI, SalI, and BglI. 1: DNA ladder; 7: pUC19-YU2(T-A) cut with EcoRI, SalI, and BglI. **C**. Sequence alignment data of pUC19-YU2(T-A) with pNL-Δψ-YU2-Env open reading frame.

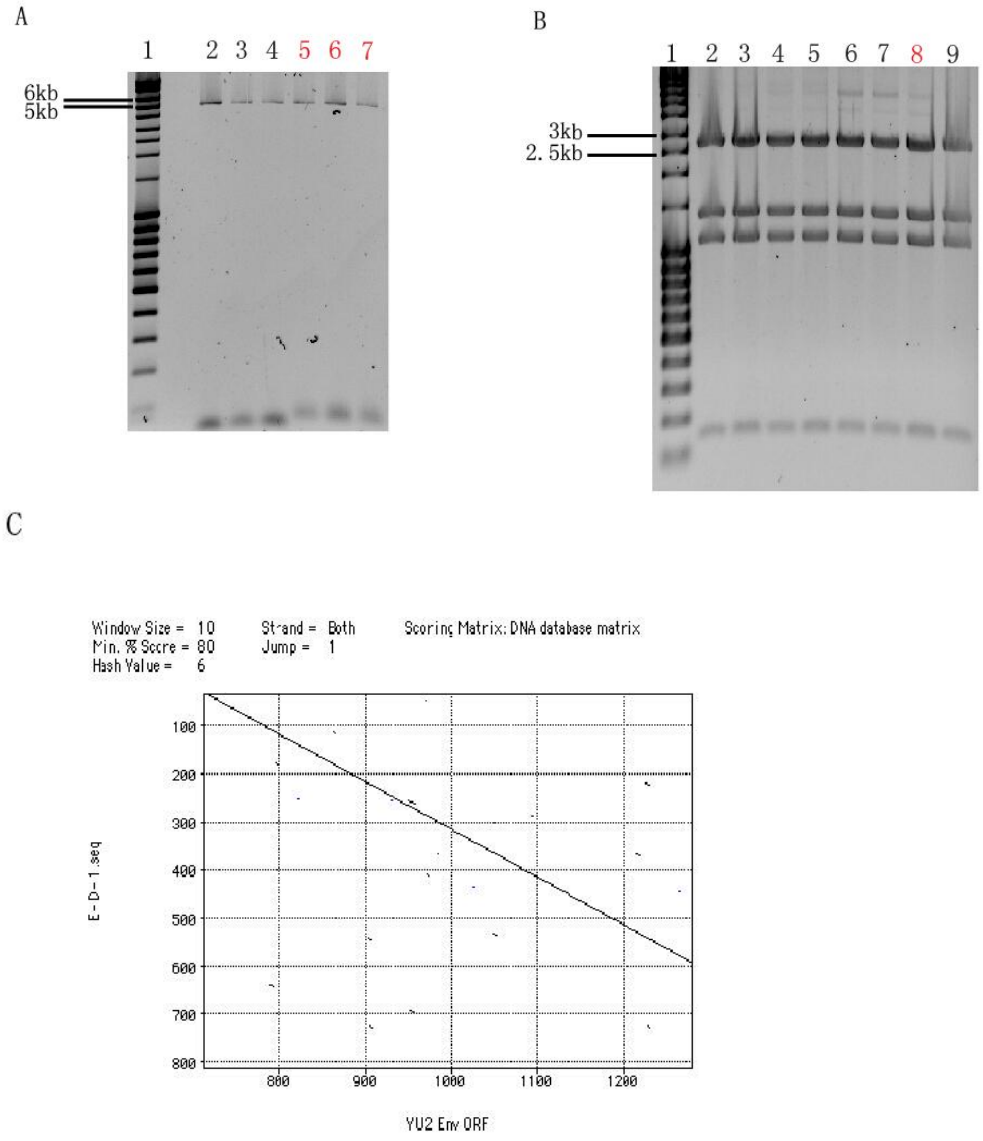

Figure 26. **A**. PCR of pUC19-YU2(E-D). 1: DNA ladder; 5-7: PCR product of pUC19-YU2(E-D) (5.3kb). **B**. Screening of pUC19-YU2(E-D) mutant clones, digested with EcoRI, SalI, and BglI. 1: DNA ladder; 8: pUC19-YU2(E-D) cut with EcoRI, SalI, and BglI. **C**. Sequence alignment data of pUC19-YU2(E-D) with pNL-Δψ-YU2-Env open reading frame.

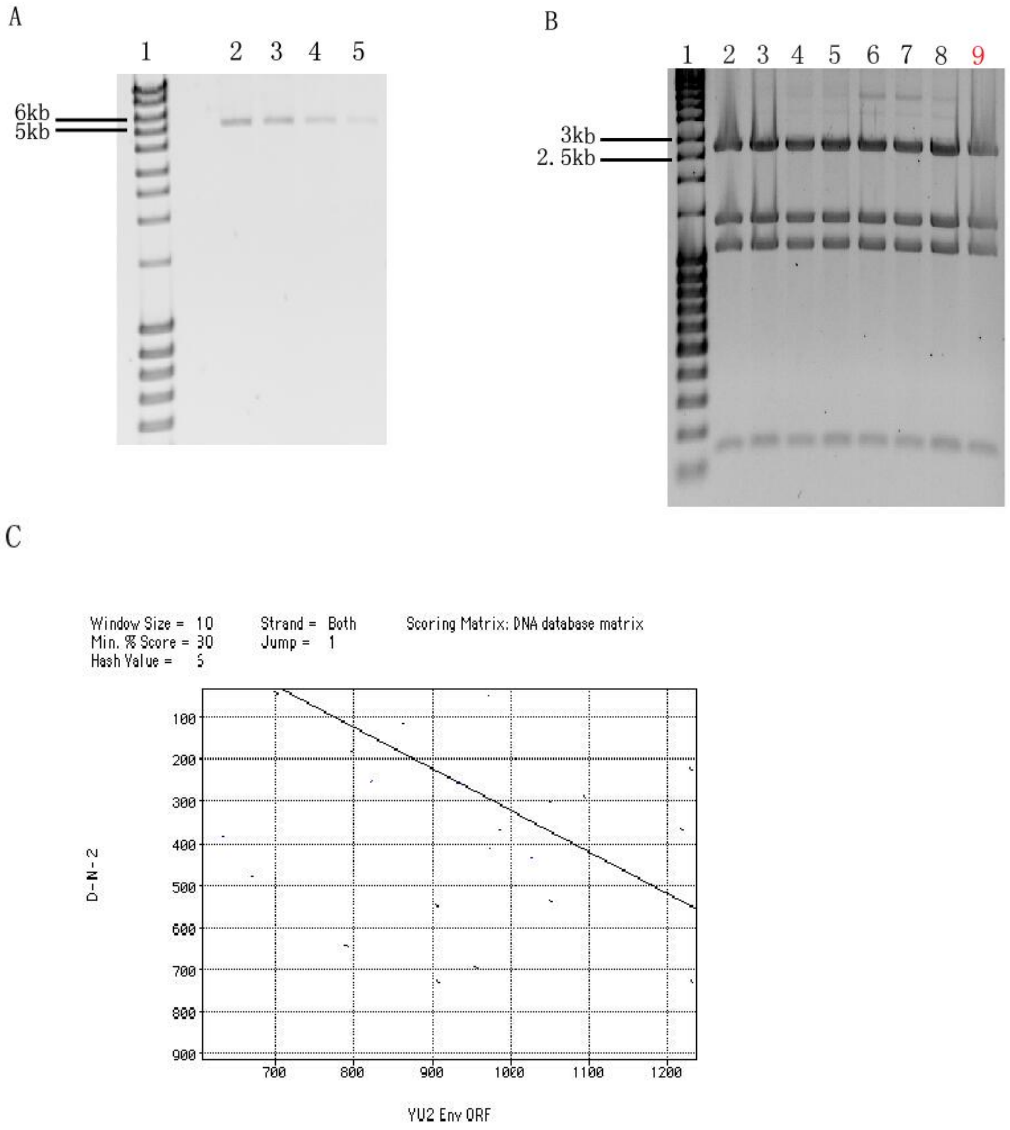

Figure 27. **A**. PCR of pUC19-YU2(D-N). 1: DNA ladder; 2-5: PCR product of pUC19-YU2(D-N) (5.3kb). **B**. Screening of pUC19-YU2(D-N) mutant clones, digested with EcoRI, SalI, and BglI. 1: DNA ladder; 9: pUC19-YU2(D-N) cut with EcoRI, SalI, and BglI. **C**. Sequence alignment data of pUC19-YU2(D-N) with pNL-Δψ-YU2-Env open reading frame.

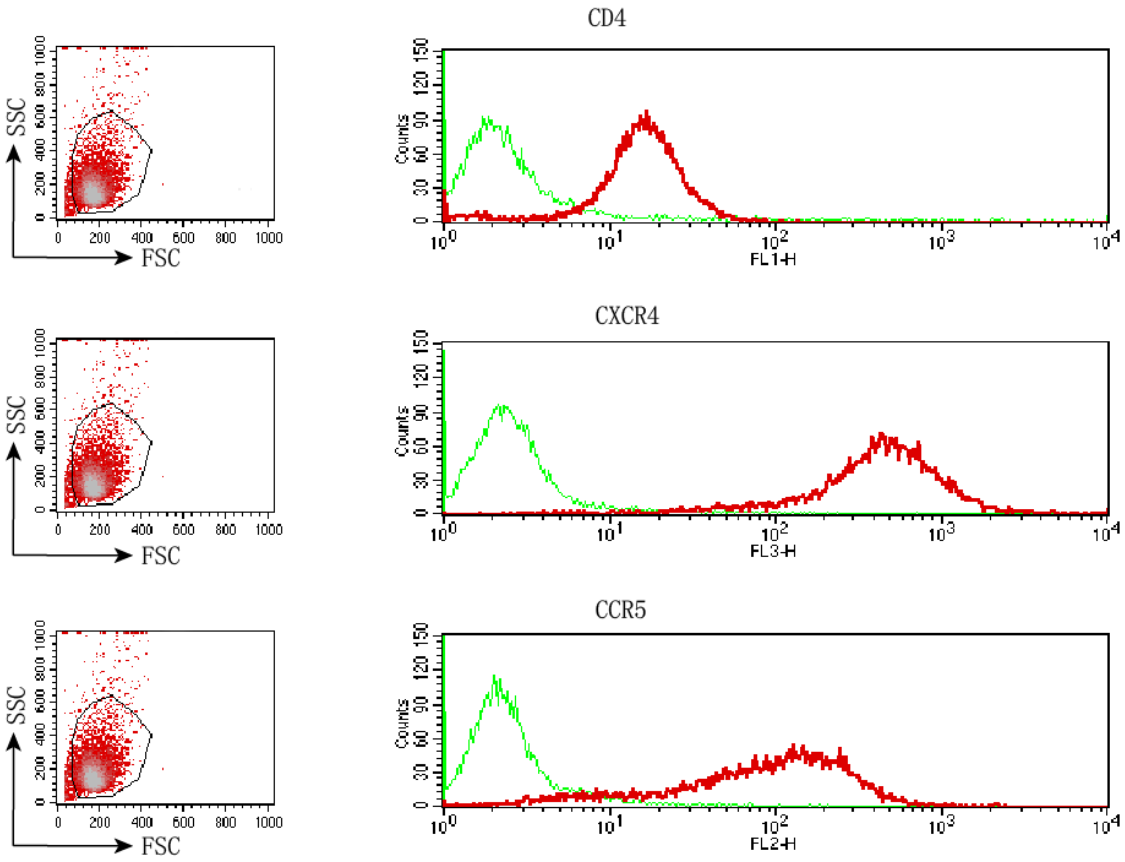

Figure 28. CD4, CXCR4, and CCR5 receptor surface staining of A3R5.7 cell line. Half million cells/tube were stained with CD4, CXCR4, CCR5 antibodies and their corresponding isotypes, respectively. Cells washed, and fixed before flow cytometry analysis. Green: Isotype. Red: Antibody.

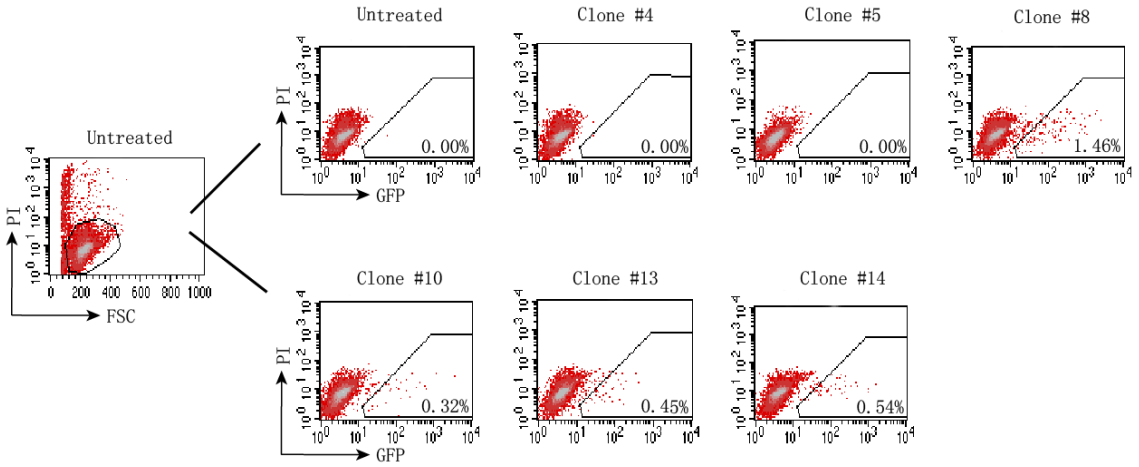

Figure 29. YU2 wildtype infectivity of A3R5.7-GFP clones. 2 x 10^5 cells/tube were infected with equal amount of YU2 wildtype viruses for 2 hours before washing. Flow cytometry data of each sample were collected every other day since 2 days post infection. A3R5.7-GFP monocolonal cell line with highest GFP expression was selected. Untreated: cells only. Clone #4-14: A3R5.7-GFP single cell clones infected with YU2 wildtype viruses.

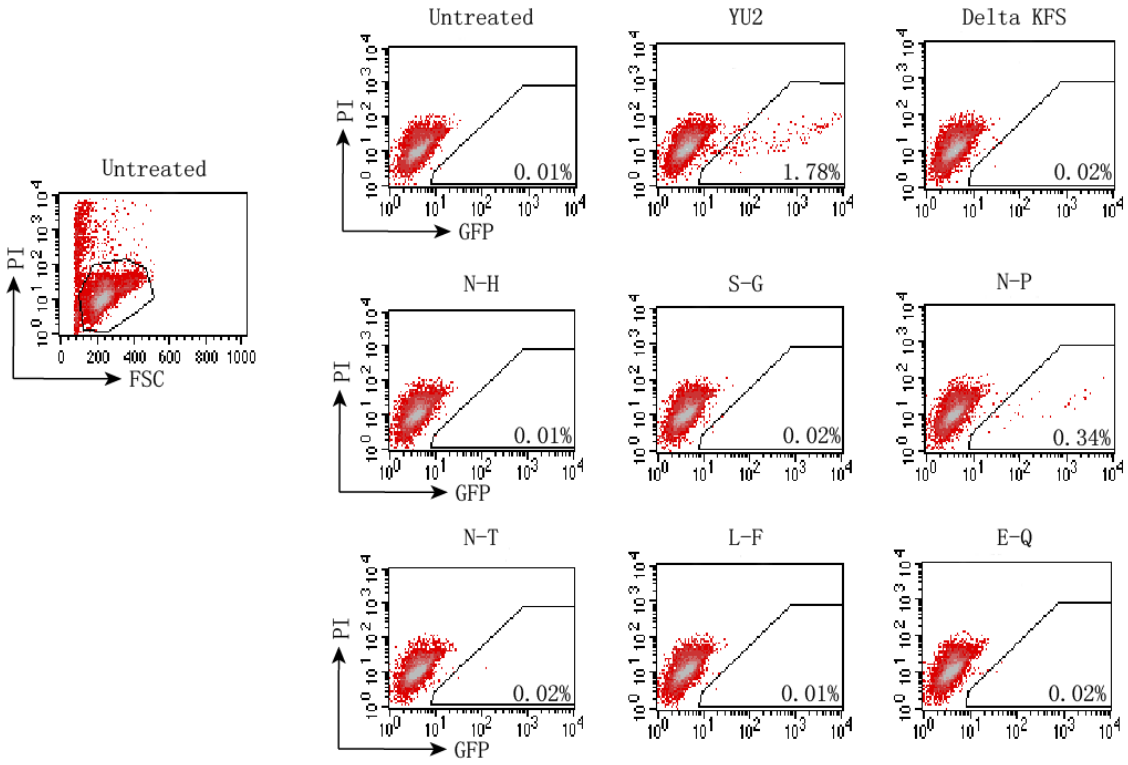

Figure 30. YU2 wildtype and YU2 mutants infectivity of A3R5.7-GFP clone #8 cells (1200g, 4 dpi). 2 x 10^5 cells/tube were infected with equal amount of p24 of pNL-Δφ-YU2-Env lentiviral particles, NL4-3 (KFS)Δgp160 lentiviral particles, and pNL-Δφ-YU2-Env mutants lentiviral particles, respectively. Infection was taken with spinoculation of 1200g at room temperature for 2 hours. Cells were then washed and incubated for 48 hours. Flow cytometry data of each sample were collected every other day since 2 days post infection. Propyl iodide (PI) was added to indicate the dead cells. GFP expression was measured to indicate the infectivity of the viruses.

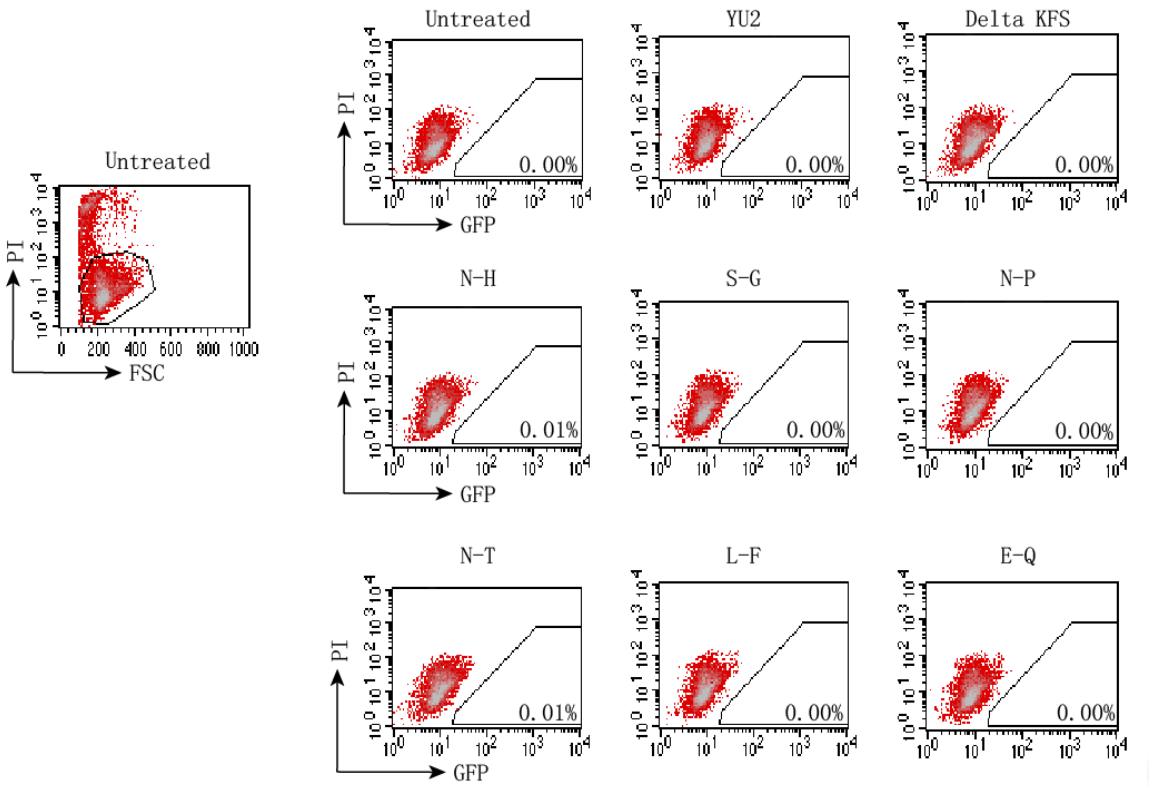

Figure 31. YU2 wildtype and YU2 mutants infectivity of Clone X cells (1200g, 4 dpi). 2 x 10^5 cells/tube were infected with equal amount of p24 of pNL-Δφ-YU2-Env lentiviral particles, NL4-3 (KFS)Δgp160 lentiviral particles, and pNL-Δφ-YU2-Env mutants lentiviral particles, respectively. Infection was taken with spinoculation of 1200g at room temperature for 2 hours. Cells were then washed and incubated for 48 hours. Flow cytometry data of each sample were collected every other day since 2 days post infection. Propyl iodide (PI) was added to indicate the dead cells. GFP expression was measured to indicate the infectivity of the viruses.

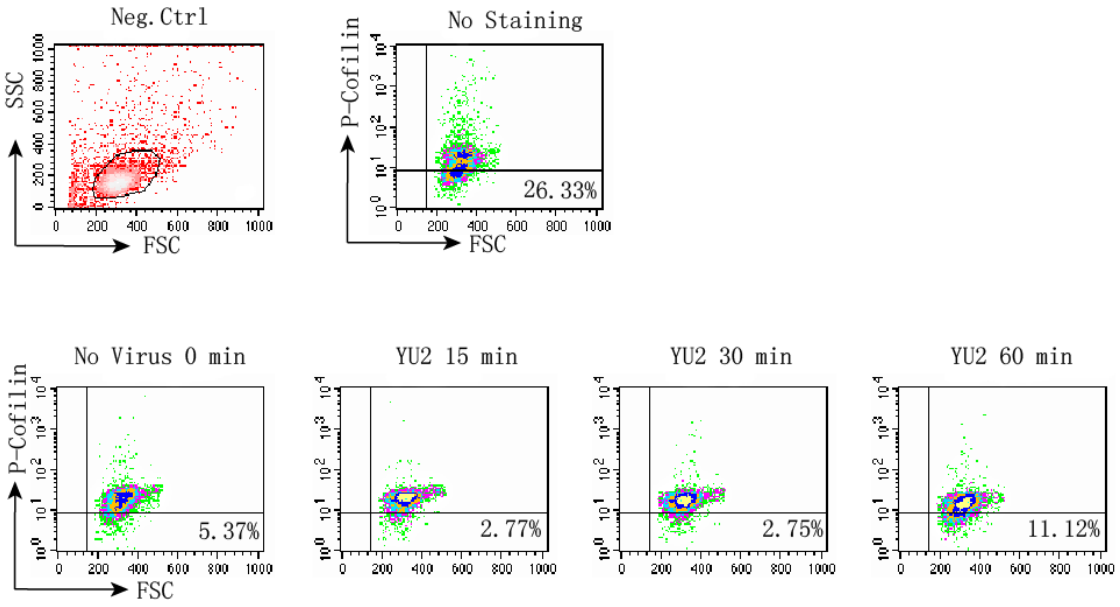

Figure 32. Flow cytometry analysis of p-cofilin intracellular staining of Memory cells with pNL-Δφ-YU2-Env stimulation. Half million memory cells purified from blood were infected with equal amount of p24 of pNL-Δφ-YU2-Env viruses at different time points ranging from 15 minutes, 30 minutes, to 60 minutes. P-cofilin antibody was added to each tube and incubated for 1 hour. Secondary antibody was added to each tube and incubated for 30 minutes. Cells for each time point were then examined by flow cytometry. No staining: cells only. No virus: Cells only + p-cofilin antibody + secondary antibody. X axis: cell size. Y axis: p-cofilin. Donor#04172014.

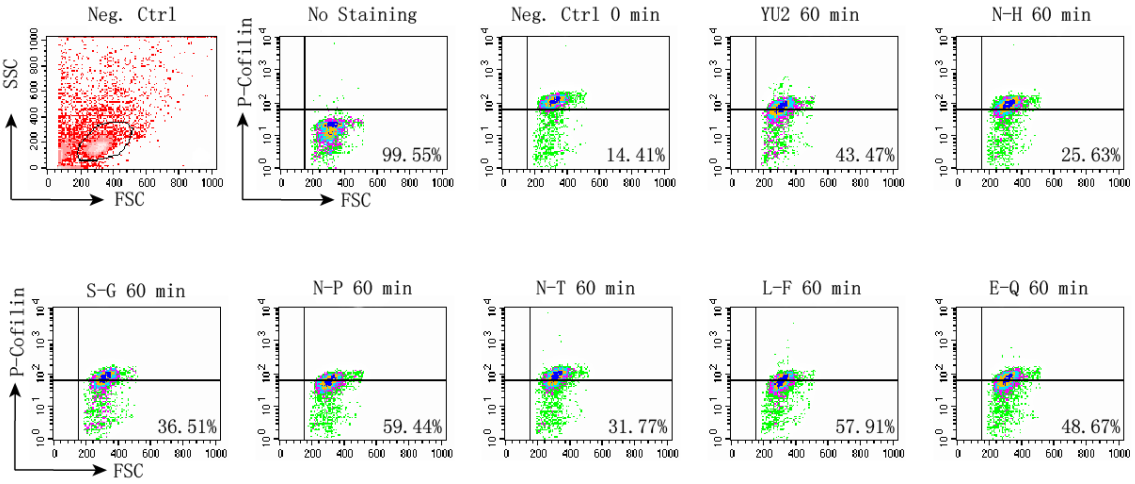

Figure 33. Flow cytometry analysis of p-cofilin intracellular staining of Memory cells with pNL-Δφ-YU2-Env and pNL-Δφ-YU2-Env mutants stimulation. Half million memory cells purified from blood were infected with equal amount of p24 of pNL-Δφ-YU2-Env and pNL-Δφ-YU2-Env mutants lentiviral particles for 60 minutes. P-cofilin antibody was added to each tube and incubated for 1 hour. Secondary antibody was added to each tube and incubated for 30 minutes. Cells for each time point were then examined by flow cytometry. No staining: Cells only + secondary antibody. Negative control: Cells only + p-cofilin antibody + secondary antibody. X axis: cell size. Y axis: p-cofilin. Donor# 04172014.

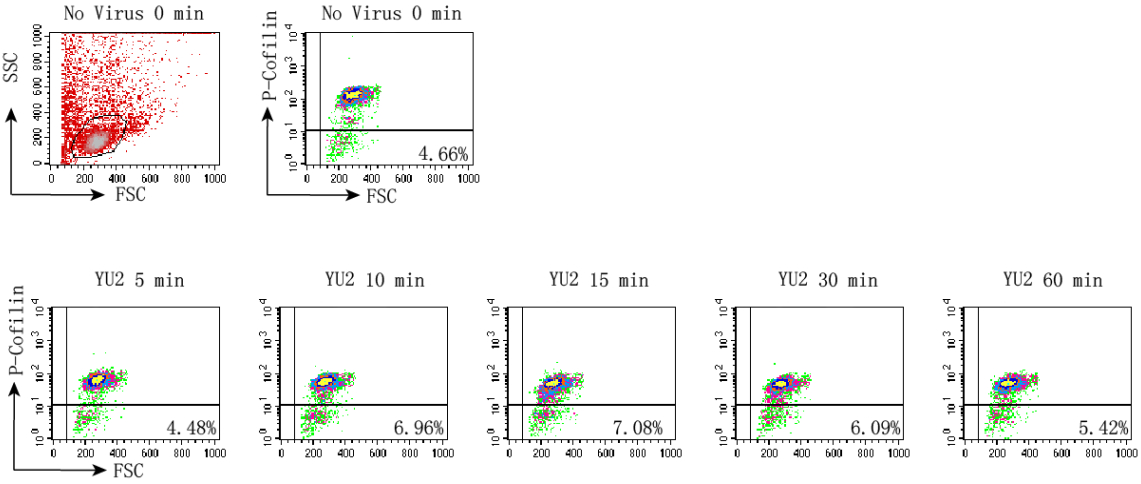

Figure 34. Flow cytometry analysis of p-cofilin intracellular staining of Memory cells with pNL-Δφ-YU2-Env stimulation. Half million memory cells purified from blood were infected with equal amount of p24 of pNL-Δφ-YU2-Env viruses at different time points ranging from 5 minutes, 10 minutes, 15 minutes, 30 minutes, to 60 minutes. P-cofilin antibody was added to each tube and incubated for 1 hour. Secondary antibody was added to each tube and incubated for 30 minutes. Cells for each time point were then examined by flow cytometry. No virus: Cells only + p-cofilin antibody + secondary antibody. X axis: cell size. Y axis: p-cofilin. Donor# 04222014.

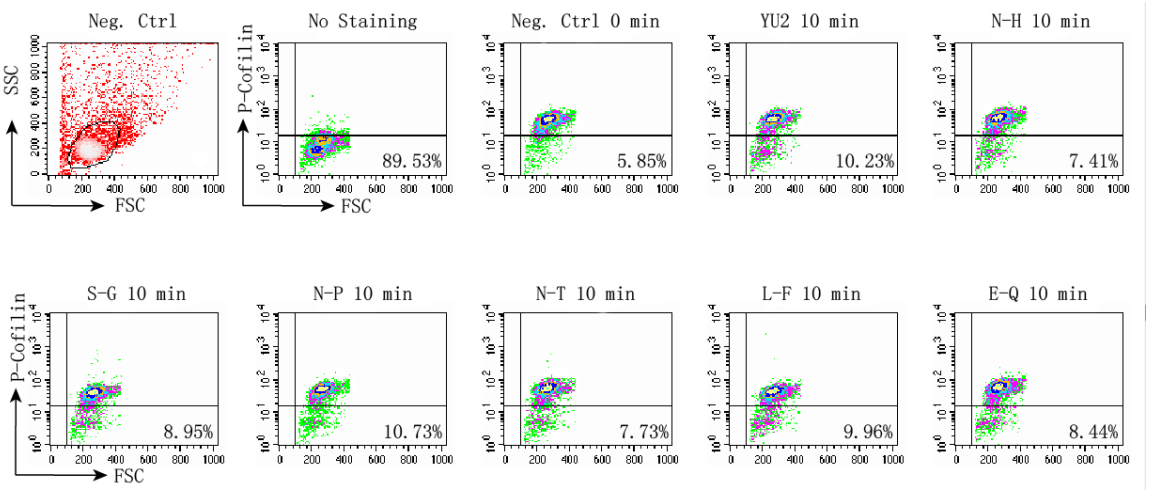

Figure 35. Flow cytometry analysis of p-cofilin intracellular staining of Memory cells with pNL-Δφ-YU2-Env and pNL-Δφ-YU2-Env mutants stimulation. Half million memory cells purified from blood were infected with equal amount of p24 of pNL-Δφ-YU2-Env and pNL-Δφ-YU2-Env mutants lentiviral particles for 10 minutes. P-cofilin antibody was added to each tube and incubated for 1 hour. Secondary antibody was added to each tube and incubated for 30 minutes. Cells for each time point were then examined by flow cytometry. No staining: Cells only + secondary antibody. Negative control: Cells only + p-cofilin antibody + secondary antibody. X axis: cell size. Y axis: p-cofilin. Donor# 04222014.

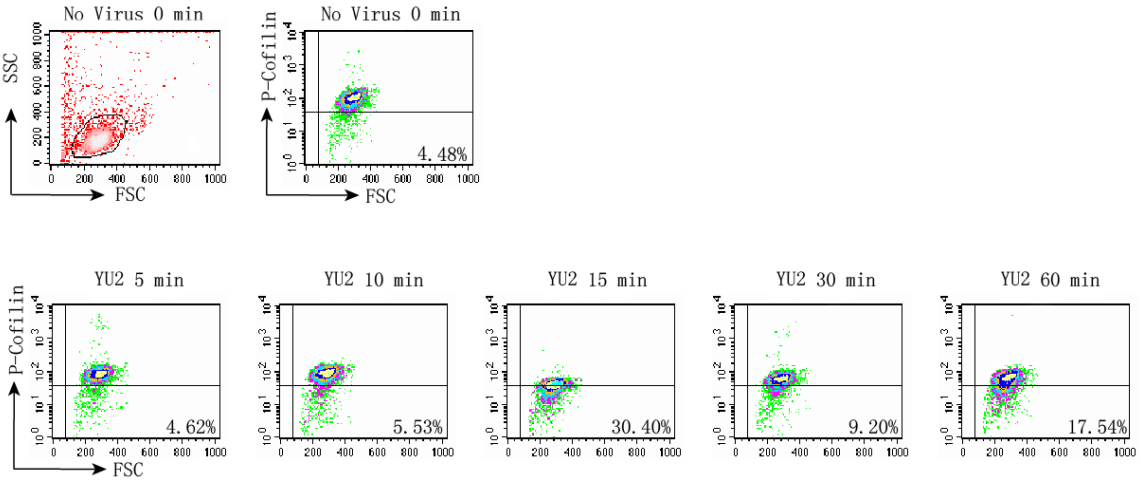

Figure 36. Flow cytometry analysis of p-cofilin intracellular staining of Memory cells with pNL-Δφ-YU2-Env stimulation. Half million memory cells purified from blood were infected with equal amount of p24 of pNL-Δφ-YU2-Env viruses at different time points ranging from 5 minutes, 10 minutes, 15 minutes, 30 minutes, to 60 minutes. P-cofilin antibody was added to each tube and incubated for 1 hour. Secondary antibody was added to each tube and incubated for 30 minutes. Cells for each time point were then examined by flow cytometry. No virus: Cells only + p-cofilin antibody + secondary antibody. X axis: cell size. Y axis: p-cofilin. Donor# 08052014.

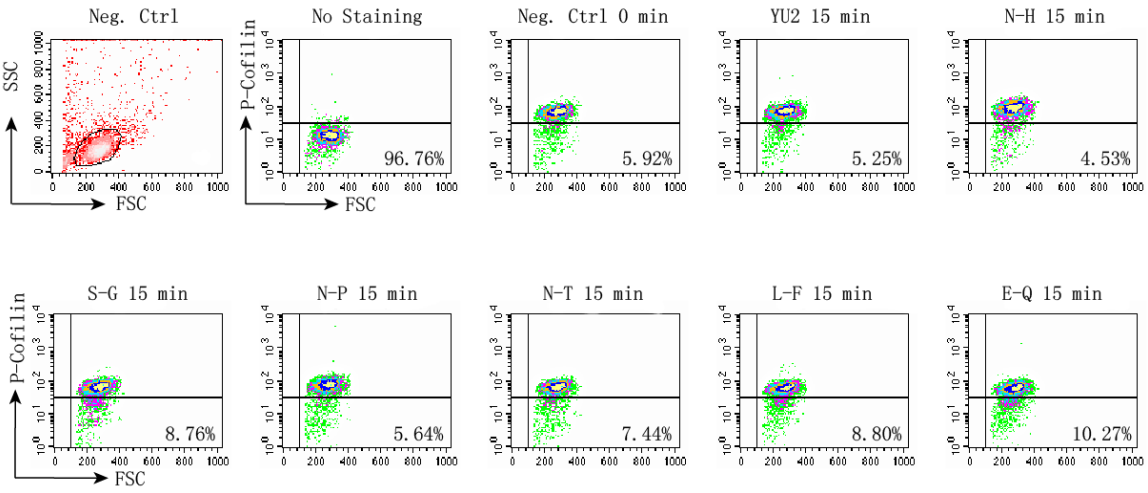

Figure 37. Flow cytometry analysis of p-cofilin intracellular staining of Memory cells with pNL-Δφ-YU2-Env and pNL-Δφ-YU2-Env mutants stimulation. Half million memory cells purified from blood were infected with equal amount of p24 of pNL-Δφ-YU2-Env and pNL-Δφ-YU2-Env mutants lentiviral particles for 15 minutes. P-cofilin antibody was added to each tube and incubated for 1 hour. Secondary antibody was added to each tube and incubated for 30 minutes. Cells for each time point were then examined by flow cytometry. No staining: Cells only + secondary antibody. Negative control: Cells only + p-cofilin antibody + secondary antibody. X axis: cell size. Y axis: p-cofilin. Donor# 08052014.

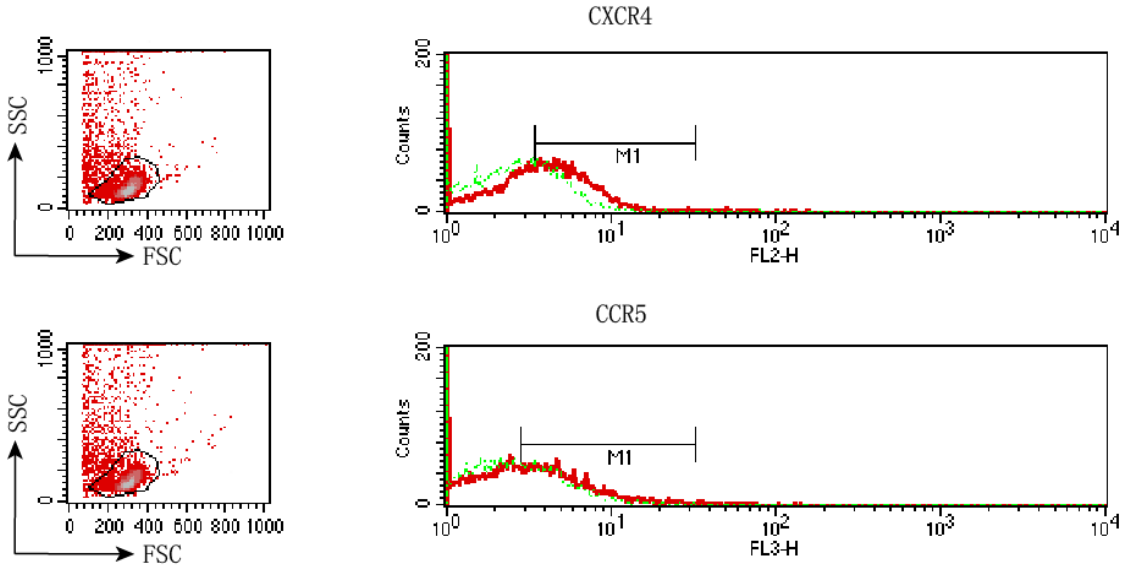

Figure 38. CXCR4 and CCR5 receptor surface staining of total CD4 T cell population purified from blood. Half million cells/tube were stained with CXCR4, CCR5 antibodies and their corresponding isotypes, respectively. Cells were washed, and fixed before flow cytometry analysis. Green: Isotype. Red: Antibody. Donor# 06182014.

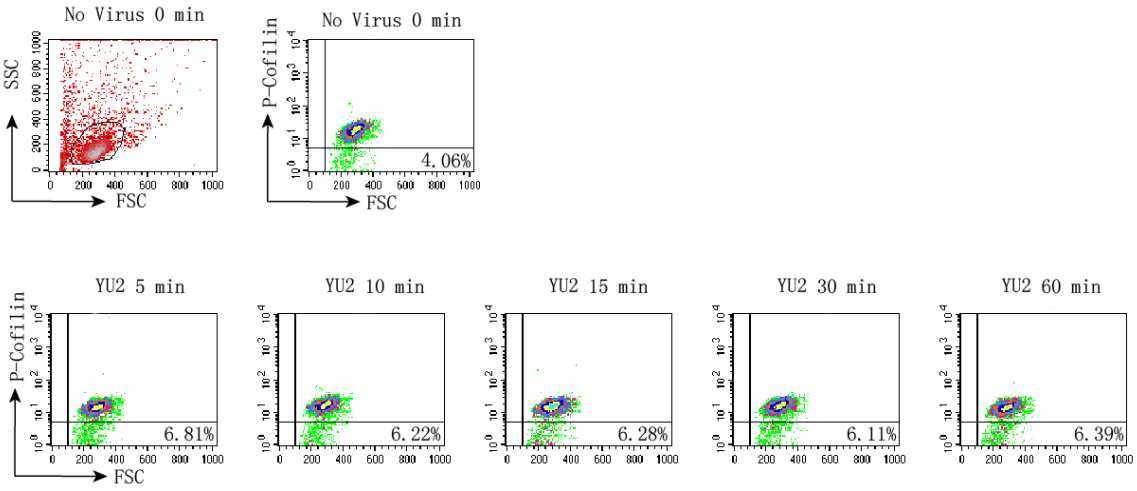

Figure 39. Flow cytometry analysis of p-cofilin intracellular staining of total CD4 T cells (CCR5-) with pNL-Δφ-YU2-Env stimulation. Half million memory cells purified from blood were infected with equal amount of p24 of pNL-Δφ-YU2-Env viruses at different time points ranging from 5 minutes, 10 minutes, 15 minutes, 30 minutes, to 60 minutes. P-cofilin antibody was added to each tube and incubated for 1 hour. Secondary antibody was added to each tube and incubated for 30 minutes. Cells for each time point were then examined by flow cytometry. No virus: Cells only + p-cofilin antibody + secondary antibody. X axis: cell size. Y axis: p-cofilin. Donor# 06182014.

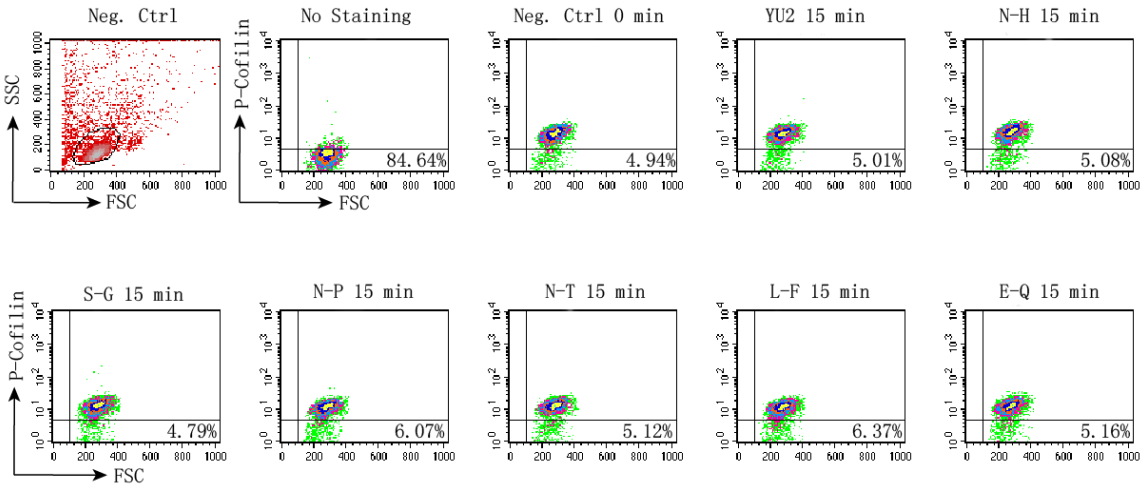

Figure 40. Flow cytometry analysis of p-cofilin intracellular staining of total CD4 T cells (CCR5-) with pNL-Δφ-YU2-Env and pNL-Δφ-YU2-Env mutants stimulation. Half million memory cells purified from blood were infected with equal amount of p24 of pNL-Δφ-YU2-Env and pNL-Δφ-YU2-Env mutants lentiviral particles for 15 minutes. P-cofilin antibody was added to each tube and incubated for 1 hour. Secondary antibody was added to each tube and incubated for 30 minutes. Cells for each time point were then examined by flow cytometry. No staining: Cells only + secondary antibody. Negative control: Cells only + p-cofilin antibody + secondary antibody. X axis: cell size. Y axis: p-cofilin. Donor# 06182014.

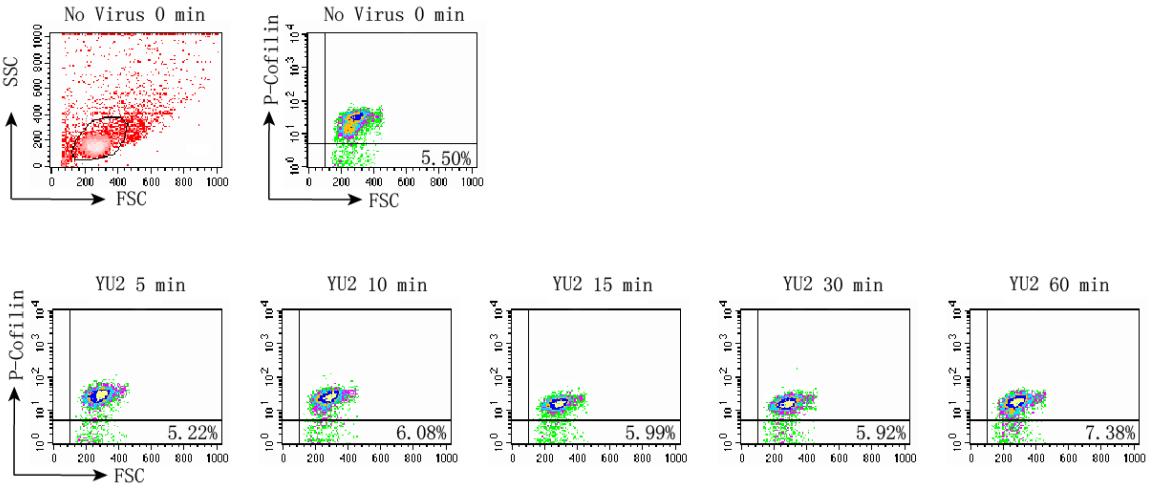

Figure 41. Flow cytometry analysis of p-cofilin intracellular staining of total CD4 T cells (CCR5-) with pNL-Δφ-YU2-Env stimulation. Half million memory cells purified from blood were infected with equal amount of p24 of pNL-Δφ-YU2-Env viruses at different time points ranging from 5 minutes, 10 minutes, 15 minutes, 30 minutes, to 60 minutes. P-cofilin antibody was added to each tube and incubated for 1 hour. Secondary antibody was added to each tube and incubated for 30 minutes. Cells for each time point were then examined by flow cytometry. No virus: Cells only + p-cofilin antibody + secondary antibody. X axis: cell size. Y axis: p-cofilin. Donor# 0722014.

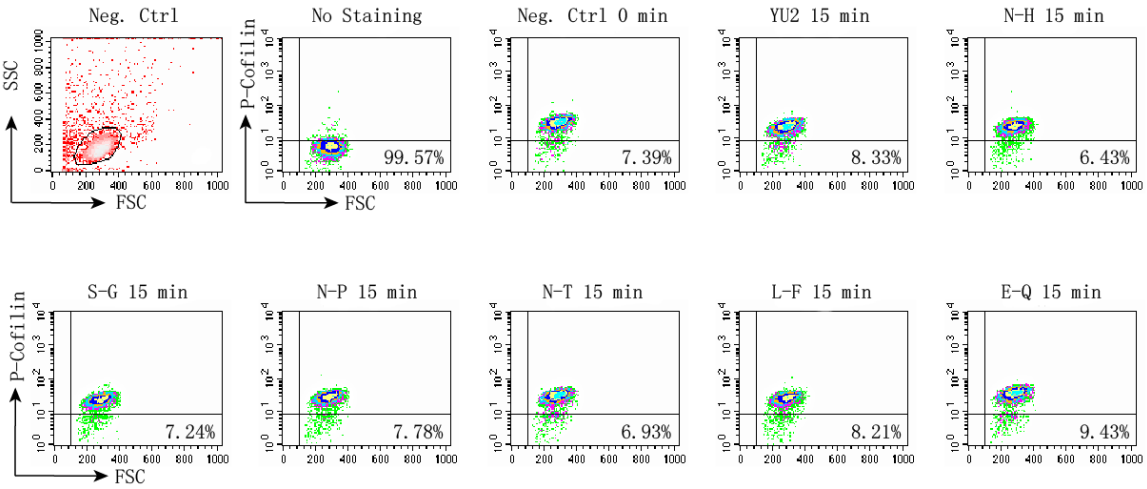

Figure 42. Flow cytometry analysis of p-cofilin intracellular staining of total CD4 T cells (CCR5-) with pNL-Δφ-YU2-Env and pNL-Δφ-YU2-Env mutants stimulation. Half million memory cells purified from blood were infected with equal amount of p24 of pNL-Δφ-YU2-Env and pNL-Δφ-YU2-Env mutants lentiviral particles for 15 minutes. P-cofilin antibody was added to each tube and incubated for 1 hour. Secondary antibody was added to each tube and incubated for 30 minutes. Cells for each time point were then examined by flow cytometry. No staining: Cells only + secondary antibody. Negative control: Cells only + p-cofilin antibody + secondary antibody. X axis: cell size. Y axis: p-cofilin. Donor# 07222014.

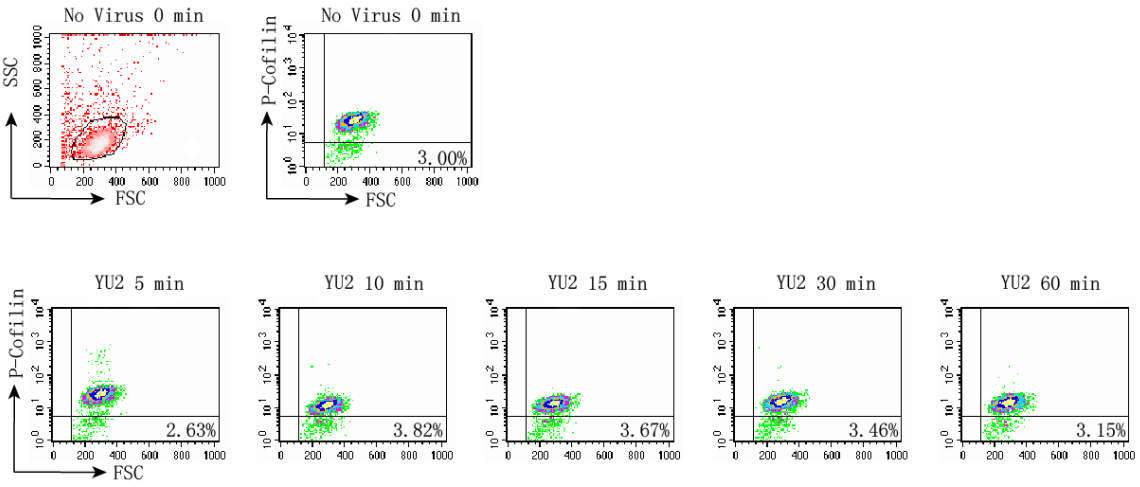

Figure 43. Flow cytometry analysis of p-cofilin intracellular staining of total CD4 T cells (CCR5-) with pNL-Δφ-YU2-Env stimulation. Half million memory cells purified from blood were infected with equal amount of p24 of pNL-Δφ-YU2-Env viruses at different time points ranging from 5 minutes, 10 minutes, 15 minutes, 30 minutes, to 60 minutes. P-cofilin antibody was added to each tube and incubated for 1 hour. Secondary antibody was added to each tube and incubated for 30 minutes. Cells for each time point were then examined by flow cytometry. No virus: Cells only + p-cofilin antibody + secondary antibody. X axis: cell size. Y axis: p-cofilin. Donor# 0826014.

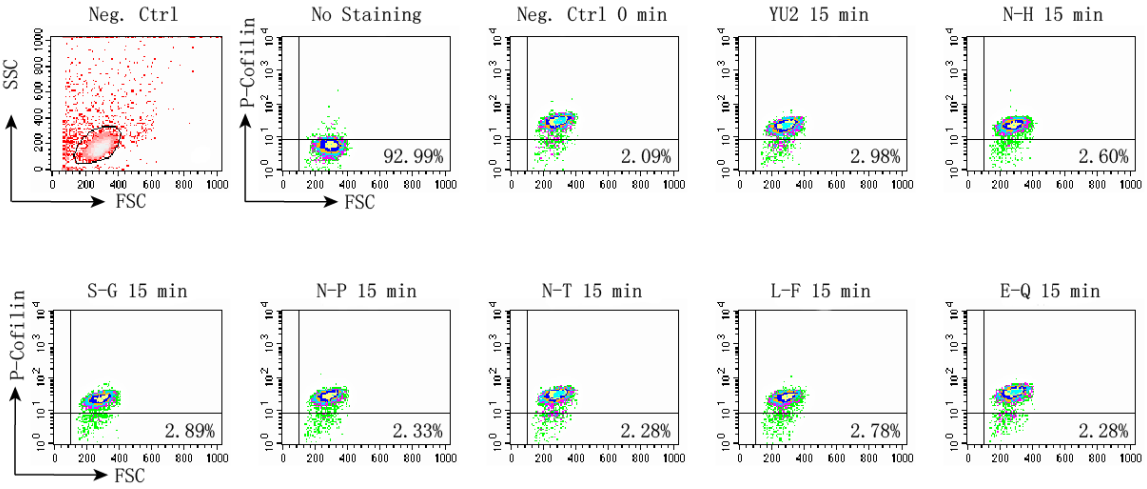

Figure 44. Flow cytometry analysis of p-cofilin intracellular staining of total CD4 T cells (CCR5-) with pNL-Δφ-YU2-Env and pNL-Δφ-YU2-Env mutants stimulation. Half million memory cells purified from blood were infected with equal amount of p24 of pNL-Δφ-YU2-Env and pNL-Δφ-YU2-Env mutants lentiviral particles for 15 minutes. P-cofilin antibody was added to each tube and incubated for 1 hour. Secondary antibody was added to each tube and incubated for 30 minutes. Cells for each time point were then examined by flow cytometry. No staining: Cells only + secondary antibody. Negative control: Cells only + p-cofilin antibody + secondary antibody. X axis: cell size. Y axis: p-cofilin. Donor# 08262014.

APPENDIX

Sequences of Six Confirmed Mutants (Data from Genewiz Company)

11 S-G

GTTCAATGGAACAGGACCATGTACAAATGTCAGCACAGTACAATGTACACAT
GGAATTAGGCCAGTAGTATCAACTCAACTGCTGTTAAATGGCAGTCTAGCAG
AAGAAGAGATAGTAATTAGATCTGAAAATTTCACAAACAATGCTAAAACTAT
AATAGTACAGCTGAACGAATCTGTAGTAATTAATTGTACAAGACCCAACAAC
AATACAAGAAAA**GGA**ATAAATATAGGACCAGGGAGAGCATTGTATACAACA
GGAGAAATAATAGGAGATATAAGACAAGCACATTGTAACCTTAGTAAAACA
CAATGGGAAAACACTTTAGAACAGATAGCTATAAAATTAAAAGAACAATTTG
GGAATAATAAAACAATAATCTTTAATCCATCCTCAGGAGGGGACCCAGAAAT
TGTAACACACAGTTTTAATTGTGGAGGGGAATTTTTCTACTGTAATTCAACAC
AACTGTTTACTTGGAATGATACTAGAAAGTTAAATAACACTGGAAGAAATAT
CACACTCCCATGTAGAATAAAACAAATTATAAATATGTGGCAGGAAGTAGGA
AAAGCAATGTATGCCCCTCCCATCAGAGGACAAATTAGATGTTCATCAAATA
TTACAGGGCTGCTATTAACAAGAGATGGTGGTAAGGACACGAACGGGACTGA
GATCTTCAGACCTGGAGGAGGAGATATGAGGGACAATTGGAGAAGTGAATT
ATATAAATATAAAGTAGTAAAAATTGAACCATTAGGAGTAGCACCCACCAAG
GCAAAGAGAAGAGTGGTGCAGAGAGAAAAAAGAGCAGTGGGACTAGGAGCT
TTGTTCCTTGGGTTCTTGGGAGCAGCAGGAAGCACTATGGGCGCAGCGTCAA
TAACGCTGACGGTACAGGCCAGACAATTATTGTCTGGTATAGTGCAACAGCA
GAACAATCTGCTGAGGGCTATTGAGGCGCAACAGCACCTGTTGCAACTCACA
GTCTGGGGCATCAAGCAGCTCCAGGCA

13 N-H

GTTCAATGGAACAGGACCATGTACAAATGTCAGCACAGTACAATGTACACAT
GGAATTAGGCCAGTAGTATCAACTCAACTGCTGTTAAATGGCAGTCTAGCAG
AAGAAGAGATAGTAATTAGATCTGAAAATTTCACAAACAATGCTAAAACTAT
AATAGTACAGCTGAACGAATCTGTAGTAATTAATTGTACAAGACCCAACAAC
AATACAAGAAAAAGTATA**CAC**ATAGGACCAGGGAGAGCATTGTATACAACA
GGAGAAATAATAGGAGATATAAGACAAGCACATTGTAACCTTAGTAAAACA
CAATGGGAAAACACTTTAGAACAGATAGCTATAAAATTAAAAGAACAATTTG
GGAATAATAAAACAATAATCTTTAATCCATCCTCAGGAGGGGACCCAGAAAT
TGTAACACACAGTTTTAATTGTGGAGGGGAATTTTTCTACTGTAATTCAACAC

AACTGTTTACTTGGAATGATACTAGAAAGTTAAATAACACTGGAAGAAATAT
CACACTCCCATGTAGAATAAA

13 N-P

AGTTCAATGGAACAGGACCATGTACAAATGTCAGCACAGTACAATGTACACA
TGGAATTAGGCCAGTAGTATCAACTCAACTGCTGTTAAATGGCAGTCTAGCA
GAAGAAGAGATAGTAATTAGATCTGAAAATTTCACAAACAATGCTAAAACTA
TAATAGTACAGCTGAACGAATCTGTAGTAATTAATTGTACAAGACCCAACAA
CAATACAAGAAAAAGTATA**CCA**ATAGGACCAGGGAGAGCATTGTATACAAC
AGGAGAAATAATAGGAGATATAAGACAAGCACATTGTAACCTTAGTAAAAC
ACAATGGGAAAACACTTTAGAACAGATAGCTATAAAATTAAAAGAACAATTT
GGGAATAATAAAACAATAATCTTTAATCCATCCTCAGGAGGGGACCCAGAAA
TTGTAACACACAGTTTTAATTGTGGAGGGGAATTTTTCTACTGTAATTCAACA
CAACTGTTTACTTGGAATGATACTAGAAAGTTAAATAACACTGGAAGAAATA
TCACACTCCCATGTAGAATAAAACAAATTATAAATATGTGGCAGGAAGTAGG
AAAAGCAATGTATGCCCCTCCCATCAGAGGACAAATTAGATGTTCATCAAAT
ATTACAGGGCTGCTATTAACAAGAGATGGTGGTAAGGACACGAACGGGACTG
AGATCTTCAGACCTGGAGGAGGAGATATGAGGGACAATTGGAGAAGTGAAT
TATATAAATATAAAGTAGTAAAAATTGAACCATTAGGAGTAGCACCCACCAA
GGCAAAGAGAAGAGTGGTGCAGAGAGAAAAAAGAGCAGTGGGACTAGGAG
CTTTGTTCCTTGGGTTCTTGGGAGCAGCAGGAAGCACTATGGGCGCAGCGTC
AATAACGCTGACGGTACAGGCCAGACAATTATTGTCTGGTATAGTGCAACAG
CAGAACAATCTGCTGAGGGCTATTGAGG

13 N-T

GGAACAGGACCATGTACAAATGTCAGCACAGTACAATGTACACATGGAATTA
GGCCAGTAGTATCAACTCAACTGCTGTTAAATGGCAGTCTAGCAGAAGAAGA
GATAGTAATTAGATCTGAAAATTTCACAAACAATGCTAAAACTATAATAGTA
CAGCTGAACGAATCTGTAGTAATTAATTGTACAAGACCCAACAACAATACAA
GAAAAAGTATA**ACT**ATAGGACCCAGGGAGAGCATTGTATACAACAGGAGAA
ATAATAGGAGATATAAGACAAGCACATTGTAACCTTAGTAAAACACAATGGG
AAAACACTTTAGAACAGATAGCTATAAAATTAAAAGAACAATTTGGGAATAA
TAAAACAATAATCTTTAATCCATCCTCAGGAGGGGACCCAGAAATTGTAACA
CACAGTTTTAATTGTGGAGGGGAATTTTTCTACTGTAATTCAACACAACTGTT
TACTTGGAATGATACTAGAAAGTTAAATAACACTGGAAGAAATATCACACTC
CCATGTAGAATAAAACAAATTATAAATATGTGGCAGGAAGTAGGAAAAGCA
ATGTATGCCCCTCCCATCAGAGGACAAATTAGATGTTCATCAAATATTACAG
GGCTGCTATTAACAAGAGATGGTGGTAAGGACACGAACGGGACTGAGATCTT
CAGACCTGGAGGAGGAGATATGAGGGACAATTGGAGAAGTGAATTATATAA
ATATAAAGTAGTAAAAATTGAACCATTAGGAGTAGCACCCACCAAGGC

20 L-F

TCAATGGAACAGGACCATGTACAAATGTCAGCACAGTACAATGTACACATGG
AATTAGGCCAGTAGTATCAACTCAACTGCTGTTAAATGGCAGTCTAGCAGAA
GAAGAGATAGTAATTAGATCTGAAAATTTCACAAACAATGCTAAAACTATAA
TAGTACAGCTGAACGAATCTGTAGTAATTAATTGTACAAGACCCAACAACAA
TACAAGAAAAAGTATAAATATAGGACCAGGGAGAGCA**TTT**ATACAACAGGA
GAAATAATAGGAGATATAAGACAAGCACATTGTAACCTTAGTAAAACACAAT
GGGAAAACACTTTAGAACAGATAGCTATAAAATTAAAAGAACAATTTGGGA
ATAATAAAACAATAATCTTTAATCCATCCTCAGGAGGGGACCCAGAAATTGT
AACACACAGTTTTAATTGTGGAGGGGAATTTTTCTACTGTAATTCAACACAAC
TGTTTACTTGGAATGATACTAGAAAGTTAAATAACACTGGAAGAAATATCAC
ACTCCCATGTAGAATAAAACAAATTATAAATATGTGGCAGGAAGTAGGAAAA
GCAATGTATGCCCCTCCCATCAGAGGACAAATTAGATGTTCATCAAATATTAC
AGGGCTGCTATTAACAAGAGATGGTGGTAAGGACACGAACGGGACTGAGAT
CTTCAGACCTGGAGGAGGAGATATGAGGGACAATTGGAGAAGTGAATTATAT
AAATATAAAGTAGTAAAAATTGAACCATTAGGAGTAGCACCCACCAAGGCA
AAGAGAAGAGTGGTGCAGAGAGAAAAAAGAGCAGTGGGACTAGGAGCTTTG
TTCCTTGGGTTCTTGGGAGCAGCAGGAAGCACTATGGGCGCAGCGTCAATAA
CGCTGACGGTACAGGCCAGACAATTATTGTCTGGTATAGTGCAACAGCAGAA
CAATCTGCTGAGGGCTA

25 E-Q

GTTCAATGGAACAGGACCATGTACAAATGTCAGCACAGTACAATGTACACAT
GGAATTAGGCCAGTAGTATCAACTCAACTGCTGTTAAATGGCAGTCTAGCAG
AAGAAGAGATAGTAATTAGATCTGAAAATTTCACAAACAATGCTAAAACTAT
AATAGTACAGCTGAACGAATCTGTAGTAATTAATTGTACAAGACCCAACAAC
AATACAAGAAAAAGTATAAATATAGGACCAGGGAGAGCATTGTATACAACA
GGGA**CAA**ATAATAGGAGATATAAGACAAGCACATTGTAACCTTAGTAAAAC
ACAATGGGAAAACACTTTAGAACAGATAGCTATAAAATTAAAAGAACAATTT
GGGAATAATAAAACAATAATCTTTAATCCATCCTCAGGAGGGGACCCAGAAA
TTGTAACACACAGTTTTAATTGTGGAGGGGAATTTTTCTACTGTAATTCAACA
CAACTGTTTACTTGGAATGATACTAGAAAGTTAAATAACACTGGAAGAAATA
TCACACTCCCATGTAGAATAAAACAAATTATAAATATGTGGCAGGAAGTAGG
AAAAGCAATGTATGCCCCTCCCATCAGAGGACAAATTAGATGTTCATCAAAT
ATTACAGGGCTGCTATTAACAAGAGATGGTGGTAAGGACACGAACGGGACTG
AGATCTTCAGACCTGGAGGAGGAGATATGAGGGACAATTGGAGAAGTGAAT
TATATAAATATAAAGTAGTAAAAATTGAACCATTAGGAGTAGCACCCACCAA
GGCAAAGAGAAGAGTGGTGCAGAGAGAAAAAAGAGCAGTGGGACTAGGAG
CTTTGTTCCTTGGGTTCTTGGGAGCAGCAGGAAGCACTATGGGCGCAGCGTC
AATAACGCTGACGGTACAGGCCAGACAATTATTGTCTGGTATAGTGCAACAG
CAGA

VI. REFERENCES

Agnew, B. J., L. S. Minamide, and J. R. Bamburg. 1995. Reactivation of phosphorylated actin depolymerizing factor and identification of the regulatory site. *J Biol Chem* 270:17582-17587.

Arber, S., F. A. Barbayannis, H. Hanser, C. Schneider, C. A. Stanyon, O. Bernard, and P. Caroni. 1998. Regulation of actin dynamics through phosphorylation of cofilin by LIM-kinase. *Nature* 393:805-809.

Arrildt, Kathryn T, S. B. Joseph, and R. Swanstrom. 2012. The HIV-1 Env Protein: A Coat of Many Colors. *Curr HIV/AIDS Rep*. 9(1): 52-63.

Basmaciogullari, Stephane, G J. Babcock, D V. Ryk, W Wojtowicz, and Joseph Sodroski. 2002. Identification of conserved and variable structures in the human immunodeficiency virus gp120 glycoprotein of importance of CXCR4 binding. Journal of Virology. Vol 76(21): 10791-10800

Cao, J., Sullivan, N., Desjardin, E., Parolin, C., Robinson, J., Wyatt, R., and Sodroski, J. (1997). Replication and neutralization of human immunodeficiency virus type 1 lacking the V1 and V2 variable loops of the gp120 envelope glycoprotein. *Journal of Virology.***71**(12)**:** 9808-12

Cardozo, T, Kimura T, Philpott S, Weiser B, Burger H, and Zolla-Pazner S. 2007. Structural basis for coreceptor selectivity by the HIV type 1 V3 loop. *AIDS Res Hum Retroviruses*. 23(2): 415-26.

Chirmule, Narendra, and Savita Pahwa. 1996. Envelop Glycoproteins of Human Immunodeficiency Virus Type 1: Profound Influences on Immune Functions. *Microbiological Review*. Vol 60, No.2: p386-406.

Connor, R. I., and D. D. Ho. 1994. Human Immunodeficiency virus type 1 variants with increased replicative capacity develop during the asymptomatic stage before disease progression. *J. Virol*. 68:4400-4408

Cormier, E., and Dragic, T. (2002). The crown and stem of the V3 loop play distinct roles in human immunodeficiency virus type 1 envelope glycoprotein interactions with the CCR5 coreceptor. *Journal of Virology* **76**(17)**,** 8953-8957.

Costin, Joshua. M.. 2007 Cytopathic Mechanisms of HIV-1. *Virology Journal* 2007, **4**:100

Freed, Eric O, and Malcolm A. Martin. 1995. The Role of Human Immunodeficiency Virus Type 1 Envelope Glycoproteins in Virus Infection. *J Biol Chem.* 270(41):23883-6

Freed, Eric O. 2003. HIV-1 Replication. *Somat Cell Mol Genet* **26**(1-6)**,** 13-33.

Freed, Eric O. 1998. HIV-1 Gag Proteins: Diverse Functions in the Virus Life Cycle. *Virology* 251: 1-15

Gallo, Robert C., and Luc Montagnier. (2003) The discovery of HIV as the cause of AIDS. *N Engl J Med*; 349:2283-2285. doi: 10.1056/NEJMp038194

Guttman, Miklos, Maria Kahn, Natalie K. Garcia, Shiu-Lok Hu, and Kelly K. Lee. 2012. Solution structure, conformational dynamics, and CD4-induced activation in full-length, glycosylated, monomeric HIV gp120. *Journal of Virology*. 86:8750-8764.

Hartley, Oliver, Per Johan Klasse, Quentin J. Sattentau, and John P. Moore. 2005. V3: HIV's Switch-Hitter. *AIDS Research and Human Retroviruses*. Vol 21(2): 171-189.

Hoffman, Noah G, Francoise Seillier-Moiseiwitsch, JaeHyung Ahn, Jason M. Walker, and Ronald Swanstrom. 2002. Variability in human immunodeficiency virus type 1 gp120 env protein linked to phenotype-associated changes in the V3 loop. *J. Virol.* 76.8: 3852-3864.

Hsu, Shang-Te D. and Alexandre M.J.J. Bonvin. 2004. Atomic Insight into the CD4 binding-induced conformational changes in HIV-1 gp120. Protein: Structure, Function, and Bioinformatics. 55: 582-593

Kallings, L. O. (2008). The first postmodern pandemic: 25 years of HIV/AIDS. *Journal of Internal Medicine,* 263: 218–243. doi: 10.1111/j.1365-2796.2007.01910.x

Koot, M., I. P. Keet, A. H. Vos, R. E. de Goede, M. T. Roos, R. A. Coutinho, F. Miedema, P. T. Schellekens, and M. Tersmette. 1993. Prognostic value of HIV-1 syncytium-inducing phenotype for rate of CD4+ cell depletion and progression to AIDS. *Ann. Intern. Med*. 118:681-688

Marsden, Matthew D., and Jerome A. Zack. 2013. HIV/AIDS eradication. *Bioorg Med Chem Lett*. 23(14): 4003–4010.

Moriyama, K., K. Iida, and I. Yahara. 1996. Phosphorylation of Ser-3 of cofilin regulates its essential function on actin. *Genes Cells* 1:73-86.

Naif, H. M. 2013. Pathogenesis of HIV infection. *Infect Dis Rep.* 5(Suppl 1):e6. doi: 10.4081/idr.2013.s1.e6. eCollection 2013.

Nebl, G., S. C. Meuer, and Y. Samstag. 1996. Dephosphorylation of serine 3 regulates nuclear translocation of cofilin. *J Biol Chem* 271:26276-80.

Pantophlet, Ralph, and Dennis R. Burton. 2006. GP120: Target for Neutralizing HIV-1 Antibodies. *Annu. Rev. Immunol*. 24: 739-769

Richman, D. D., and S. A. Bozzette. 1994. The impact of the syncytium-inducing phenotype of human immunodeficiency virus on disease progression. *J. Infect. Dis*. 169:968-974

Romani, Bizhan, S. Engelbrecht, and R. H. Glashoff. 2010. Functions of Tat: the versatile protein of human immunodeficiency virus type 1. *Journal of General Virology*. 91:1-12

Samstag Y., C. Eckerskorn, S. Wesselborg, S. Henning, R. Wallich and S. C. Meuer. 1994. Costimulatory signals for human T-cell activation induce nuclear translocation of pp19/cofilin. *Proc Natl Acad Sci U S A* 91:4494-4498.

Samstag, Y., S. M. Eibert, M. Klemke, and G. H. Wabnitz. 2003. Actin cytoskeletal dynamics in T lymphocyte activation and migration. *J Leukoc Viol* 73:30-48.

Sander, O, T. Sing, I. Sommer, A. J. Low, P. K. Cheung, P. R. Harrigan, T. Lengauer, and F. S. Domingues. 2007. Structural descriptors of gp120 V3 loop for the prediction of HIV-1 coreceptor usage. *PLos Comput Biol*. 3(3):e58

Scoggins, Robert M., James R. Tayor, Jr., James Patrie, Angelique B. van'tWout, Hanneke Schuitemaker, and David Camerini. 2000. Pathogenesis of Primary R5 Human Immunodeficiency Virus Type 1 Clones in SCID-hu Mice. *Journal of Virology*. 74(7): 3205-3216.

Spear, M., J Guo, and Y. Wu. 2012. The trinity of the cortical actin in the initiation of HIV-1 infection. *Retrovirology*. 9:45

Thali, M., Moore, J. P., Furman, C., Charles, M., Ho, D. D., Robinson, J., and Sodroski, J. (1993). Characterization of conserved human immunodeficiency virus type 1 gp120 neutralization epitopes exposed upon gp120-CD4 binding. *Journal of Virology*. **67**(7)**:** 3978-88

Wyatt, R., Sullivan, N., Thali, M., Repke, H., Ho, D., Robinson, J., Posner, M., and Sodroski, J. (1993). Functional and immunologic characterization of human immunodeficiency virus type 1 envelope glycoproteins containing deletions of the major variable regions. *Journal of Virology*. **67**(8)**:** 4557-65.

Xiang, S., Peter D. Kwong, Rishi Gupta, Carlo D. Rizzuto, David J. Casper, Richard Wyatt, Liping Wang, Wayne A. Hendrickson, Michael L. Doyle, and Joseph Sodroski. 2002. Mutagenic Stabilization and/or Disruption of a CD4-Bound State Reveals Distinct Conformations of the Human Immunodeficiency Virus Type 1 gp120 Envelope Glycoprotein. *Journal of Virology*. 76(19)9888-9899

Yang, N., O. Higuchi, K. Ohashi, K. Nagata, A. Wada, K. Kangawa, E. Nishida, and K. Mizuno. 1998. Cofilin phosphorylation by LIM-kinase 1and its role in Rac-mediated actin reorganization. *Nature* 393:809-812.

Yoder, A, D. Yu, L. Dong, S. R. Iyer, X. Xu, J. Kelly, J. Liu, W. Wang, P. J. Vorster, L. Agulto, D. A. Stephany, J. N. Cooper, J. W. Marsh, and Y. Wu. 2008. HIV envelope-CXCR4 signaling activates cofilin to overcome cortical actin restriction in resting CD4 T cells. *Cell* 134:782-792.

Younai, Fariba S. 2013. Thirty years of the human immunodeficiency virus epidemic and beyond. *Int J Oral Sci*. 5(4): 191-199.

Zella, Davide, Oxana Barabitskaja, Jennifer M. Burns, Fabio Romerio, Daniel E. Dunn, Maria Grazia Revello, Giuseppe Gerna, Marvin S. Reitz Jr, Robert C. Gallo, and Frank F. Weichold. 1998. Interferon-γ increases expression of chemokine receptros CCR1, CCR3, and CCR5, but not CXCR4 in monocytoid U937 cells. *Blood*. 91(12): 4444-50.

BIOGRAPHY

Huizhi Liang graduated from Hangzhou Foreign Language School in China in 2006. She received her Bachelor of Science from George Mason University in 2010. She was employed as a student volunteer in a research lab in George Mason University for one year and received her Master of Science in Biology with a concentration in Microbiology and Infectious Diseases from George Mason University in 2015.